12-9-2022

Mapping forest structure in Mississippi using LiDAR remote sensing

Nitant Rai
Mississippi State University, nitant.rai07@gmail.com

Mapping forest structure in Mississippi using LiDAR remote sensing

By

Nitant Rai

Approved by:

Krishna P. Poudel (Major Professor)
Qin Ma
Austin J. Himes
Qingmin Meng
Donald L. Grebner (Graduate Coordinator)
Loren W. Burger (Dean, College of Forest Resources)

A Thesis
Submitted to the Faculty of
Mississippi State University
in Partial Fulfillment of the Requirements
for the Degree of Master of Science
in Forestry
in the Department of Forestry

Mississippi State, Mississippi

December 2022

Name: Nitant Rai

Date of Degree: December 9, 2022

Institution: Mississippi State University

Major Field: Forestry

Major Professor: Krishna P. Poudel

Title of Study: Mapping forest structure in Mississippi using LiDAR remote sensing

Pages in Study: 91

Candidate for Degree of Master of Science

This study aimed at evaluating the agreement of spaceborne Light Detection and Ranging (lidar) ICESat-2 canopy height with Airborne Laser Scanning (ALS) derived canopy height to inform about the performance of ICESat-2 canopy height metrics and understand its uncertainties and utilities. The agreement was assessed for different forest types, physiographic regions, a range of percent canopy cover, and diverse disturbance histories. Results of this study suggest that best agreements are found using strong beam data collected at night for canopy height retrieval using ICESat-2. The ICESat-2 showed great potential for estimating canopy heights, particularly in evergreen forests with high canopy cover. Statistical models were developed using fixed-effects and mixed-effects modeling approaches to predict ALS canopy height metrics using ICESat-2 parameters and other attributes. Overall, ICESat-2 showed good agreement with ALS canopy height and showed its predictive ability to characterize canopy height. The outcome of this study will help the scientific community understand the capabilities and limitations of ICESat-2 canopy heights; the study also provides a new approach to obtain wall-to-wall ALS standard canopy height maps at landscape level.

Keywords: airborne laser scanning, canopy height, ICESat-2, fixed-effects, mixed-effects model

DEDICATION

In dedication to my loving family who have always supported and encouraged my pursuit of higher education. I would not have had the opportunities that I have today without their sacrifice and support.

ACKNOWLEDGEMENTS

I would like to express my sincere gratitude to everyone who helped me throughout this project. I'm extremely grateful to my major advisor, Dr. Krishna P. Poudel, for his tremendous support and close guidance throughout my master's journey. I am deeply indebted to my former major advisor, Dr. Qin Ma, for giving me the opportunity to come to Mississippi State University. I am extremely thankful that she helped me carry out research through video conferencing and meetings even after leaving the university. I would like to express my deepest appreciation to my committee members, Dr. Austin Himes and Dr. Qingmin Meng for their willingness and participation in this project. Many thanks to my friends Karold, Mahesh and Sujan for their unwavering support throughout this process.

TABLE OF CONTENTS

LIST OF TABLES

LIST OF FIGURES

CHAPTER I

ACCURACY EVALUATION OF SPACEBORNE LIDAR (ICESAT-2) TREE HEIGHT PRODUCTS USING AIRBORNE LIDAR DERIVED TREE HEIGHT ESTIMATES

1.1 Introduction

Forests in Mississippi cover more than 65% of the state's total land area (Morgan et al., 2012). These forests provide a great deal of resources, ecosystem goods and services to local communities including timber production, biomass and carbon sequestration, regulation of temperature and rainfall, recreation, habitat for wildlife and soil protection (di Sacco et al., 2021). The provisioning of ecosystem services from these forests are often affected by human intervention and natural disturbances. Forest managers often employ management operations, such as prescribed fire and thinning that modify the forest structure (Harrod et al., 2009). Additionally, unpredictable natural phenomenon such as windstorms, flooding, hurricanes, and severe wildfires alter forest structure (Seidl et al., 2011). In Mississippi, the frequently occurring hurricanes (Day et al., 2007), increasing trends in forest fire severity and occurrence (Grala et al., 2017), and flooding severely impact the state's forests (Oswalt, 2019). As a result, forest productivity and ecosystem services are negatively impacted. There is a need for robust evaluation of the patterns in forest structure caused by the disturbances and how these forest stands recover after disturbances.

Forest structure is a three-dimensional characteristic of a forest describing the spatial arrangement of trees' trunks, branches, and canopy heights in the forest (Tello et al., 2018).

Important forest structural attributes include tree height, diameter, basal area, stand density, canopy cover, and leaf area index (Guan et al., 2020). Quantifying forest structure is a critical step to understand aboveground biomass and carbon dynamics (Alves et al., 2010), as well as for other forest monitoring applications, such as growth modeling and fire risk assessment (van Leeuwen & Nieuwenhuis, 2010). To describe forest structure, structural heterogeneity in the horizontal and vertical dimensions need to be considered. The horizontal structure reflects size, density, and arrangement of stand whereas vertical structure accounts for tree height variability and vertical distribution of canopy (Tello et al., 2018). This study focused on the vertical structure of the forest, specifically tree height since it is one of the most important parameters for characterizing forest structure (Rödig et al., 2018).

Traditionally forest structure characterization has been based on field-based inventory, and forest structure metrics have been derived based on the measurement of individual tree information, such as height, basal area, canopy dimensions, species composition, and/or stand density (Tello et al., 2018). The forest structure maps produced from large-scale field inventories become outdated quickly and are prone to error (Kayitakire et al., 2006). With the advent of remote sensing techniques, researchers have been able to precisely estimate forest structure more rapidly. Use of remote sensing techniques help alleviate time consuming and costly field work covering large areas, which may not be logistically feasible in all situations (Zahawi et al., 2015). Various studies have demonstrated the accuracy and reliability of measurements made using remote sensing techniques. For example, Rahimizadeh et al., (2020) estimated canopy gap by object-and pixel-based methods with 91% accuracy when compared with field-based inventory. Hyyppä et al., (2000) compared various data sources to estimate forest stand attributes and found that the remote sensing profiling instrument presented an equivalent accuracy to conventional

forest inventory with R^2 of 0.77, 0.59, and 0.68 in estimating mean height, basal area, and stem volume respectively. Ma et al., (2017) used very-high-resolution (VHR) optical imagery to classify tree crown cover with 93% overall accuracy. However, optical methods suffer from saturation effects causing decreased sensitivity of the backscatter since electromagnetic radiations from the sun cannot penetrate the upper forest canopy directly (Chen et al., 2007). In recent years, remote sensing technologies such as waveform Light Detection and Ranging (lidar) and Synthetic Aperture Radar (SAR) have allowed the measurement of 3-D forest information. Researchers have used SAR (Tello et al., 2018), Terrestrial Laser Scanner (TLS) (Danson et al., 2014), Airborne Laser Scanning (ALS) and a combination of ALS and multi spectral scanners (Manzanera et al., 2016) to characterize forest structure. Research has shown higher accuracy of lidar data for measuring forest structural parameters, such as tree height, compared to the estimates of ground-based surveys and other optical remote sensing methods (Akay et al., 2009).

Lidar is a laser-based remote sensing technique that illuminates the target by emitting pulses of energy. The travel time of each laser pulse emitted from the sensor to the target provides the distance from the instrument to the target (Dubayah & Drake, 2000). This information is used to understand the overall characteristics and structure of the target, such as forest trees and terrain. Lidar can penetrate upper forest canopies and map undergrowth and ground data. Thus, lidar-based forest structure data and high-resolution Digital Elevation Models (DEMs) have been widely used in forest inventory, managing forest fires, planning forest operations, and measuring forest structures at landscape scales (Wulder et al., 2008). At local scales, traditional in-situ forest inventory methods measure forest structure precisely, while airborne and spaceborne lidar datasets provide an opportunity to scale local measurements to regional and even global scales (Wulder et al., 2012).

In forested ecosystems, wise management decisions are made by comprehensively considering variables such as forest composition and structure. Information on forest structure has been used to undertake various forest management operations such as clearcutting, thinning, soil preparation and weeding, as well as monitoring forest deforestation and degradation (Holmgren et al., 1996). The new lidar technology has the ability to characterize the forest structure by directly measuring canopy height, sub-canopy topography, and vertical distribution of intercepted surfaces between the top of the canopy and the ground surface (Dubayah & Drake, 2000). Past studies that used lidar to estimate tree height have shown good results with Root-Mean Squared Error (RMSE) values ranging from 17 to 19 centimeters (cm) in pavement, low grass, and evergreen forests and 26 cm in deciduous forests (Hodgson & Bresnahan, 2004). Although the application of lidar to ecological problems has shown promising results, current airborne lidar acquisitions remain prohibitively expensive for large scale monitoring projects and regional studies (Beland et al., 2019).

Spaceborne lidar missions such as ICESat-2 (Ice, Cloud, and land Elevation Satellite) and GEDI (Global Ecosystem Dynamics Investigation) are capable of directly measuring canopy heights which could improve our understanding of forest structure at near global scale (Neuenschwander & Magruder, 2019). GEDI is the first spaceborne lidar instrument specifically optimized to measure vegetation structure and forms the basis of critical reference datasets. GEDI lidar observations are used to create data sets on canopy height, canopy cover and vertical profile, leaf area index and profile, topography, and footprint-level and gridded Above Ground Biomass Density (AGBD) within 51.5° latitude (Dubayah et al., 2020). On the other hand, ICESat-2 is the only space-based lidar system that collects data above 51.5° latitude. As such,

ICESat-2 data will provide a new opportunity to directly measure the height and distribution of forests at higher latitudes than GEDI.

The ICESat-2 consists of three pairs of beams, each pair separated by about 3 kilometers (km) cross-track with a pair spacing of 90 meters (m). Each of the beams has a nominal 17 m diameter footprint with an along-track sampling interval of 0.7 m. The ICESat-2 ATL08 (Land and Vegetation Height) dataset contains the along-track terrain elevation and canopy heights (Neuenschwander et al., 2016). The ATL08 product is developed from ATL03 using DRAGANN (Differential, Regressive, and Gaussian Adaptive Nearest Neighbor), algorithm specifically designed for extracting terrain and canopy heights. It provides estimates of terrain and canopy height and canopy cover of a segment at every 100 m step size in the along-track direction (Neuenschwander et al., 2020). For the ICESat-2 ATL08 product, the terrain and canopy parameters are consecutively provided at a fixed step-size of 100 m along the ground track, referred to as a segment, and along track distance of 0.7 m. This ensures there are a sufficient number of photons to estimate terrain and canopy height (Liu et al., 2021).

Current spaceborne lidar acquisitions from missions like ICESat-2 offer opportunities for mapping canopy height at regional scales, but the accuracies of these canopy height products have not been systematically evaluated over the southern USA, particularly in recently disturbed areas. Many airborne lidar datasets have been acquired over time under the USGS 3D Elevation Program (3DEP). They provide opportunities to build synergies for consistent and spatially complete characterization of vertical forest structures (Thatcher et al., 2020). Although spaceborne lidar like ICESat-2 has the advantage of large-area coverage over airborne lidar systems, it is still not certain that they can fully replace airborne lidar. Comparing height estimates from airborne and spaceborne lidar datasets in a variety of scenarios would help

validate the usefulness of spaceborne lidar data and provide information on the uncertainties, their scientific utility, and conditions for their reliability.

While the ICESat-2's ATL08 product is increasingly utilized by researchers, validation of its canopy height data is still limited. Studies have assessed ICESat-2 terrain height and canopy height data over different regions. For example, Neuenschwander & Magruder, (2019) reported on ICESat-2 ATL08 product, with RMSEs of 0.85 m and 3.69 m for terrain and canopy height retrievals, respectively on forests of Finland. Liu et al., (2021) in assessing ICESat-2 canopy height using all data pairs, regardless of data acquisition time and beam intensity reported an RMSE values of 40.2% and R^2 value of 0.61. Mulverhill et al., (2022) compared 95th percentile canopy heights derived from ICESat-2 with National Terrestrial Ecosystem Monitoring System (NTEMS) data and reported a RMSE of 4.87 m. These efforts to validate height estimates from the ICESat-2's products have largely focused on a single biome or ecoregion (Neuenschwander et al., 2020), or assess terrain heights (Tian & Shan, 2021). Malambo & Popescu, (2021) conducted a study to assess canopy height over different biomes, however they did not focus on the disturbance history and forest types within the study area. Therefore, to inform the performance of ICESat-2 for characterizing the vertical structure of forests, there is a need to evaluate a variety of canopy height metrics over various vegetation types and disturbance histories.

This study aims to evaluate the accuracy and uncertainties associated with estimating canopy heights from ICESat-2. Canopy height from ICESat-2 was validated using data from ALS across different physiographic regions and forest types in Mississippi. The disturbance maps from Vegetation Change Tracker (VCT) and LANDFIRE were used to identify the occurrence of the initial disturbance, its location, extent and frequency and the last occurrence of

disturbance between 1986 to 2016. This information was used to see how the spaceborne lidar determines the canopy height over previously disturbed areas as well as undisturbed areas. The findings presented in this research will provide information on the accuracy of the ICESat-2 canopy height product and its accuracy over different scenarios. It demonstrates the value and potential of integrating diverse data sources for forest structure monitoring. Additionally, it will help to develop a model to map forest structure on multi-spatial and temporal scales.

1.2 Objective

The overall objective of this study was to compare spaceborne lidar tree height data with airborne lidar data over 27 counties of Mississippi. The specific objective was to evaluate the accuracy and uncertainties of ICESat-2 canopy height products using airborne lidar derived tree height estimates.

1.3 Materials and methods

1.3.1 Study area

The study area covers 27 counties of Mississippi (Figure 1.1). The study area boundary map was obtained from Mississippi Automated Resource Information System (MARIS, 2022). Mississippi state encompasses about 125,460 km² with elevation ranging from 30 to 200 m above mean sea level. The mean annual temperatures range from 16 degrees Celsius (°C) to 20°C and precipitation ranges from about 1270 to 1650 millimeters (mm) across the state from north to south (Department of Geosciences at Mississippi State University, 2022). Major tree species include loblolly pine (*Pinus taeda*), elm (*Ulmus spp.*), ash (*Fraxinus spp.*), cottonwood (*Populus deltoides*), oak (*Quercus spp.*), cypress (*Cupressus spp.*), sweetgum (*Liquidambar styraciflua*), black willow (*Salix nigra*), and hickory (*Carya spp.*) (Oswalt, 2019).

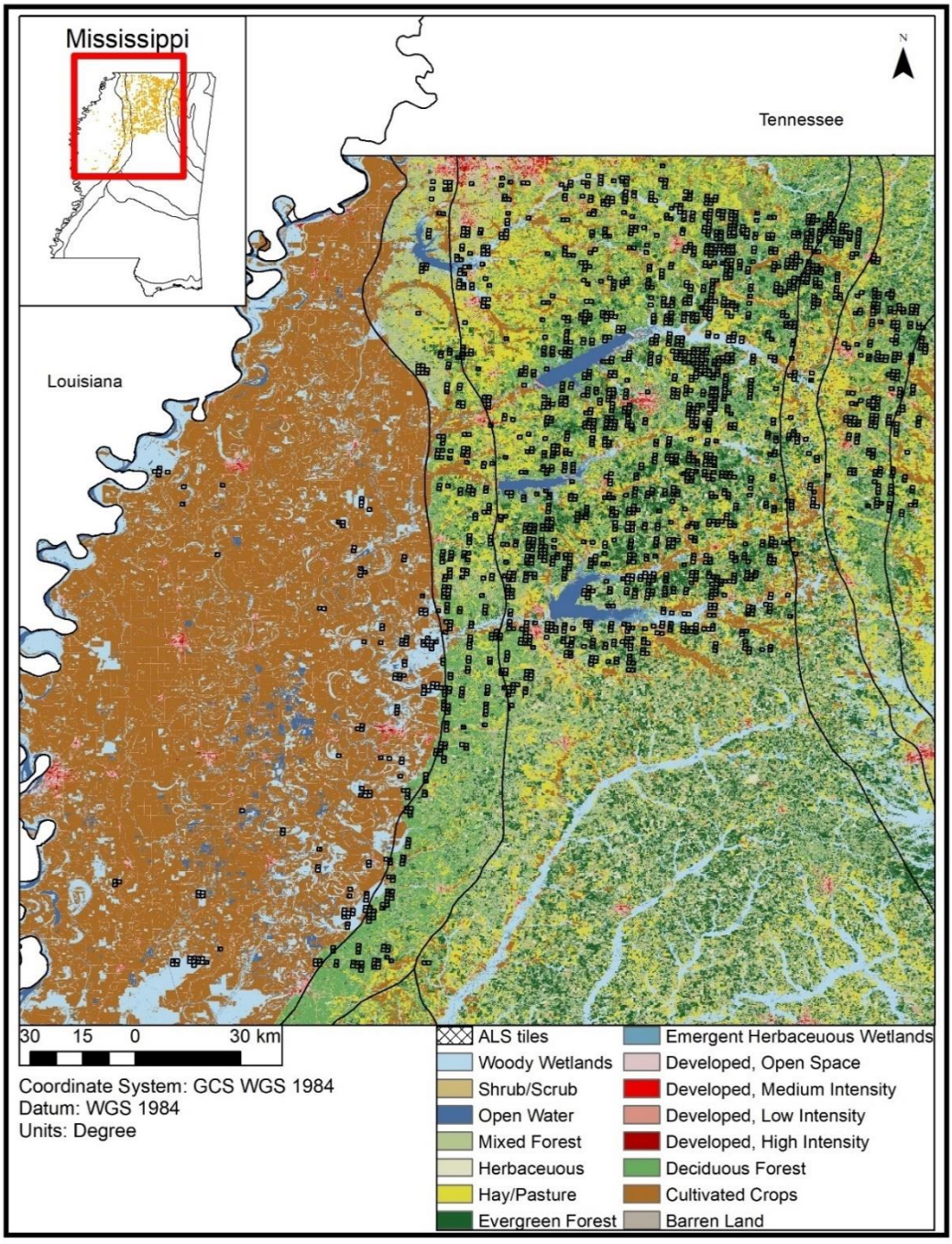

Figure 1.1 Map showing study area within Mississippi. The land use and land cover types are extracted from the National Land Cover Database (NLCD) 2019 (MRLC, 2022).

1.3.2 Dataset

Lidar data from both airborne and spaceborne platforms were used in this study. The datasets used in this study were ICESat-2 ATL08 data, ALS data, National Land Cover Database (NLCD), and disturbance maps collected from VCT and LANDFIRE. These datasets were processed to examine the agreement between canopy height estimates from ICESat-2 and corresponding height estimates from ALS. Two approaches were used to compare the ALS canopy height with the ICESat-2. First, we compared ICESat-2 data with Canopy Height Model (CHM) derived canopy heights and second approach was to compare ICESat-2 data with ALS relative metrics i.e., ALS derived maximum height (ALS max) and ALS 99th percentile height (RH99). The overall flow of the study is shown in the Figure 1.2.

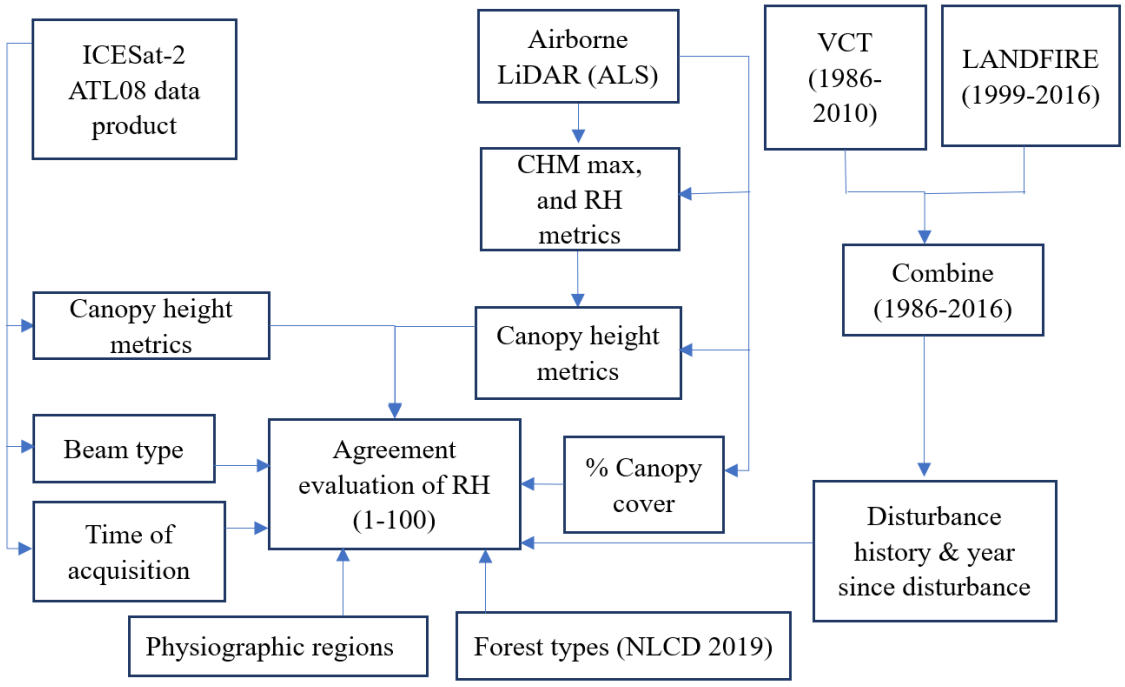

Figure 1.2 Flowchart for assessing the agreement between ICESat-2 and ALS derived canopy height

1.3.3 ICESat-2 data acquisition and processing

ICESat-2 ATL08 canopy height data collected between 2018 October to 2020 December was downloaded from the Earthdata Search website (https://search.earthdata.nasa.gov). ICESat-2 carries the Advanced Topographic Laser Altimeter System (ATLAS), a single-photon sensitive lidar instrument that can detect individual photons reflected from vegetation canopy (Queinnec et al., 2021). It transmits three pairs of laser beams at a wavelength of 532 nm (green) and each pair of beams consists of a weak beam and a strong beam with a transmitted energy of approximately 1:4 ratio transmitted at a rate of 10 kHz. ATLAS can record a transmitted laser pulse every 70 cm from a nominal orbit altitude of 500 km and can detect up to approximately 10 signal photons per footprint over highly reflective surfaces such as ice and snow surfaces, and between 0 and 4 signal photons over land and vegetation (Neuenschwander et al., 2016; Neuenschwander & Magruder, 2019). As a result, the amount of data captured is directly proportional to the difference in transmitted beam energy. In the case of vegetation, the level of penetration and subsequent characterization of the understory structure may be influenced by beam energy, atmospheric effects and noise levels. Another important factor for a photon-counting lidar system like ICESat-2 is acquisition time. When detected with ICESat-2's own transmitted laser pulse, similar green energy from solar radiation is highest during the day, resulting in higher levels of background noise for day acquisitions than for night acquisitions (Neuenschwander et al., 2020).

This study used the Level-4 Land and Vegetation Height data product (ATL08), for the canopy heights above the WGS84 ellipsoid. The ATL08 data is characterized by each of the six ground tracks. Each ground track group on the ATL08 data product contains subgroups for land and canopy heights as well as for beam and reference parameters utilized in the ATL08

processing. The ATL08 data provides along track terrain and canopy height metrics in 100 m segment including estimates like relative heights (RH or the height from the ground at which a certain quantile of energy is returned) of canopy and descriptive statistics of terrain elevation including mean, minimum, maximum, median, standard deviation, mode, and skewness of the terrain height within each 100 m step (Liu et al., 2021). All available version 4 ATL08 granules between October 2018 and December 2020 were downloaded. After spatial and data quality filtering of 337 HDF5 files, 1,057,848 sample segments were obtained over Mississippi containing valid measurements (Figure 1.3).

ICESat-2 reports three canopy height metrics: h_max_canopy (maximum canopy height relative to the ground), h_canopy (RH98, 98% relative height) and canopy_h_metrics (height metrics based on the cumulative distribution of relative heights above the interpolated ground surface, calculated at 5% intervals for percentages 10-95). The most significant challenge to the ICESat-2 algorithm comes from the effect of solar background noise; thus, the data acquisition time and beam intensity affect the accuracy of labeled ground photons and canopy photons by affecting the number of photons in the segment (n_seg_ph) and the signal-to-noise ratio (SNR). For ICESat-2, the RH98 parameter is recommended as a measurement of the top canopy height rather than the maximum of canopy photons owing to the signal-to-noise uncertainty at the top of the canopy (Neuenschwander et al., 2020; Neuenschwander & Pitts, 2019).

This study examined the RH metrics including 25^{th}, 50^{th}, 75^{th}, 95^{th}, 98^{th} and maximum canopy height percentile from ICESat-2 and ALS over different scenario as shown in Table 1.1. This study compared the RH98 from ICESat-2 with RH99 of ALS because the RH metric closest to RH98 given by ALS was RH99.

Table 1.1 Variables used to assess the agreement of ICESat-2 and ALS.

Variable	Scenario
Beam type	Strong, and weak
Time of acquisition	Day, and night
Beam type and time of acquisition	Strong day, strong night, weak day, and weak night
Forest types	Deciduous forest, evergreen forest, mixed forest, and woody wetlands
Physiographic regions	Black prairie, Pontotoc ridge, flatwoods, north central hills, loess hills, and alluvial plain
% Canopy cover	0 - 1
Disturbance frequency	0, 1, 2, and >2
Year since disturbance	<20, 20-25, 25-30, and >30

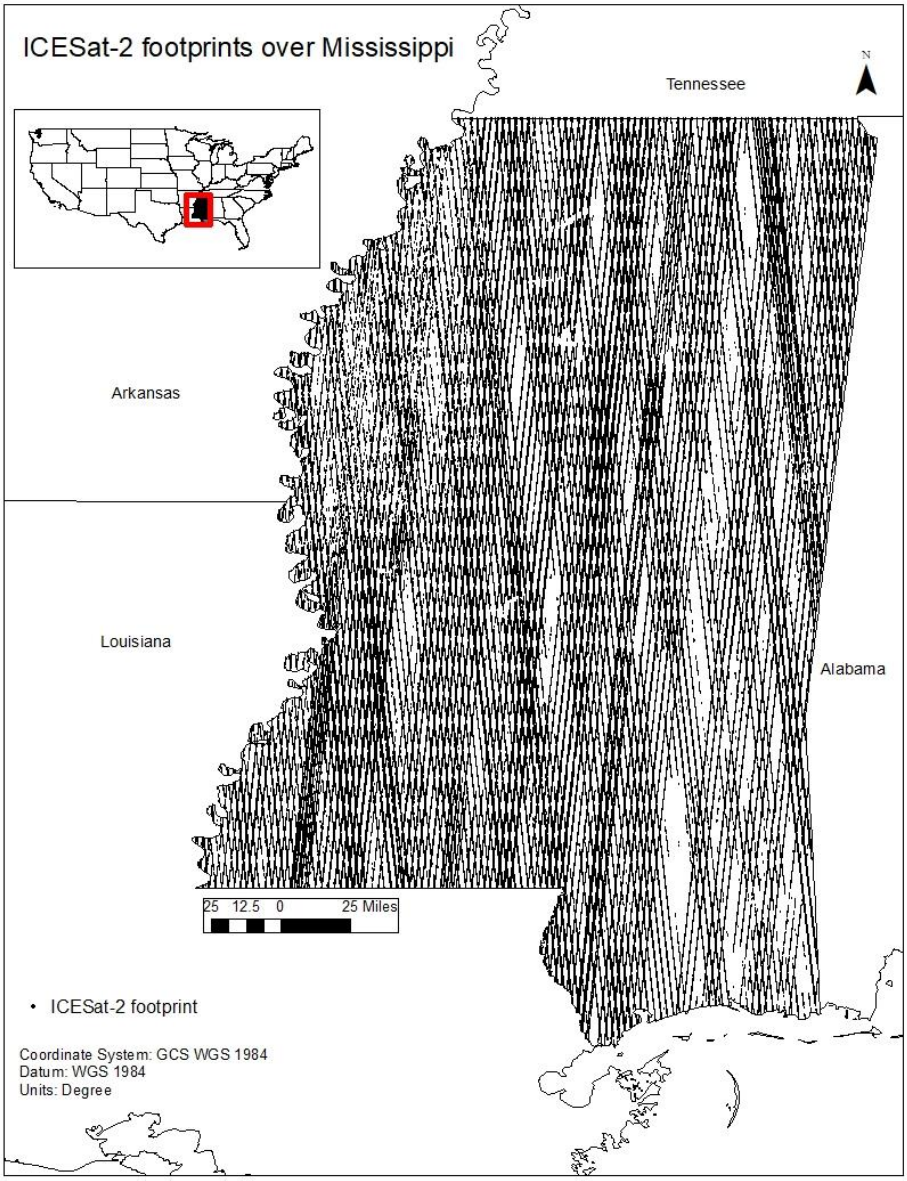

Figure 1.3 Lidar footprints observed in Mississippi. A total of 1,057,848 ICESat-2 records were observed from 2018-2020.

1.3.4 ALS data acquisition and processing

Airborne Laser Scanning (ALS) data of some regions within Mississippi were downloaded from a publicly available dataset to verify the accuracy of the canopy height retrieved in this study. ALS data was downloaded from 3DEP LiDAR Explorer website (http://prd-tnm.s3.amazonaws.com/LidarExplorer/index.html#/). This data was collected in three

phases as Mississippi Delta A1 2018 (February 18, 2018 - February 8, 2019), Mississippi Delta A2 2018 (January 24, 2019 - February 29, 2019) and Mississippi Delta A3 2018 (February 26, 2018 - December 13, 2020) with point density of 2 pts/m^2. The downloaded ALS data was located in 6 of the 11 physiographic regions of Mississippi. The metadata for the ALS data suggests that its RMSEz value is ≤10 cm (USGS, 2020), which is an order of magnitude lower than the canopy height error of ICESat-2. Therefore, the use of this ALS product as reference data is a good indicator of the canopy height accuracy of ICESat-2.

Over 11,337 ALS tiles were downloaded, each tile covering an area of 1 km^2, and sampling was carried out to select tiles for further processing due to the processing and memory limitations. This study used the location of all the Forest Inventory and Analysis (FIA) plots across Mississippi to sample the tiles, and only those tiles that were within a 1 km buffer around the FIA sites were chosen. The FIA plot location was used for sampling because it collects data on forest vegetation and related attributes, using a systematic plot design that covers the conterminous United States (Tinkham et al., 2018). The resulting 2145 tiles were processed using LIDAR360 software. A total of 47,482 ICESat-2 segments across all sites were evaluated to assess the agreement between ICESat-2 and ALS canopy heights.

Canopy height metrics from ALS were derived using LiDAR360 software Version 5.2 (GreenValley International, 2022). LiDAR360 software provides tools required for effectively interacting and manipulating lidar point cloud data. Two different kinds of individual tree segmentation algorithms are provided in the software to derive individual tree parameters, the CHM-based marker-controlled watershed segmentation algorithm (Conrad et al., 2015) and point-cloud based algorithm (Li et al., 2012). This study used CHM for further analysis. The first step in CHM segmentation includes outlier removal function and then classifying the ground

points (filter) to generate Digital Surface Model (DSM) and Digital Elevation Model (DEM). The DEM and DSM were calculated from the lidar ground returns and first returns with the ordinary kriging method at 1 m spatial resolution (Guo et al., 2010). Then, CHM was calculated as the difference between DSM and DEM. Relative height (RH) metrics were also calculated using the LiDAR360 software to get parameters related to point cloud elevation. It was used to calculate the RH metrics by 100 m × 12 m segment polygons which gave RH (1-100) within the segment to correlate with the ICESat-2 data.

1.3.5 Disturbance map

This study used VCT and LANDFIRE disturbance maps both with a spatial resolution of 30 m. The VCT algorithm uses time series observations from Landsat images to map the location, timing, and spectral magnitudes of forest disturbance events (Huang et al., 2010) whereas the LANDFIRE disturbance maps the location, extent, type, and severity of major disturbances for the entire US using Landsat images (Landfire, 2011). Although the name suggests LANDFIRE would only show wildfire, it includes disturbance from different sources such as clearcutting, thinning, prescribed fire, and development activities. The VCT disturbance maps from 1986 - 2010 were downloaded from ORNL DAAC website (https://daac.ornl.gov). Similarly, the LANDFIRE disturbance maps were downloaded from LANDFIRE website (https://landfire.gov/hdist.php) for years 1999 - 2016. Between the LANDFIRE and VCT, only LANDFIRE provides information about the severity of the disturbance from low to high. Our preliminary analysis showed that the VCT and LANDFIRE were similar when LANDFIRE disturbance maps were filtered by only high and medium disturbance severity. After comparison, we combined LANDFIRE and VCT maps for the overlapping map years (1999 - 2010) of high and medium severity areas. This produced a uniform disturbance map for years 1986 - 2016,

which was then analyzed in ArcGIS and Python version 3.7 (Van Rossum & Drake, 2009). Then, ICESat-2 footprints were overlaid over the disturbance maps and were evaluated if the footprint locations were disturbed within study period. The ICESat-2 footprints were also grouped as undisturbed, disturbed once, disturbed twice, disturbed more than twice, and years since disturbance.

1.3.6 National Land Cover Database (NLCD) and Physiographic Regions Map

NLCD provides nationwide data on land cover and land cover change based on Landsat-8 multispectral satellite images at 30 m resolution. NLCD is an operational land cover monitoring program providing updated land cover and related information for the United States (Wickham et al., 2021). For this study, NLCD land cover data from 2019 was downloaded from Multi-Resolution Land Characteristics Consortium website (https://www.mrlc.gov/data). Among the total of 16 land cover types in NLCD 2019, this study used the 4 different land covers, namely deciduous forest, evergreen forest, mixed forest, and woody wetlands. The NLCD map was used to evaluate ICESat-2 estimated tree height over different forest types and was supplementary data to assist our assessment.

Similarly, a Physiographic Regions map of 2013 was downloaded from MARIS website (www.maris.state.ms.us/). 6 of the 11 physiographic regions in Mississippi namely the North Central Hills, Flatwoods, Pontotoc Ridge, Black Prairie, Alluvial Plain, and Loess Hills were covered by the ALS tiles used in the study. Therefore, this study includes only these physiographic regions for further analysis.

1.3.7 Data processing and height metrics extraction

The geolocation (horizontal) accuracy of ICESat-2 is <5 m and tend to be 2-3 m which is much better than that of GEDI (20 m for the first version and 10 m for the second version) (Liu et al., 2021). Since several different elevation data sets are involved in this study, it is necessary to co-register them correctly. Prior to extracting canopy height metrics from ICESat-2 and ALS, a few preprocessing or data correction steps were carried out to enhance the comparison. The first critical step taken was to ensure that the ICESat-2 and ALS data were co-registered well to each other. Before calculating corresponding height metrics from ALS data, all data were projected from their respective coordinate systems to the Albers Conic equal area coordinate system.

ICESat-2 product provides each segment with an uncertainty index "h_canopy_uncertainty" for the uncertainty of the relative canopy height for the segment. This uncertainty index incorporates all systematic uncertainties (e.g., timing, orbits, geolocation, etc.) as well as the uncertainty in photon identification. An "invalid" value (3.4028E + 38) is reported if the number of ground photons in the segment is ≤5% of total number of signal photons per 100 m segment. Without a sufficient number of ground photons in a segment, the calculated terrain height has little confidence. Thus, the segments with the "invalid" value in the h_canopy_uncertainty attribute in the ICESat-2 product, noted as invalid segments, were eliminated from evaluation. Preliminary analysis showed that there were many outliers, which may have been caused by incorrect ground interpolation due to cloud or solar noise. Therefore, the outliers were removed by removing those observations that are higher than the tallest trees in Mississippi. FIA database suggested the maximum canopy height of 60 m over Mississippi,

therefore, all the observations above this value were eliminated. Further, ICESat-2 footprints were filtered using the following criteria:

1. A relative uncertainty value of less than 20 m for canopy height (h_canopy_uncertainty <20 m) (Liu et al., 2022);
2. Estimated forest canopy height should be greater than 2 m and less than 60 m.

In order to examine the robustness of our approach for retrieval of canopy height through integration of ICESat-2 and ALS products, the approach was applied to different ICESat-2 tracks in Mississippi at different segment sizes such as diameters of 13 m, 17 m, and 100 m (along-track) × 12 m (across-track) segment. The R^2 and Root Mean Square Deviation (RMSD) between retrieved ICESat-2 canopy height and corresponding ALS metrics were calculated and used as indicators for assessing the effectiveness of the proposed approach. We found that 100 m × 12 m segment had the greatest agreement with R^2 of 0.52 followed by 13 m and 17 m diameter with R^2 of 0.34 and 0.21 respectively. Also, studies have suggested that ICESat-2 ALT08 product is sampled using continuous 100 m × 12 m segments, therefore we also used 100 m × 12 m segments around ICESat-2 footprints to compare with the ALS in our study (Liu et al., 2021).

The centroids of the first and last segments were used to calculate the track inclination, and then a rectangular buffer of 100 m × 12 m around the centroids of the segments were created. LiDAR360 software was used for processing the ALS data as discussed in section 1.3.4. From the processed ALS data, canopy heights were extracted for each ICESat-2's 100 m × 12 m segment and corresponding height metrics were obtained per segment. Canopy height metrics such as canopy height, max canopy height and other relative canopy height metrics along with canopy cover were also calculated for each segment.

1.3.7.1 Data analysis

This study performed exploratory data analysis to get the summary statistics and graphics to understand the data. For statistical visualization, the study used histograms, scatterplots, boxplots, and density plots to comprehend the data. R statistical software version 4.1.1 (R Core Team 2021) was used for creating statistical graphs.

1.3.7.2 Equivalence test

Equivalence test was employed to check if the canopy height derived from ICESat-2 and ALS were statistically equivalent. This study used two one-sided t-test (TOST) procedures for testing the equivalence. Here, the null hypothesis is the non-agreement of the heights derived from ICESat-2 and ALS. Thus, rejecting the null hypothesis indicates agreement of canopy height metrics between ICESat-2 and ALS. The equivalence test is based on a range within which differences between test and reference data are considered negligible (Robinson & Froese, 2004). The TOST approach aims to specify a lower and upper bound, such that results falling within this range are considered equivalent. The observed data are compared against lower and upper bounds in two one-sided tests. If the p-value for both tests is less than the level of significance, the null hypothesis is rejected i.e., ICESat-2 and ALS derived canopy height are statistically equivalent for a given threshold value; else, we fail to reject the null hypothesis indicating the ICESat-2 and ALS derived canopy height are statistically different for a given threshold value. Having established the threshold value, it then determines whether difference between ICESat-2 and ALS canopy height lies within the region. If the region of indifference completely encompasses the confidence interval, then the height metrics measured by ICESat-2 and ALS are deemed statistically similar. If not, then the null hypothesis of difference is not rejected. In this study various intervals of tree height were established as the region of

indifference and the probabilities of rejecting the null hypothesis of dissimilarity under a range of sample sizes at α=0.05 were calculated. The null hypothesis (Equation 1.1) and alternative hypothesis (Equation 1.2) in each case were:

$$H_0: \mu_{ALS} - \mu_{ICESat-2} \neq 0 \tag{1.1}$$

$$H_1: \mu_{ALS} - \mu_{ICESat-2} = 0 \tag{1.2}$$

where μ_{ALS} refers to the ALS derived mean canopy height of 100 × 12 m segment and $\mu_{ICESat-2}$ refers to ICESat-2 canopy height.

This study used equivalence test to evaluate the agreement between ICESat-2 canopy height metrics and ALS derived canopy height metrics by beam type, time of acquisition, forest type, physiographic regions, canopy cover, disturbance frequency, and years since disturbance.

1.3.8 Accuracy assessment

Based on canopy height metrics extracted from ALS products as a reference, we applied several statistical measures to assess the accuracy of ICESat-2 canopy height. Statistical measures to evaluate the height agreement of ICESat-2 were computed by forest types, physiographic regions, percent canopy cover, disturbance history, and years since disturbance. Below are the equations (Equation 1.3 – 1.6) of statistical measures employed to evaluate the height agreement:

$$Mean\ Deviation\ (MD) = \frac{1}{n}\sum_{i=1}^{n}(h_{ICESat-2} - h_{ALS}) \tag{1.3}$$

$$\%Deviation = 100\frac{\sum_{i=1}^{n}(h_{ICESat-2} - h_{ALS})}{\sum_{i=1}^{n}(h_{ALS})} \tag{1.4}$$

$$Root\ Mean\ Square\ Deviation\ (RMSD) = \sqrt{\frac{1}{n}\sum_{i=1}^{n}(h_{ICESat-2} - h_{ALS})^2} \quad (1.5)$$

$$\%RMSD\ = \left(\frac{RMSE}{\bar{h}_{ALS}}\right)100\% \quad (1.6)$$

where, n is the total number of ICESat-2 segments evaluated; $h_{ICESat-2}$ is the ICESat-2 ATL08 height metric, h_{ALS} is the corresponding ALS height metric; and $\bar{h}_{ALS}$ is the mean ALS canopy height.

Agreement between height products was also determined based on the percentage of ICESat-2 canopy heights falling within the 95% confidence interval of the ALS mean canopy height (mean ± 1.96 SD), and then summarized across each forest type and physiographic regions.

1.4 Results

1.4.1 Overall agreement of ALS and ICESat-2

In this study, the greatest agreement was found between ICESat-2 RH98 (the height from the ground at which 98th percentile of energy is returned) and ALS RH99 (the height from the ground at which 99th percentile of energy is returned) with 90.58% of ICESat-2 RH98 heights falling within 95% confidence interval of ALS RH99 heights (MD -1.43 m and R^2 0.54) (Table 1.2).

Table 1.2 Agreement between height products from ICESat-2 and ALS falling within different range of ALS.

Scenario	% Within 95% CI	MD (m)	RMSD (m)	R^2
ICESat-2 max vs CHM max	90.48	-1.77	4.81	0.52
ICESat-2 max vs ALS max	90.39	-1.79	4.81	0.52
ICESat-2 R98 vs ALS RH99	90.58	-1.43	4.54	0.54
ICESat-2 RH95 vs ALS RH95	51.22	-10.48	12.03	0.24
ICESat-2 RH90 vs ALS RH90	50.44	-10.30	11.86	0.22

95% CI = 95% confidence interval (mean ± 1.96 SD), MD = mean deviation,
RMSD = root mean squared deviation, CHM = Canopy Height Model, RH = relative height

The equivalence test showed that the ICESat-2 RH98 and ALS RH99 derived canopy height metrics were statistically equivalent when the acceptable region of similarity was up to 1.38 m (TOST p-value > 0.05) whereas for ICESat-2 max paired with ALS max and CHM max derived canopy height metrics were statistically equivalent when the acceptable region of similarity was 1.8 m (TOST p-value > 0.05) (Figure 1.4).

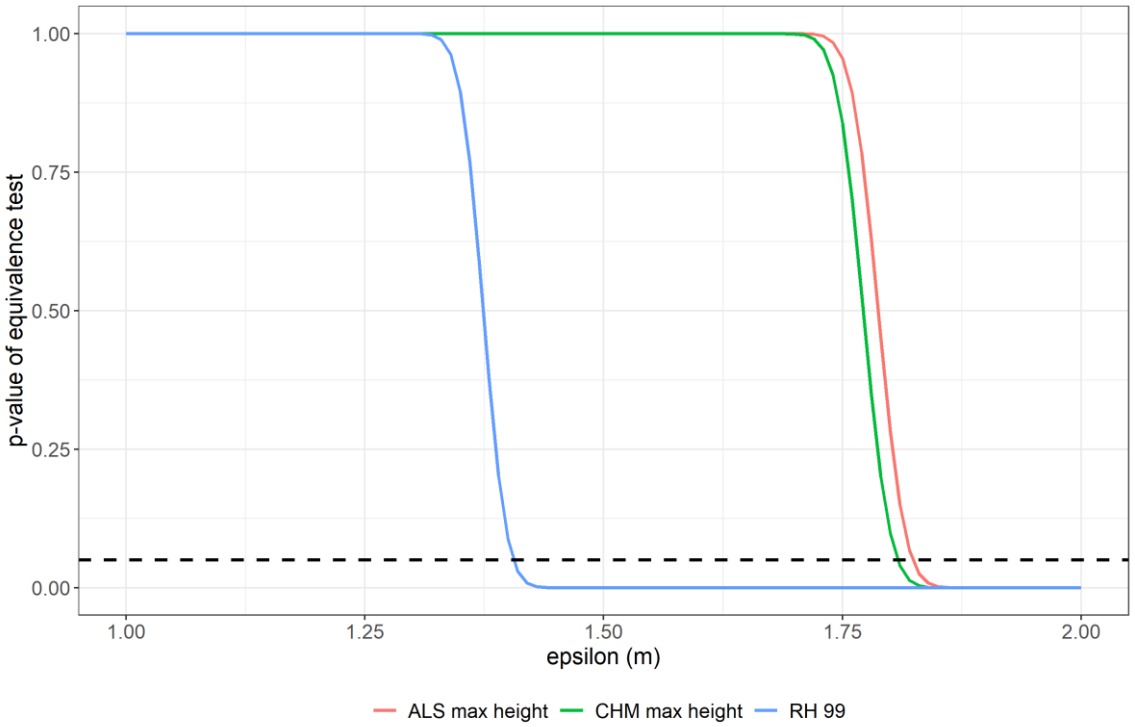

Figure 1.4 Equivalence test of ICESat-2 and ALS derived canopy height metrics.

On the other hand, 95th, 75th, 50th and 25th percentile canopy height metrics were statistically equivalent when the acceptable region of similarity was within range of 9.4 m to 11.6 m (TOST p-value > 0.05) (Figure 1.5). Among these relative heights, ICESat-2 RH98 was statistically equivalent to ALS derived RH99 pair with the lowest threshold value of 9.4 m whereas RH50 had the highest threshold value at 11.6 m. Since the region of similarity for RH25, RH50, RH75 and RH95 were large, we excluded these metrics for further study.

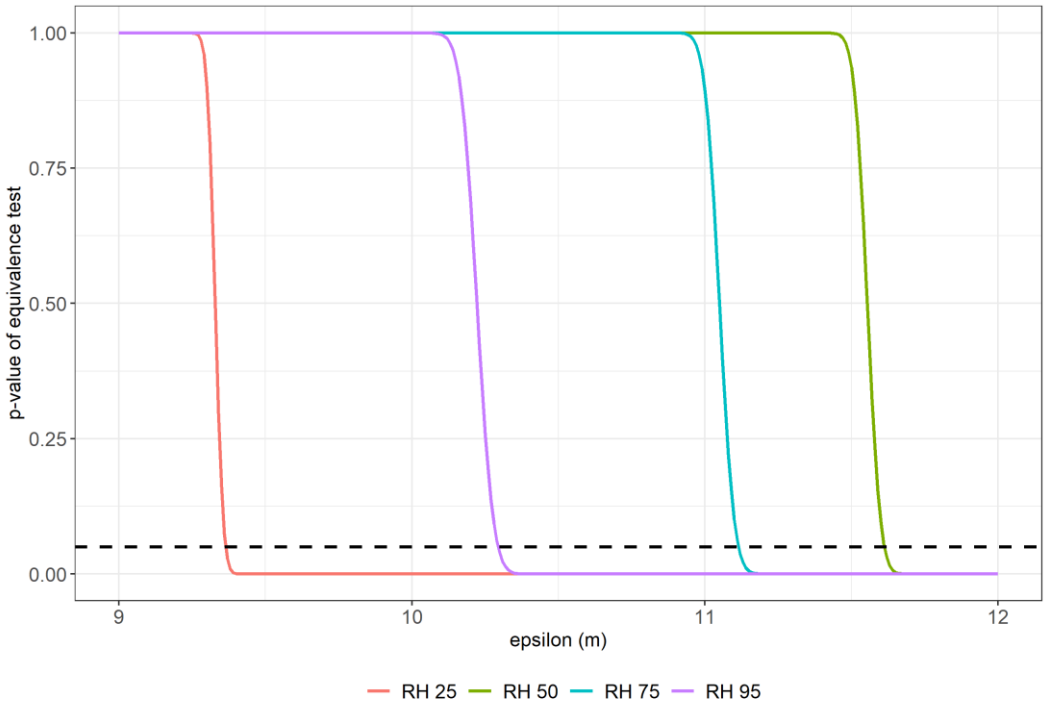

Figure 1.5 Equivalence test of different relative height metrics from ICESat-2 and ALS.

1.4.2 Relative height agreement

The canopy height agreement between ICESat-2 and ALS were evaluated by constructing three pairs: ICESat-2 max vs. CHM max, ICESat-2 max vs. ALS max, and ICESat-2 RH98 vs. ALS RH99 under different scenarios for further analysis.

The measures of agreement between ICESat-2 max with CHM max and ALS max, and between ICESat-2 RH98 and ALS RH99, respectively under different scenarios of beam intensity and data acquisition time are presented in Table 1.3 and 1.4.

Table 1.3 Canopy height agreement between ICESat-2 max, CHM max, and ALS max under different scenarios.

Scenario	% Within 95% CI	MD (m)	RMSD (m)	R^2	Sample (%)
CHM max					
Unfiltered	90.48	-1.77	4.81	0.52	100
Strong beams	91.52	-1.64	4.25	0.59	77.97
Weak beams	87.19	-2.22	6.39	0.35	22.03
Day	87.97	-1.68	5.71	0.42	46.05
Night	92.75	-1.84	3.87	0.66	53.95
Weak & Night	90.94	-2.55	4.85	0.55	8.50
Weak & Day	84.66	-2.02	7.20	0.28	13.52
Strong & Night	93.13	-1.70	3.66	0.68	45.45
Strong & Day	89.46	-1.55	4.96	0.50	32.52
ALS max					
Unfiltered	90.39	-1.79	4.81	0.52	100
Strong beams	91.45	-1.66	4.26	0.59	77.97
Weak beams	86.96	-2.25	6.39	0.35	22.03
Day	87.87	-1.69	5.71	0.42	46.03
Night	92.62	-1.88	3.88	0.66	53.97
Weak & Night	90.72	-2.59	4.85	0.56	8.51
Weak & Day	84.47	-2.03	7.20	0.28	13.51
Strong & Night	92.98	-1.74	3.67	0.68	45.46
Strong & Day	89.50	-1.54	4.97	0.50	32.52

CI = 95% confidence interval (mean ± 1.96 SD), MD = mean deviation, RMSD = root mean squared deviation, Sample (%) = % of all data.

Table 1.4 Canopy height agreement between ICESat-2 RH98 and ALS RH99 under different scenarios.

Scenario	% Within 95% CI	MD (m)	RMSD (m)	R^2	Sample (%)
Unfiltered	90.58	-1.43	4.54	0.54	100
Strong beams	91.23	-1.45	4.07	0.61	78.05
Weak beams	88.09	-1.33	5.93	0.36	21.95
Day	88.19	-1.39	5.41	0.43	45.98
Night	92.59	-1.45	3.64	0.67	54.02
Weak & Night	92.11	-1.45	4.33	0.56	8.52
Weak & Day	85.23	-1.26	6.75	0.29	13.44
Strong & Night	92.70	-1.45	3.50	0.69	45.5
Strong & Day	89.40	-1.45	4.75	0.52	32.54

CI = 95% confidence interval (mean ± 1.96 SD), MD = mean deviation, RMSD = root mean squared deviation, Sample (%) = % of all data.

Overall, ICESat-2 RH98 shows better agreement with ALS RH99 than other pairs (ICESat-2 max vs. ALS max, and ICESat-2 max vs. CHM max) regardless of the beam type and time of data acquisition with R^2 of 0.54 (Figure 1.6). The MD between ICESat-2 and ALS canopy height estimate for ICESat-2 RH98 represents an overall under estimation with a value of -1.43 m. This however shows improvement over previous study such as Neuenschwander et al., (2020) who reported an overall bias of 3.05 m in boreal forests. The overall RMSD of 4.54 m also shows variation in agreement between the two products.

Although majority of data points are clustered around one-to-one line, large differences are observed in areas with ICESat-2 max height below 10 m and above 40 m.

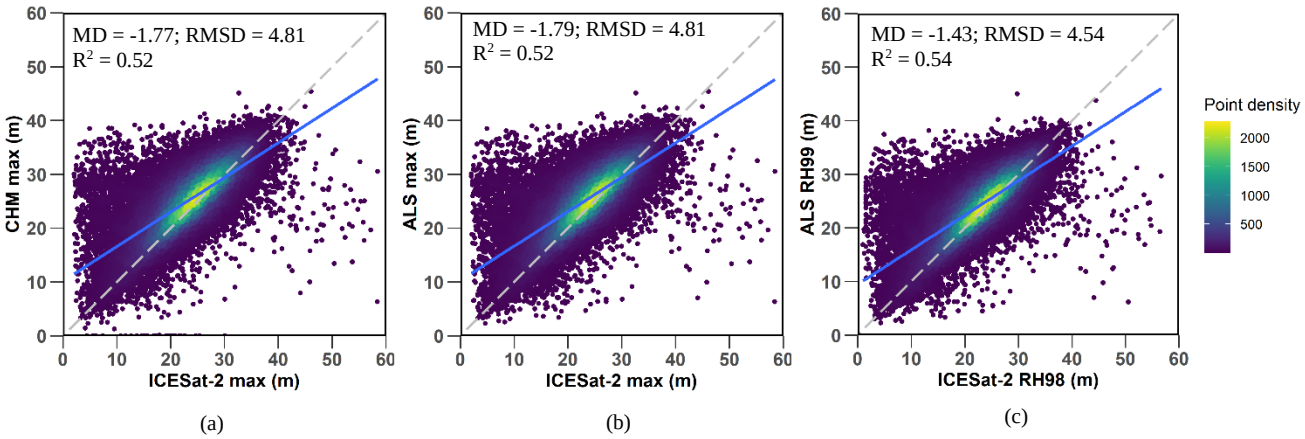

Figure 1.6 Scatterplot for ICESat-2 vs. ALS derived canopy height for (a) ICESat-2 max vs CHM max, (b) ICESat-2 max vs ALS max, and (c) ICESat-2 RH98 vs ALS RH99.

The effect of beam intensity and data acquisition time on the accuracy of the ICESat-2 canopy heights in comparison with CHM max, ALS max, and ALS RH99, ALS RH98 showed lower MD for weak beams (MD -1.33 m) compared to strong beams (MD -1.45 m) across metrics (Figure 1.7). The ICESat-2 RH98 and ALS RH99 were statistically equivalent when the

acceptable region of similarity was up to 1.43 m for weak and 1.48 for strong beam (Appendix A, Figure A.1). This threshold was 1.64 m and 2.35 m for strong and weak beam respectively for CHM max and ALS max.

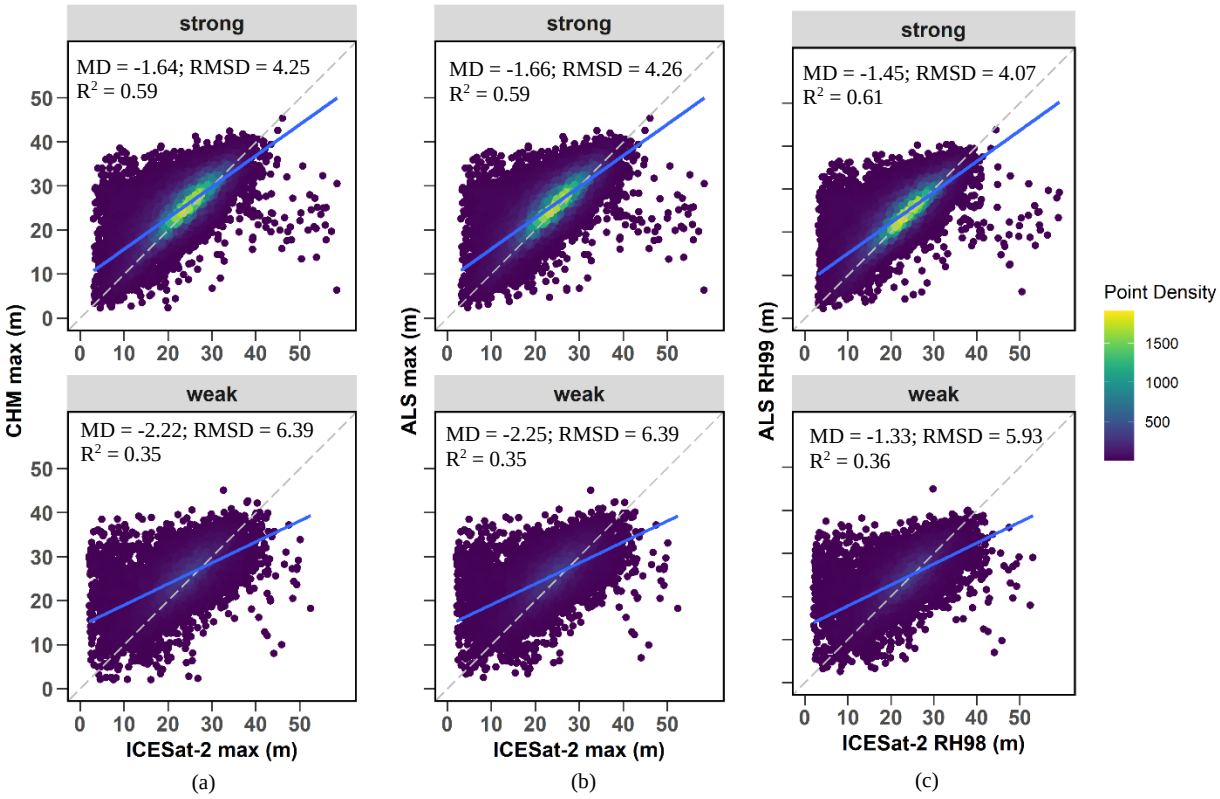

Figure 1.7 Scatterplot of ICESat-2 vs. ALS derived canopy height for strong and weak beam for (a) ICESat-2 max vs CHM max, (b) ICESat-2 max vs ALS max, and (c) ICESat-2 RH98 vs ALS RH99

Night acquisitions showed higher mean deviation (MD -1.45, R^2 0.67) compared to day acquisitions (MD -1.39, R^2 0.43) (Figure 1.8). The equivalence test results for time of acquisition also showed that ICESat-2 and ALS derived canopy height metrics for daytime acquisition were statistically equivalent when the acceptable region of similarity was up to 1.45 m which is lower than that of nighttime acquisition which is 1.49 m (TOST p-value > 0.05) (Appendix A, Figure A.2).

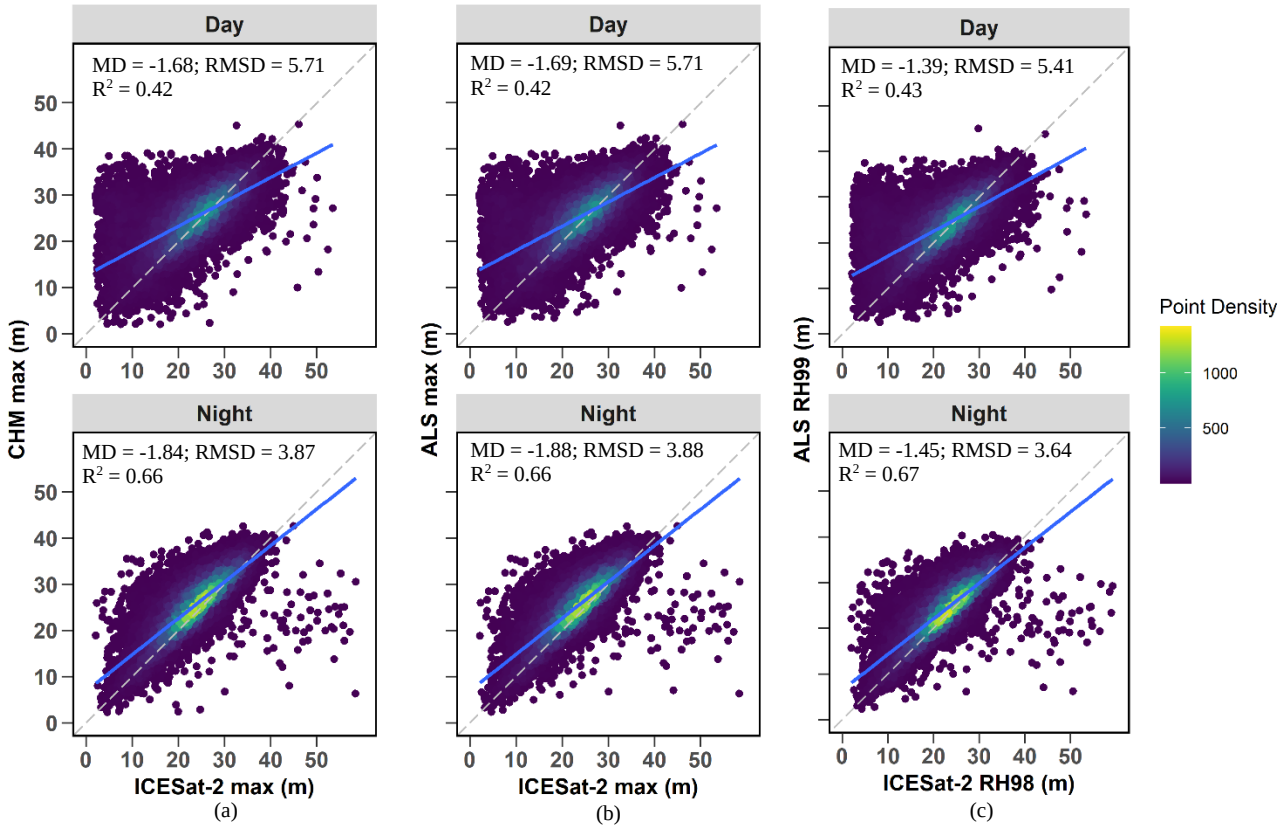

Figure 1.8 Scatterplot of ICESat-2 vs. ALS derived canopy height for day and night for (a) ICESat-2 max vs CHM max, (b) ICESat-2 max vs ALS max, and (c) ICESat-2 RH98 vs ALS RH99.

For ICESat-2, the strong beam data acquired at night have the lowest statistical error in all pairs (Table 1.3 and 1.4). This is because the strong beam has greater penetration and can extract canopy information more accurately, and the data acquired at night are less affected by background noise caused by solar radiation. For ICESat-2 RH98 vs. ALS RH99 pair, in terms of RMSD, strong beams (RMSD 4.07 m) showed better results than weak beams (RMSD 5.93 m). Similarly, night data acquisition showed better performance (RMSD 3.64 m) than daytime acquisition (RMSD 5.41 m). The use of nighttime, strong beam data largely eliminates the outliers, except when the ICESat-2 max are greater than 40 m, yielding RMSD value of 3.5 m, and R^2 value of 0.69 (Figure. 1.9). The MD between the ICESat-2 canopy height estimates and the ALS reference values are also negative, indicating that the canopy height is still

underestimated. Overall, the accuracy of the ICESat-2 canopy height estimates is better when using only strong beam data acquired at night.

Based on the equivalence test, ICESat-2 max, paired with CHM max and ALS max canopy height were statistically equivalent when the acceptable region of similarity was up to 1.77 m and 1.6 m when filtered by strong beam data acquired at night and strong beam data acquired at day respectively (TOST p-value > 0.05) (Appendix A, Figure A.3). For ICESat-2 RH98 and ALS RH99 pair, using strong day and strong night had similar region of similarity i.e., 1.5 m.

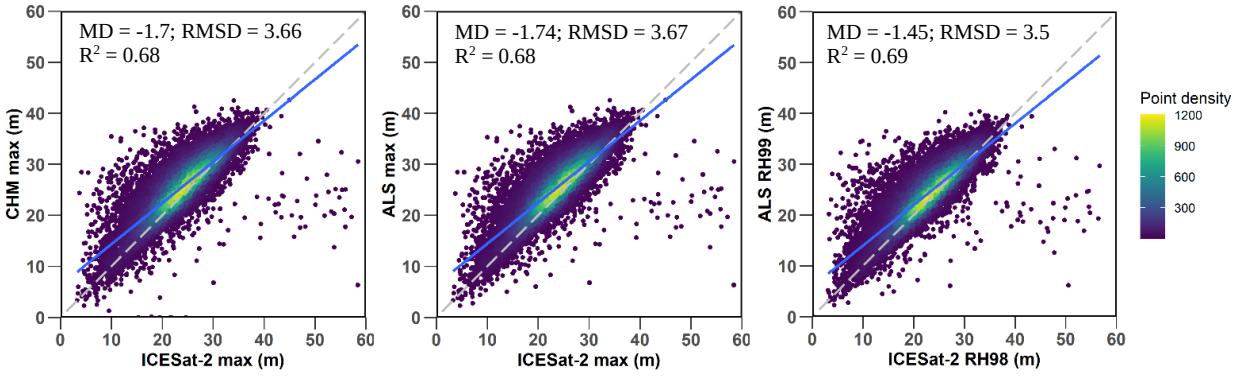

Figure 1.9 Scatterplot of ICESat-2 vs. ALS derived canopy height using only strong beam data acquired at night for (a) ICESat-2 max vs CHM max, (b) ICESat-2 max vs ALS max, and (c) ICESat-2 RH98 vs ALS RH99.

1.4.2.1 Agreement by forest type

Canopy height measured in evergreen forest had the highest agreement whereas woody wetlands had the lowest agreement, with underestimation of 0.75 m and 2.29 m respectively (Table 1.5). The forest type with the lowest correspondence were woody wetlands with less than 90% of ICESat-2 max falling within the 95% confidence interval of CHM max height.

Conversely, evergreen forest had among the highest correspondence between products, with 91% of ICESat-2 heights falling within the 95% confidence interval of CHM max height values. The ICESat-2 RH98 canopy heights underestimated ALS RH99 canopy heights across all forest types with smallest underestimation in evergreen (MD 0.47 m, RMSD 3.63 m) and greatest in woody wetlands and deciduous forest across all pairs (Table 1.6). The evergreen forests had the lowest MD and RMSD in all three pairs of ICESat-2 and ALS. ALS RH99 showed highest MD and RMSD in deciduous forest whereas CHM and ALS max showed highest MD and RMSD in woody wetlands. Woody wetlands had the greatest R^2 (0.55 to 0.58) but also had highest MD and RMSD (MD = 2.33 m and RMSD 5.37 m for ALS max).

Table 1.5 Correspondence between ICESat-2 max, CHM max and ALS max canopy height products by forest type in terms of percentages of ICESat-2 height falling within different ranges of ALS predictions.

Forest types	% Within 95% CI	MD (m)	RMSD (m)	R^2	Sample (%)
CHM max					
Deciduous	90.34	-2.20	5.16	0.52	32.39
Evergreen	91.53	-0.75	3.78	0.54	24.05
Mixed	90.15	-1.61	4.53	0.46	18.04
Woody Wetlands	88.45	-2.29	5.36	0.55	25.52
ALS max					
Deciduous	90.27	-2.21	5.17	0.52	32.38
Evergreen	91.51	-0.76	3.78	0.54	24.05
Mixed	89.88	-1.64	4.53	0.46	18.02
Woody Wetlands	88.33	-2.33	5.37	0.55	25.55

CI = 95% confidence interval (mean ± 1.96 SD), MD = mean deviation, RMSD = root mean squared deviation, Sample (%) = % of all data.

Table 1.6 Correspondence between ICESat-2 RH98 and ALS RH99 canopy height products by forest type in terms of percentages of ICESat-2 height falling within different ranges of ALS predictions.

Forest types	% Within 95% CI	MD (m)	RMSD (m)	R^2	Sample (%)
Deciduous	90.12	-1.92	4.95	0.53	32.41
Evergreen	91.63	-0.47	3.63	0.55	24.07
Mixed	90.59	-1.36	4.35	0.48	18.03
Woody wetlands	89.17	-1.75	4.89	0.58	25.49

CI = 95% confidence interval (mean ± 1.96 SD), MD = mean deviation, RMSD = root mean squared deviation, Sample (%) = % of all data.

In general, there is more variation in the ICESat-2 max distributions with a slightly greater spread of values relative to the distribution of the ALS (Figure 1.10).

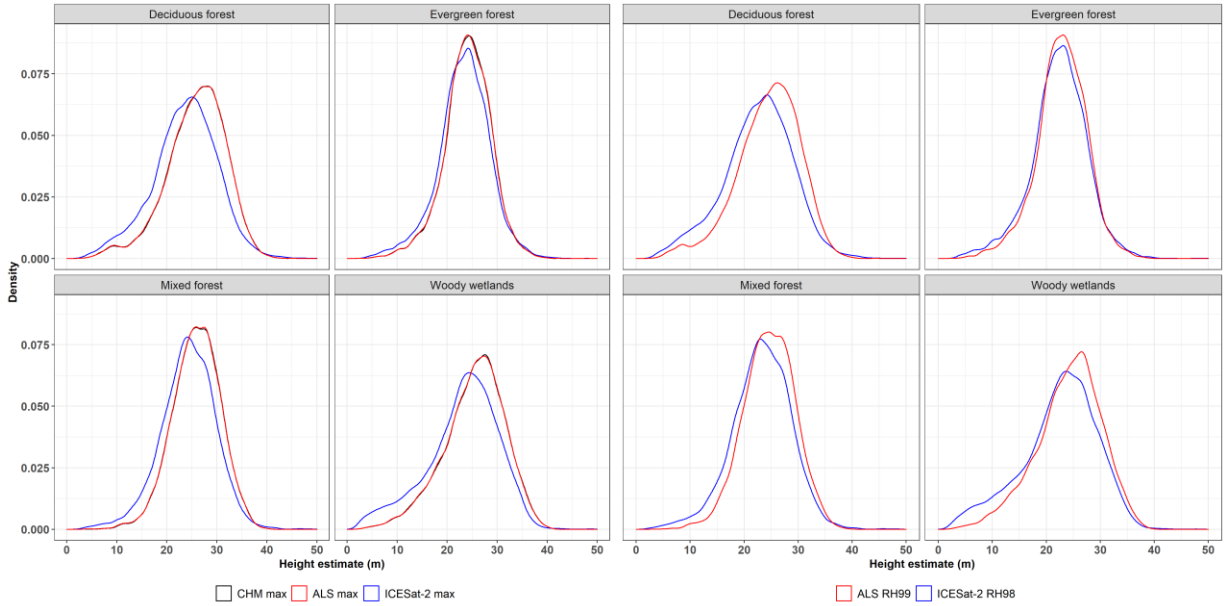

(a) (b)

Figure 1.10 Density plot showing the distribution of ICESat-2 and ALS canopy height metrics by forest types for (a) ICESat-2 max, CHM max, and ALS max (b) ICESat-2 RH98 and ALS RH99. CHM max and ALS max have similar distribution and are seen overlapping.

Further analysis by the ALS derived height class indicated that for all height class except for height class 0-10 m, the ICESat-2 median canopy height is lower than the corresponding ALS value (Figure 1.11 and 1.12). Additionally, for all forest types in 11-20 m height class, the

median values of ALS and ICESat-2 are similar particularly in evergreen forest. It indicates that the ICESat-2 overestimates the tree heights of 0-10 m height class and underestimates the higher height classes.

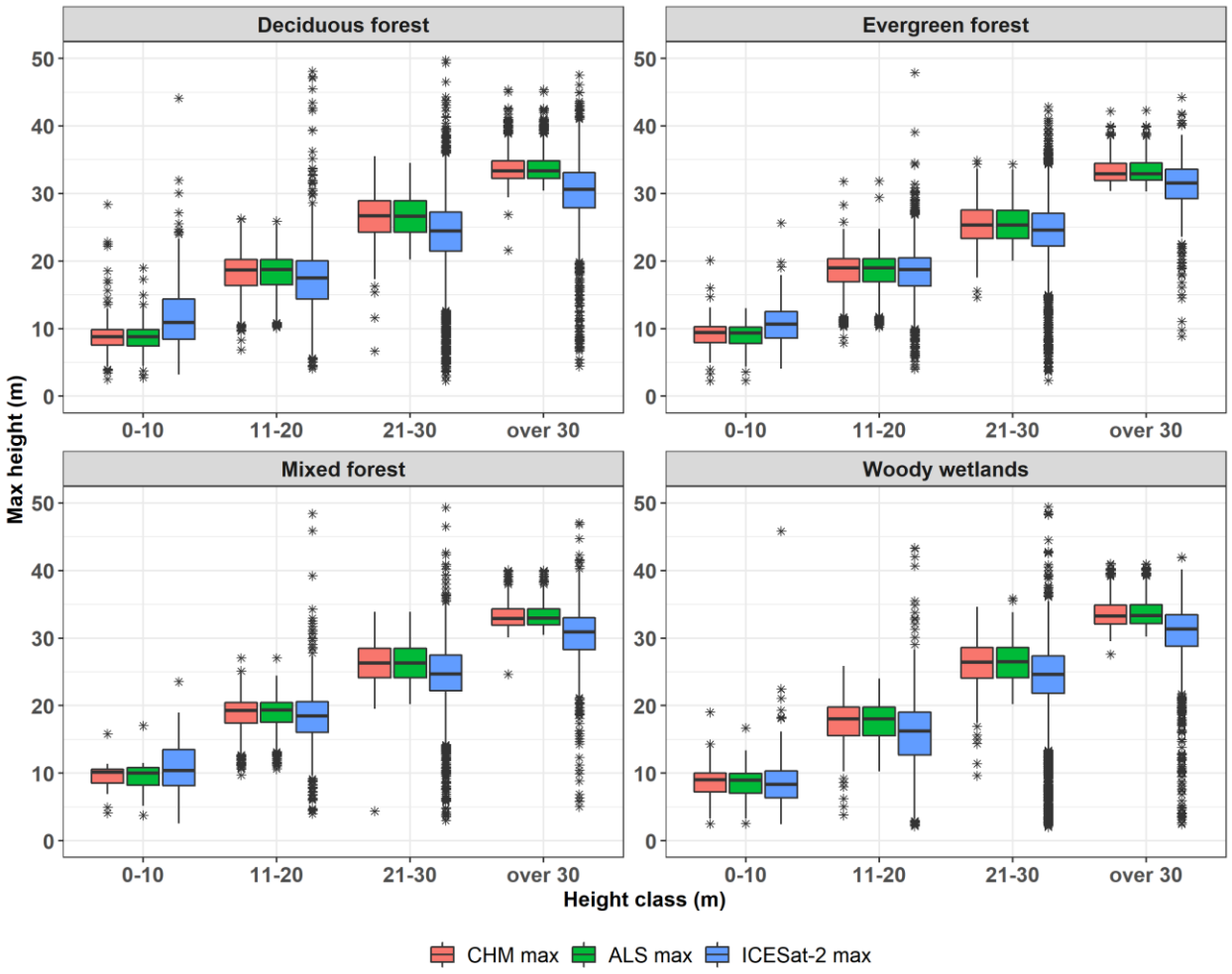

Figure 1.11 Distribution of ICESat-2 max, CHM max and ALS max canopy heights by forest type and 10 m height classes derived from ALS. Boxplots represent median, interquartile range, and extreme values.

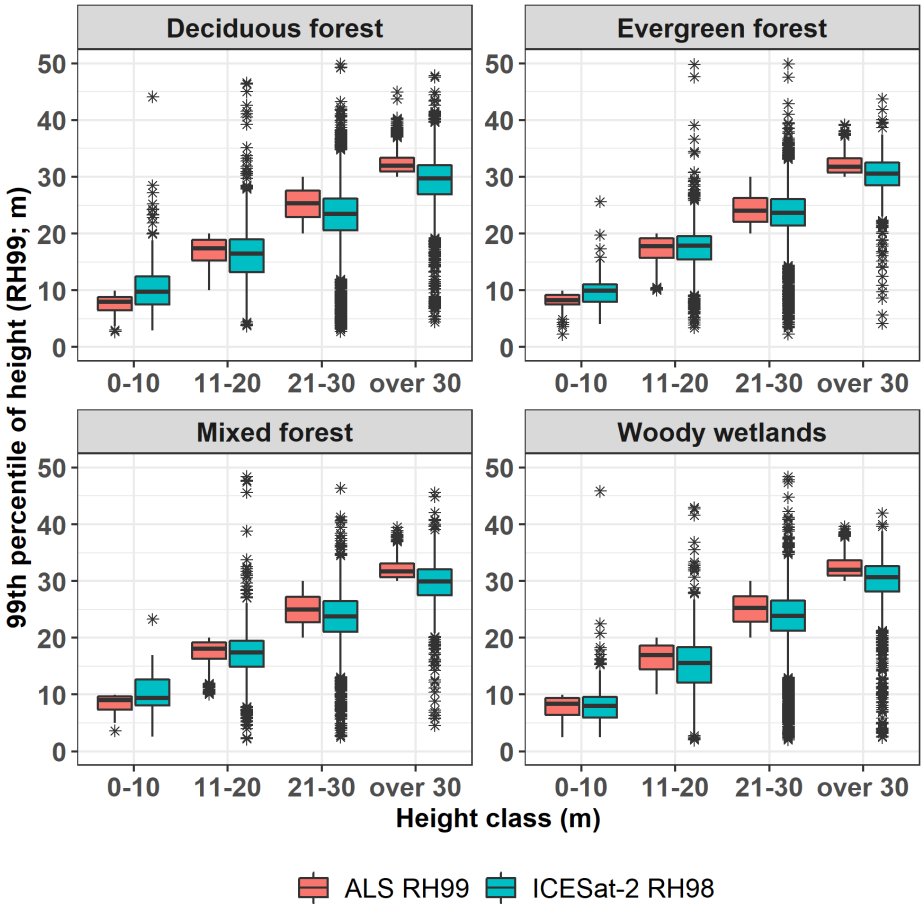

Figure 1.12 Distribution of ICESat-2 RH98 and ALS RH99 canopy heights by forest type and 10 m height classes derived from ALS. Boxplots represent median, interquartile range, and extreme values.

The equivalence test showed that the ICESat-2, and CHM max and ALS max derived canopy height metrics were statistically equivalent with similar acceptable region of similarity (TOST p-value > 0.05) in different forest types (Figure 1.13). Evergreen forest had the lowest value of acceptable threshold ranging from 0.5 m in ALS RH99 pair to 0.8 m in CHM and ALS max. In ALS RH99 pair, deciduous forest showed the lowest threshold value of 2 m whereas CHM and ALS max showed greatest threshold value of 2.4 m.

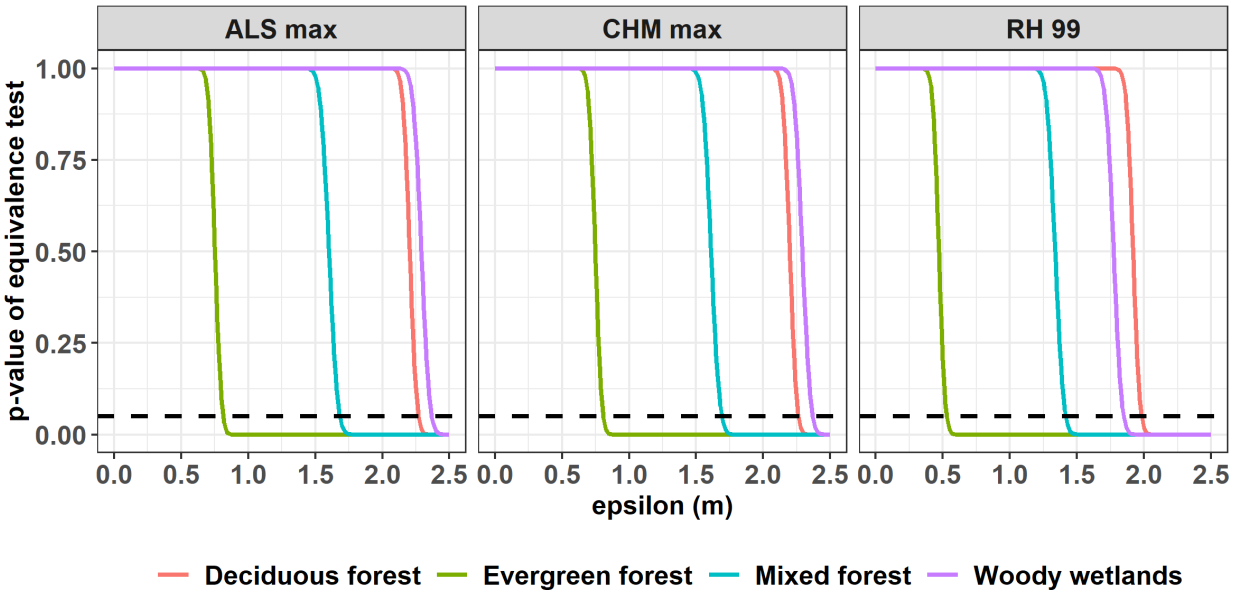

Figure 1.13 Equivalence test showing p-value and epsilon for ICESat-2 and ALS derived canopy height metrics for different forest types. Dashed line represents 0.05 p-value.

1.4.2.2 Agreement by physiographic regions

Wide variation in agreement was observed when ICESat-2 data were analyzed by the physiographic regions (Table 1.7 and 1.8). The physiographic region with the lowest correspondence was the alluvial plain with less than 90% of ICESat-2 falling within the 95% confidence interval of ALS canopy height. Conversely, the black prairie had the highest correspondence between products, with 93% of ICESat-2 canopy heights falling within the 95% confidence interval of ALS canopy height values. The ICESat-2 canopy heights underestimated ALS canopy heights across all physiographic regions with greatest underestimate in the alluvial plain (MD -1.76 m, RMSD 4.98 m for ICESat-2 RH98 vs. ALS RH99 pair) and lowest in the black prairie (MD -0.86 m, RMSD 3.78 m). Based on R^2, best agreement was observed in the alluvial plain (R^2 0.59) despite having greatest MD and RMSD.

Table 1.7 Correspondence between ICESat-2 max, CHM max, and ALS max canopy height products by physiographic regions, in terms of the percentage of ICESat-2 heights falling within different ranges of ALS predictions.

Physiographic regions	% Within 95% CI	MD (m)	RMSD (m)	R^2	Sample (%)
CHM max					
Black Prairie	93.00	-1.00	4.16	0.43	0.97
Pontotoc Ridge	90.76	-1.95	5.95	0.34	6.22
Flatwoods	90.13	-1.98	4.62	0.56	2.84
North central hills	90.68	-1.63	4.64	0.53	68.65
Loess hill	90.28	-2.03	4.68	0.49	11.7
Alluvial plain	88.93	-2.32	5.36	0.59	9.62
ALS max					
Black Prairie	92.54	-1.01	4.13	0.44	0.97
Pontotoc Ridge	90.73	-1.96	5.95	0.34	6.22
Flatwoods	89.87	-1.98	4.65	0.56	2.84
North central hills	90.59	-1.65	4.65	0.53	68.65
Loess hill	90.19	-2.04	4.68	0.49	11.67
Alluvial plain	88.83	-2.35	5.39	0.59	9.65

CI = 95% confidence interval (mean ± 1.96 SD), MD = mean deviation, RMSD = root mean squared deviation, Sample (%) = % of all data.

Table 1.8 Correspondence between ICESat-2 RH98 and ALS RH99 canopy height products by physiographic regions, in terms of the percentage of ICESat-2 heights falling within different ranges of ALS predictions.

Physiographic regions	% Within 95% CI	MD (m)	RMSD (m)	R^2	Sample (%)
Black Prairie	92.54	-0.86	3.78	0.51	0.97
Pontotoc Ridge	90.46	-1.56	5.73	0.35	6.23
Flatwoods	90.3	-1.61	4.38	0.57	2.84
North central hills	90.72	-1.33	4.38	0.55	68.63
Loess hill	89.86	-1.68	4.48	0.5	11.68
Alluvial plain	89.95	-1.76	4.98	0.61	9.65

CI = 95% confidence interval (mean ± 1.96 SD), MD = mean deviation, RMSD = root mean squared deviation, Sample (%) = % of all data.

In general, there is more variation in the ICESat-2 distributions with skewness at lower heights relative to the ALS distribution (Figure 1.14 and 1.15).

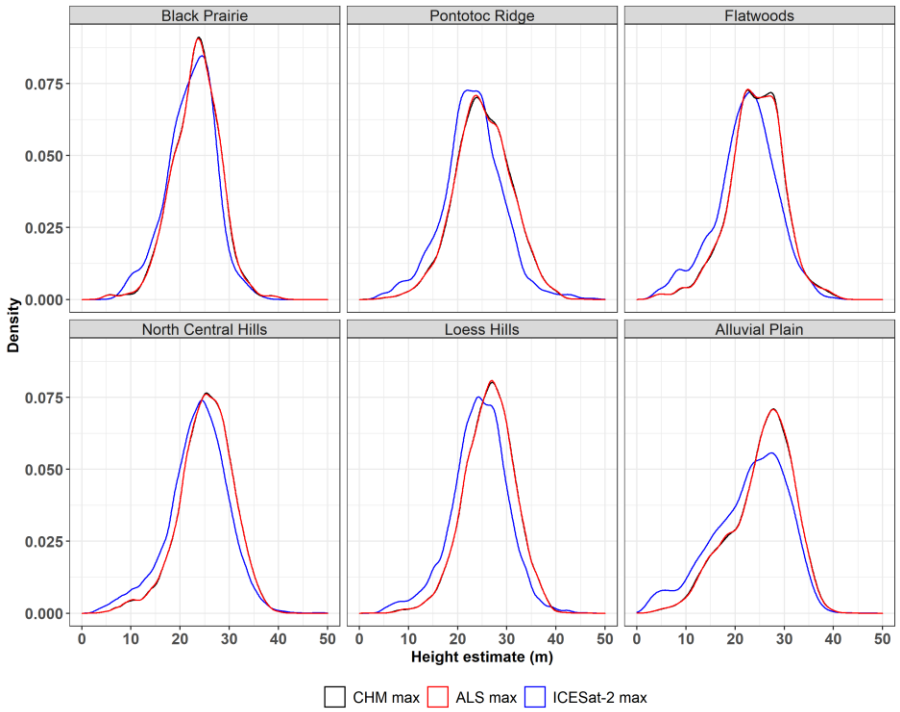

Figure 1.14 Density plot showing the distribution of ICESat-2 and ALS canopy height metrics by physiographic regions for (a) ICESat-2 max, CHM max, and ALS max (b) ICESat-2 RH98 and ALS RH99. CHM max and ALS max have similar distribution and are seen overlapping.

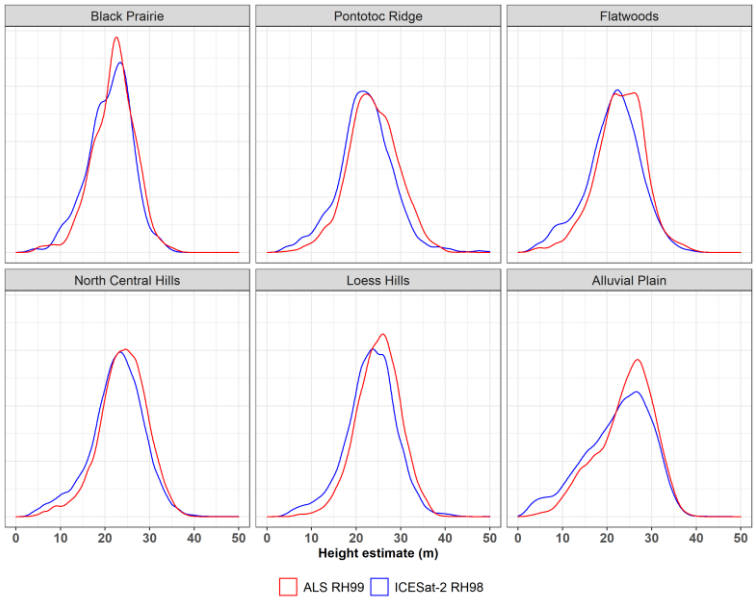

Figure 1.15 Density plots showing the distribution of ICESat-2 RH98 and ALS RH99 canopy height by physiographic regions.

Further analysis by the ALS derived height class indicated that for all height class except for height class 0-10 m, the ICESat-2 median is lower than the corresponding ALS value (Figure 1.16 - 1.17). As indicated in the figure, ICESat-2 overestimated for 0-10 m height class for all physiographic regions except for the flatwoods and alluvial plain. For height class 11-20 m, the ICESat-2 overestimated only in the black prairie whereas it underestimated for other regions. For height class >20 m ICESat-2 underestimated canopy height.

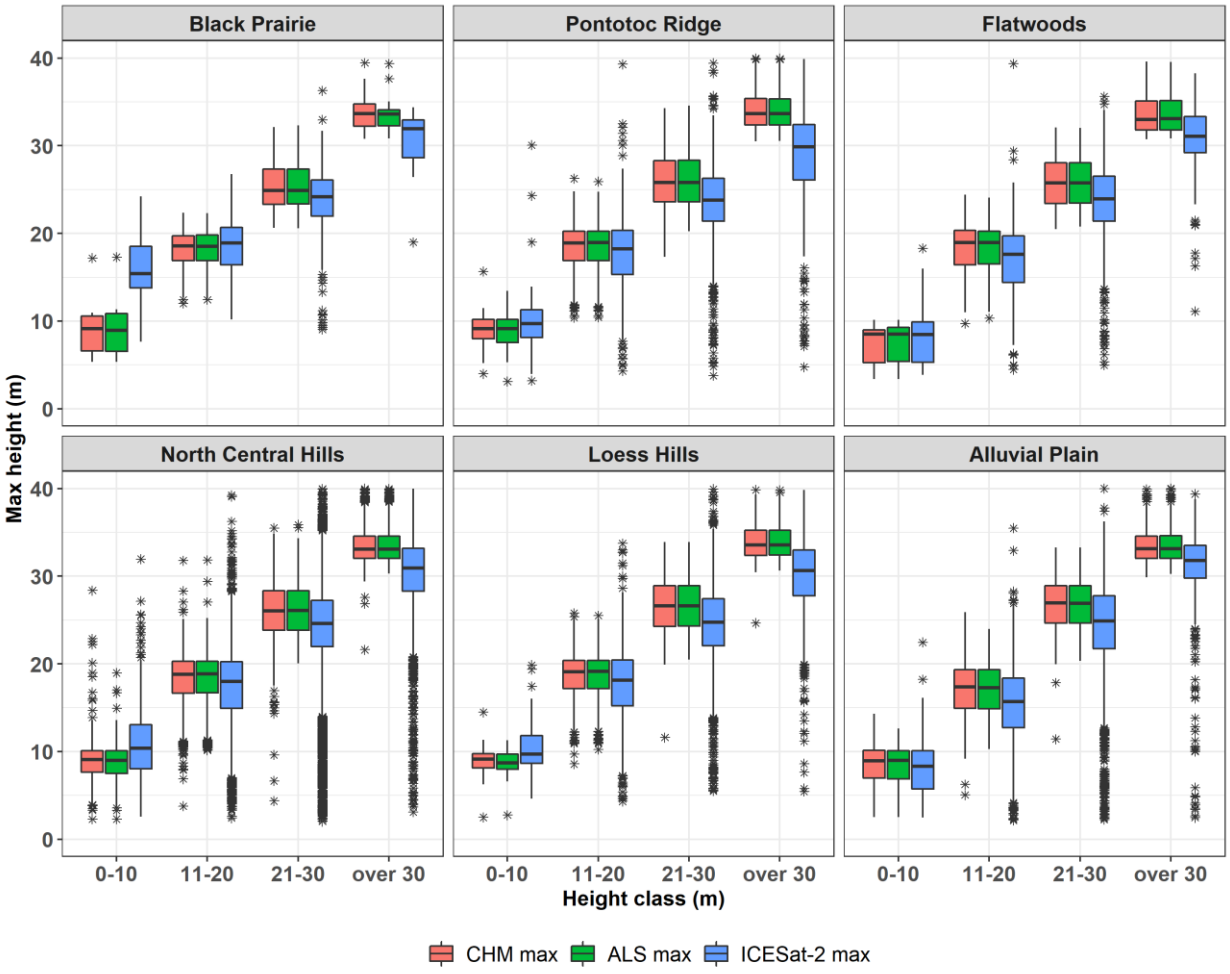

Figure 1.16 Distribution of ICESat-2 max, CHM max, and ALS max canopy heights by physiographic regions and 10 m height classes derived from ALS. Boxplots represent median, interquartile range, and extreme values.

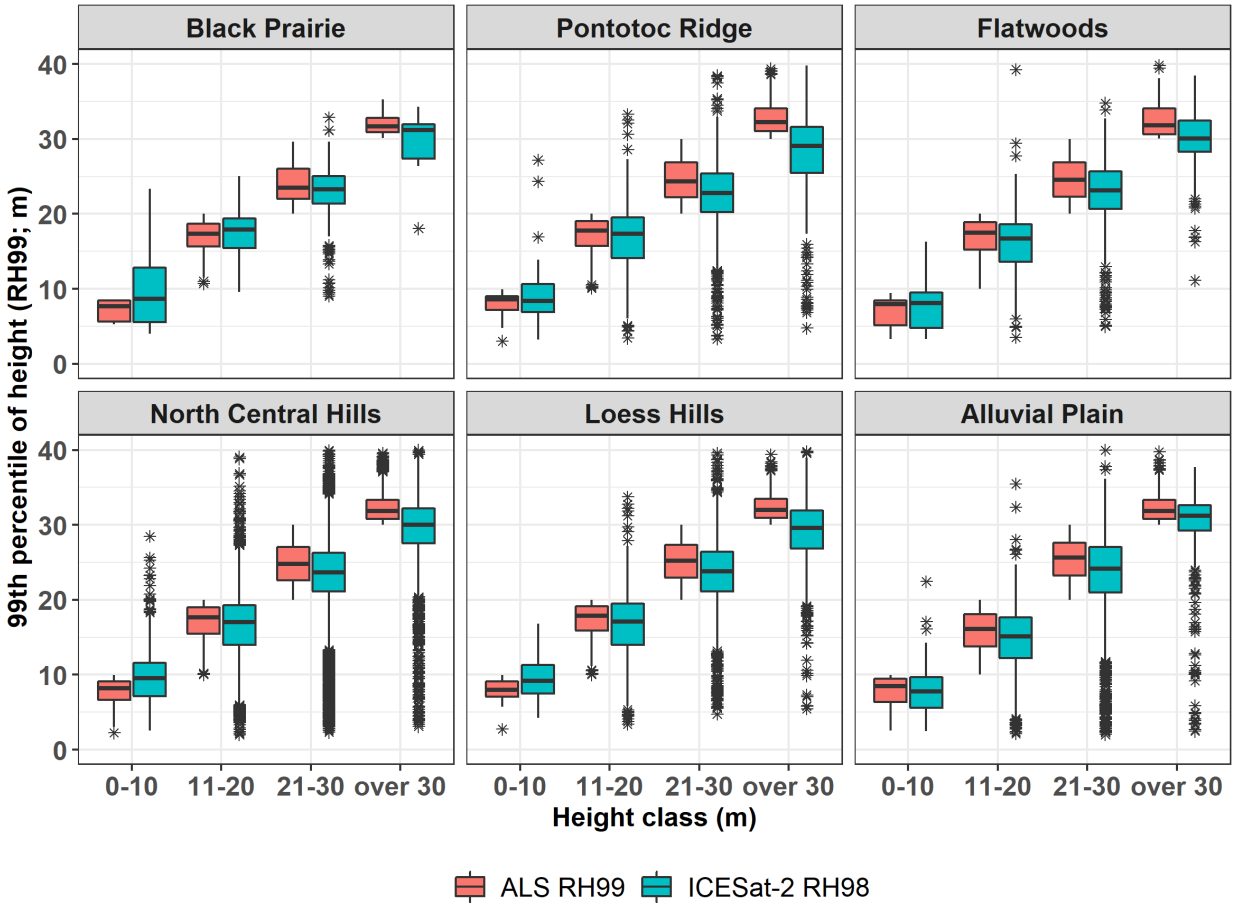

Figure 1.17 Distribution of ICESat-2 RH98 and ALS RH99 canopy heights by physiographic regions and 10 m height classes derived from ALS. Boxplots represent median, interquartile range, and extreme values.

With the equivalence test, we found that the canopy height estimation from CHM max and ALS max with the ICESat-2 max were similar in different physiographic regions. All three pairs were statistically equivalent with the lowest threshold value in the black prairie (TOST p-value > 0.05) (Figure 1.18). In the case of ICESat-2 RH98 vs. ALS RH99 pair, the canopy heights were statistically equivalent when the acceptable region of similarity was up to 2 m, particularly in the black prairie physiographic zone with lowest threshold value of 1.15 m. However, the greatest threshold value was observed for the alluvial plain in all cases.

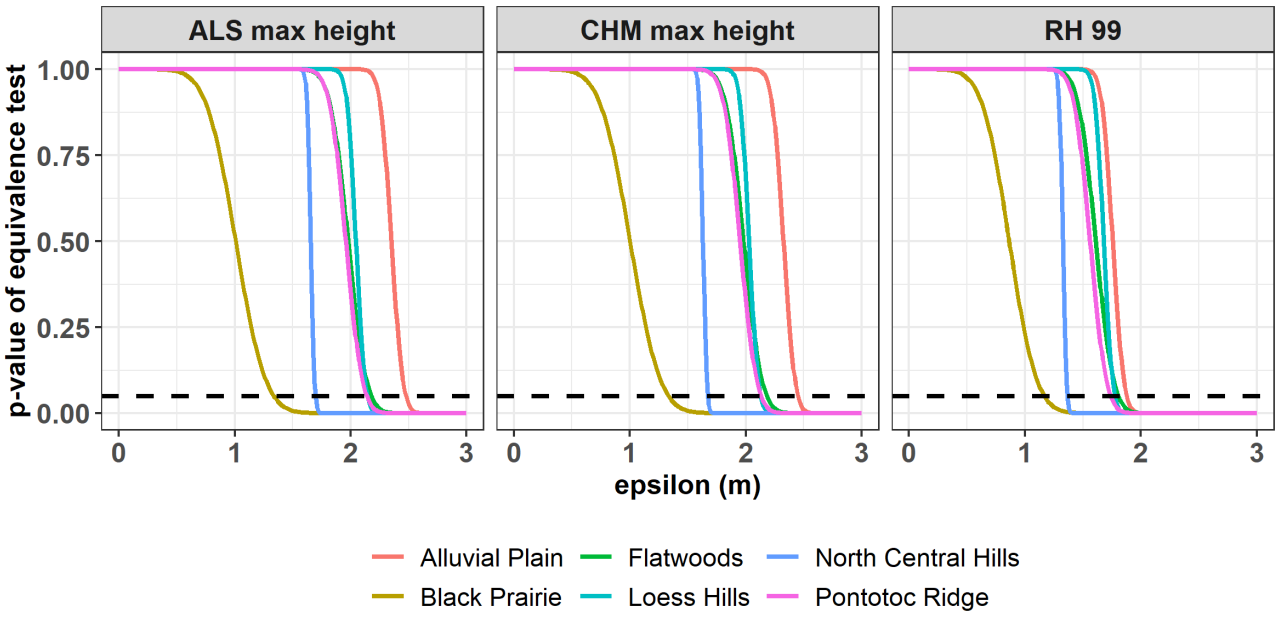

Figure 1.18 Equivalence test showing p-value and epsilon for ICESat-2 and ALS derived canopy height metrics for different physiographic regions. Dashed line represents 0.05 p-value.

1.4.2.3 Agreement by percent canopy cover

ICESat-2 ATL08 data product does not provide the estimates of canopy cover (CC) therefore we derived canopy cover using the ALS data from LiDAR360 software. The absolute MD between ALS and ICESat-2 were assessed in relation to canopy cover (Figure 1.19 - 1.21). The figures show maximum absolute MD in canopy height for lower canopy cover percentages and a gradual decrease in the absolute MD as the canopy cover increases. However, when the canopy cover was about 75%, the absolute MD slightly increased which again decreased at 80%. The best agreement between ICESat-2 and ALS was observed for canopy cover greater than 65%.

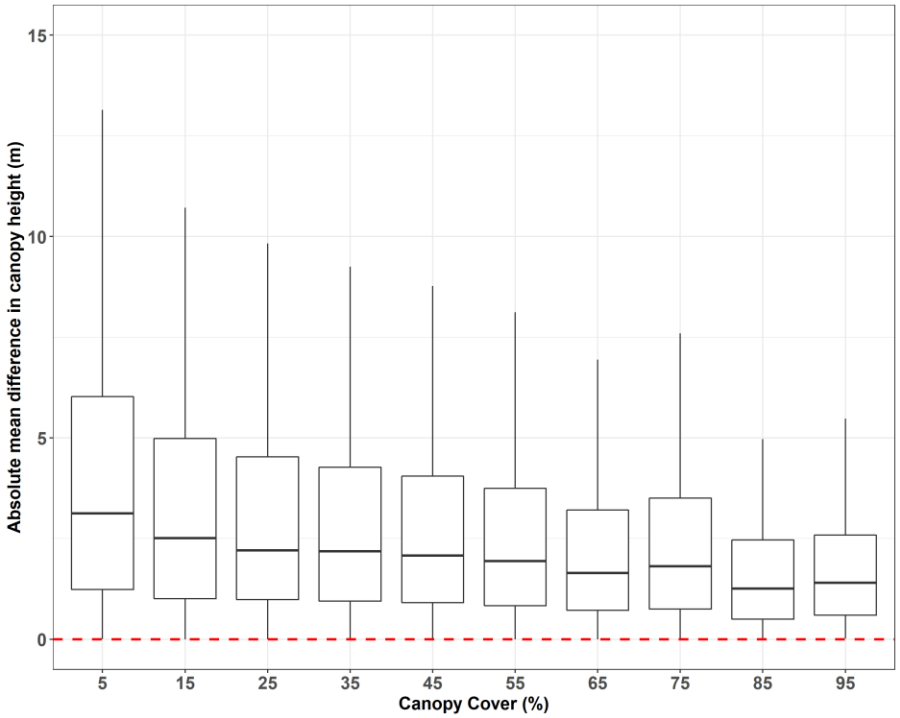

Figure 1.19 Absolute mean difference between ICESat-2 max and CHM max by canopy cover.

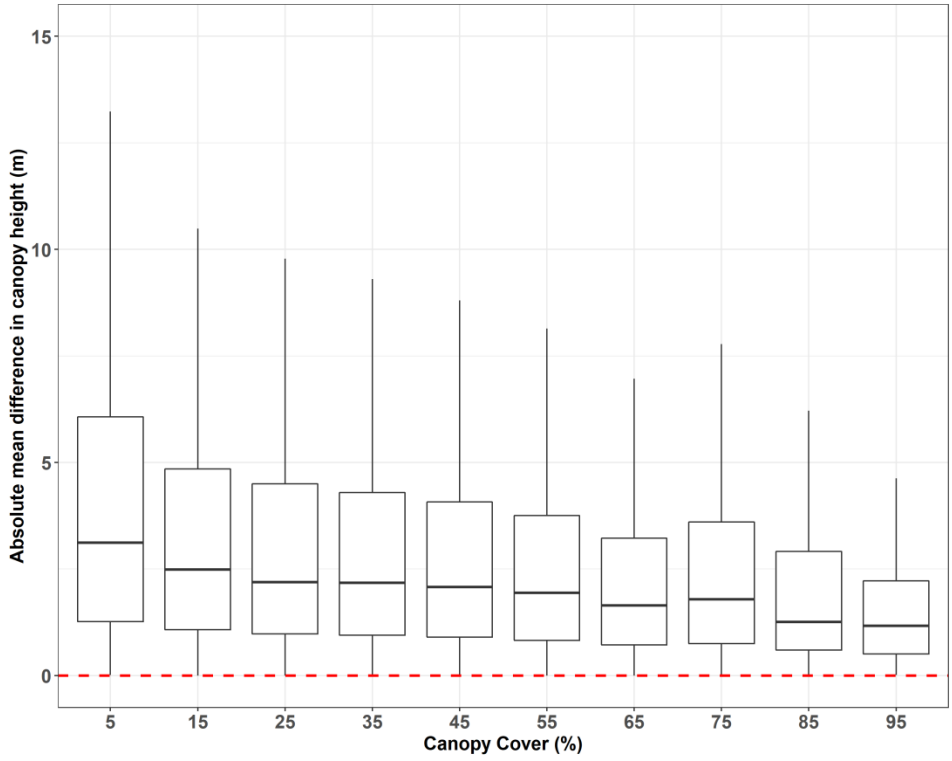

Figure 1.20 Absolute mean difference between ICESat-2 max and ALS max by canopy cover.

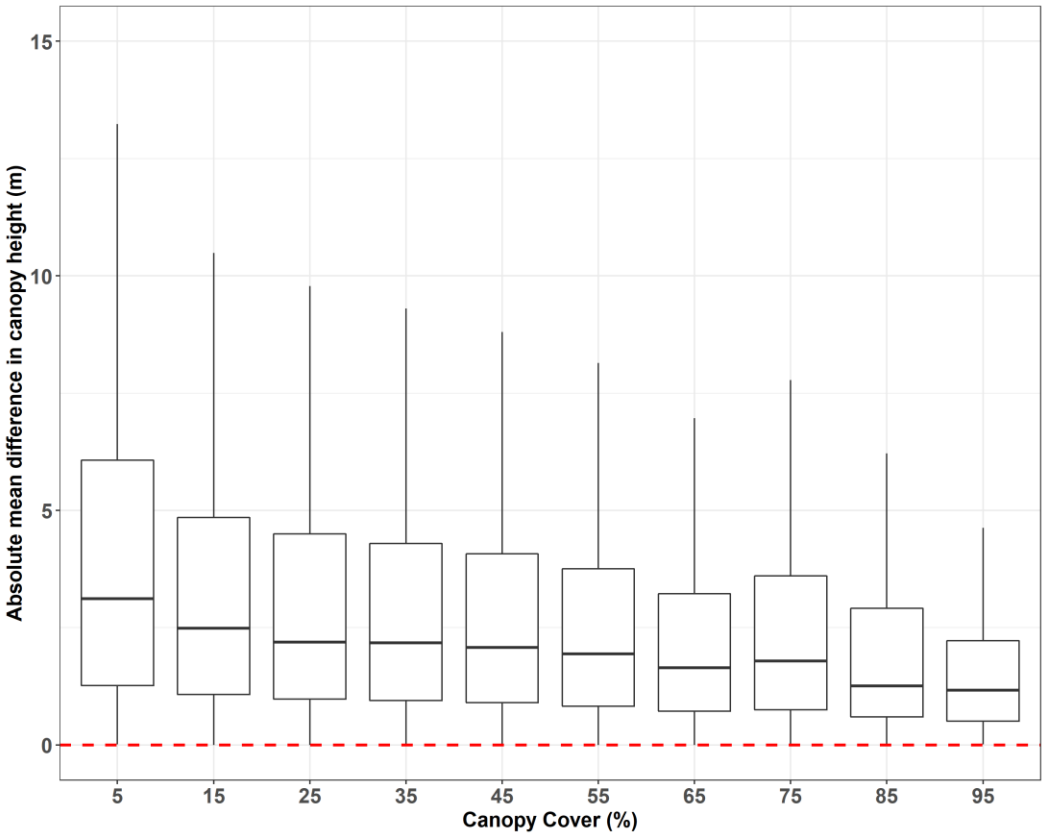

Figure 1.21 Absolute mean difference between ICESat-2 RH98 and ALS RH99 by canopy cover.

The equivalence test by percent canopy cover (Appendix A, Figure A.5 – A.7) shows that ICESat-2 RH98 and ALS RH99 are statistically equivalent with the lowest threshold value of 0.9 m for 65% CC followed by 85% and 95% CC. Similarly, ALS max pair also shows the lowest threshold value of 1.4 m for 65% CC whereas CHM max shows 95% CC with the lowest threshold value of 1.2 m followed by 65% CC. On the other hand, CHM and ALS max shows that the greatest threshold value for 15% CC.

1.4.2.4 Agreement by disturbance frequency and years since disturbance

In 0-10 m height class, the ICESat-2 overestimated the canopy height irrespective of number of disturbances (Figure 1.22). In 11-20 m height class, for area disturbed more than

twice, CHM max, ALS max, and ICESat-2 max canopy heights are similar. Also, greater difference among ICESat-2 and ALS were observed with increasing height classes. Similar results were also observed for ICESat-2 RH98 vs. ALS RH99 (Figure 1.23).

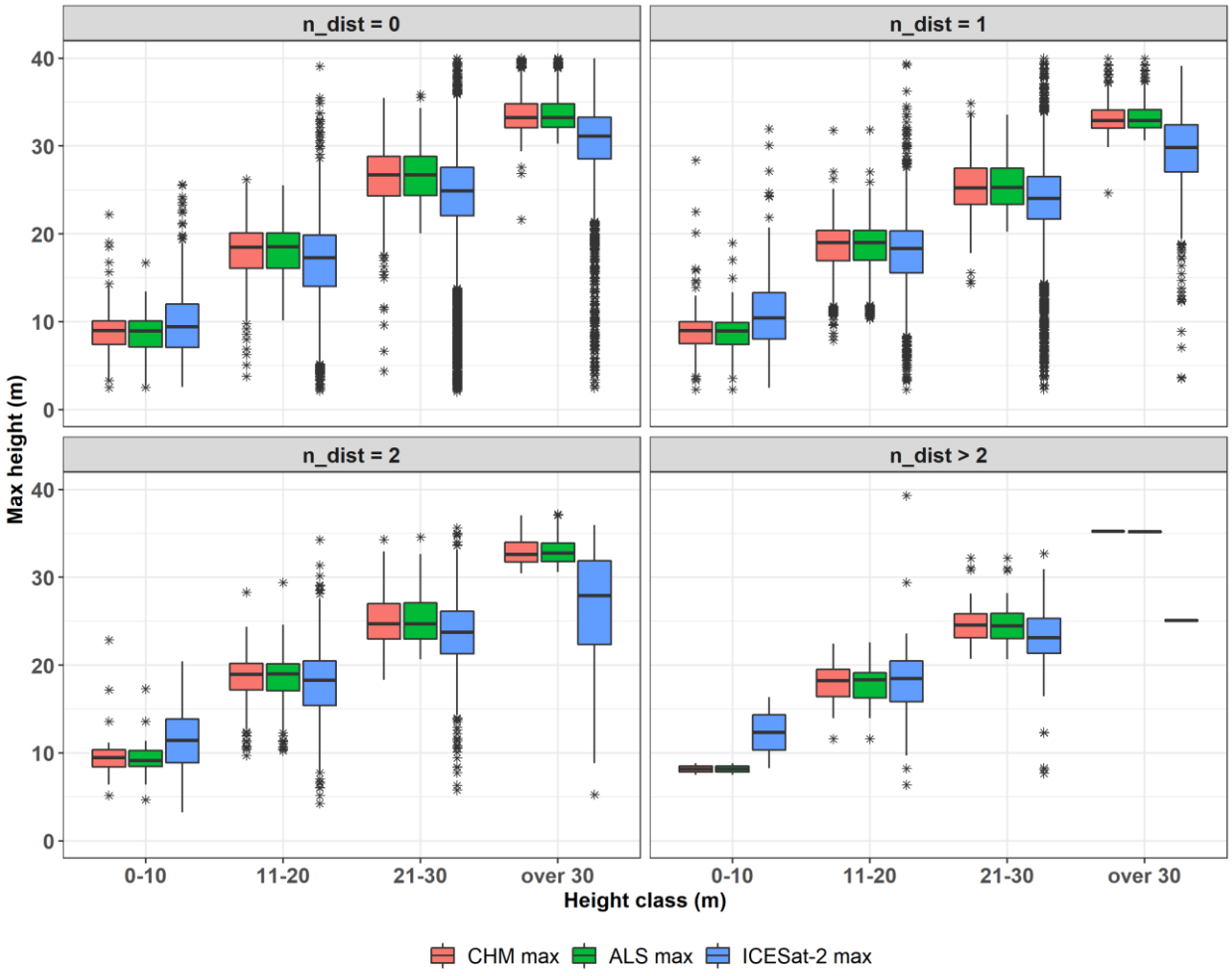

Figure 1.22 Distribution of ICESat-2 max, CHM max, and ALS max canopy heights by frequency of disturbance and 10 m height classes derived from ALS. Boxplots represent median, interquartile range, and extreme values.

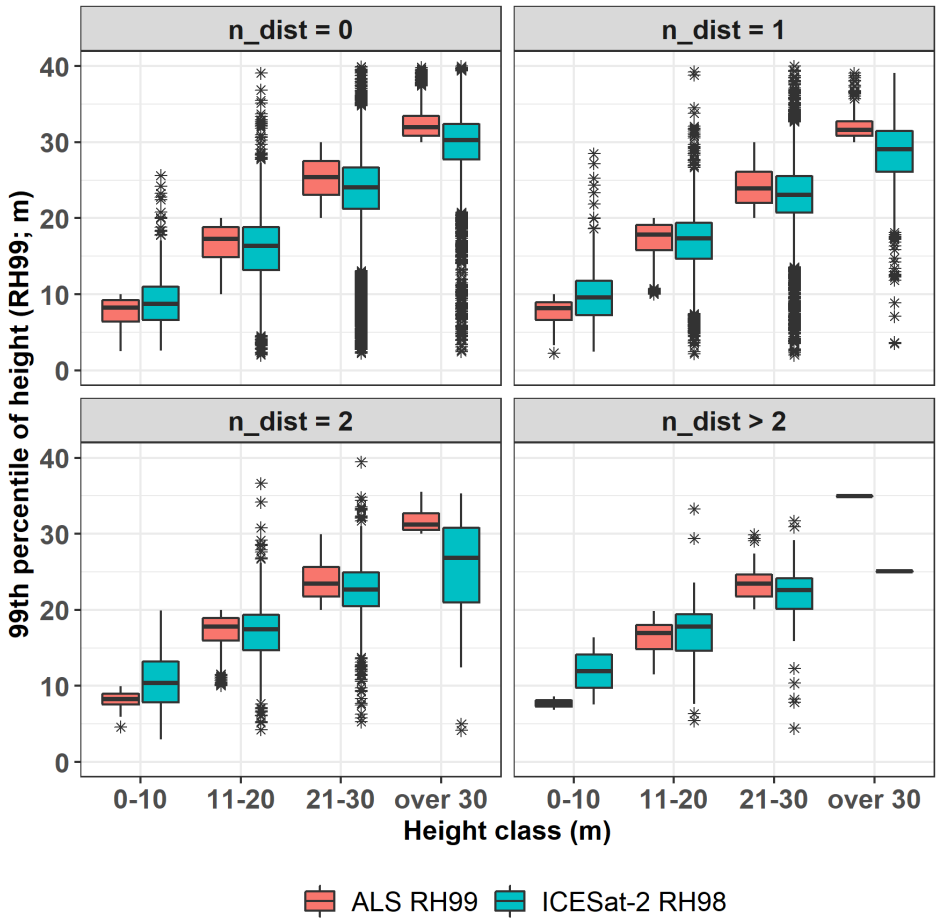

Figure 1.23 Distribution of ICESat-2 RH98 and ALS RH99 canopy heights by frequency of disturbance and 10 m height classes derived from ALS. Boxplots represent median, interquartile range, and extreme values.

The equivalence test (Appendix A, Figure A.8 – A.10) for all three pairs showed that ICESat-2 was statistically equivalent to ALS derived canopy height with a similar threshold value of 1.38 m. This threshold ranged from 1.1 m to 1.4 m for sites disturbed once and 1.6 m to 2.1 m for undisturbed sites.

In the case of time since disturbance, ICESat-2 underestimated the canopy height regardless of time since disturbance (Figure 1.24). In general, both height products captured patterns of height increase since disturbance. For a longer time following disturbance, both

ICESat-2 and ALS heights followed the expected increase in canopy height due to assumed growth.

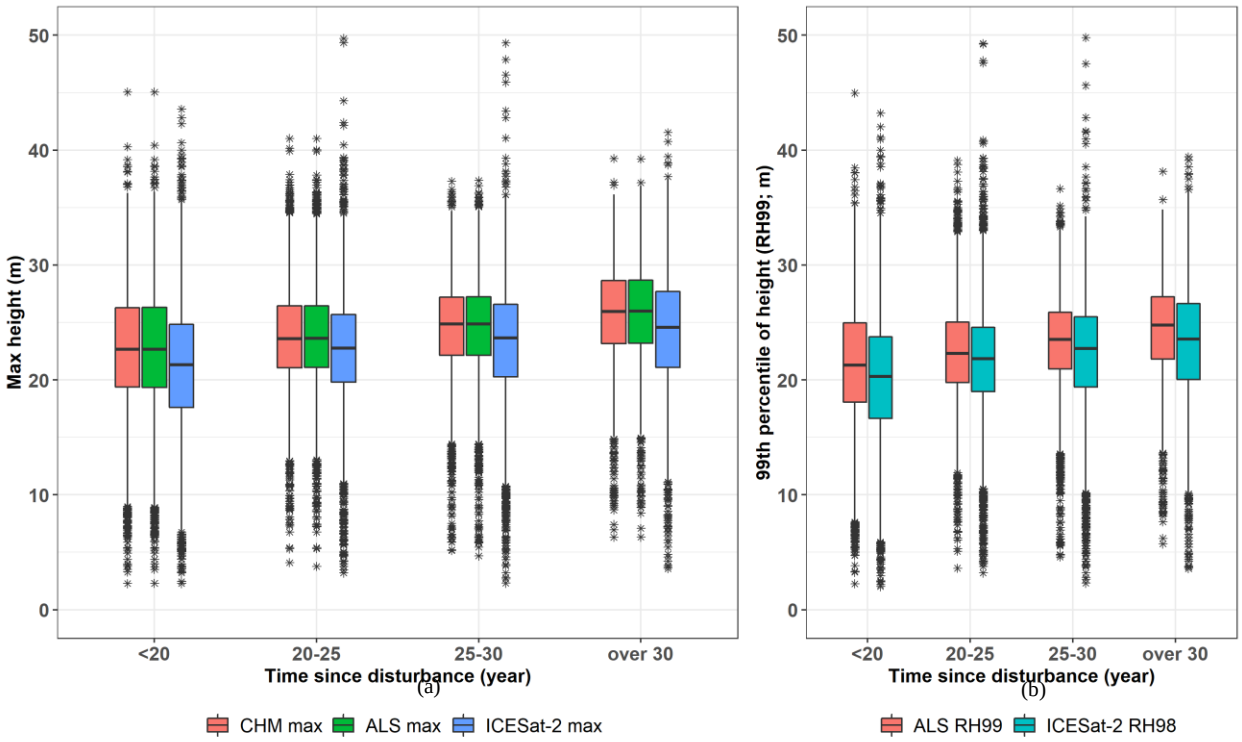

Figure 1.24 Distribution of ICESat-2 and ALS derived canopy height by year since disturbance for (a) ICESat-2 max, CHM max, and ALS max (b) ICESat-2 RH98 and ALS RH99. Boxplots represent median, interquartile range, and extreme values.

The equivalence test (Appendix A, Figure A.11 – A.13) results show that all three pairs have similar results with forests 20-25 years since disturbance having the lowest threshold value of similarity (0.6 m) in the ALS RH99 pair. This threshold was 1.2 m in ALS max whereas the largest threshold value was found for forests disturbed <20 years ago ranging from 1.6 m to 1.95 m.

1.5 Discussion

This study evaluated the degree of agreement between the maximum and RH98/RH99 canopy heights measured from two different lidar systems- ICESat-2 and ALS. This study also evaluated the height agreement with respect to different sensor parameters such as beam type, time of acquisition and other factors like forest types, physiographic regions, canopy cover, disturbance frequency and year since disturbance.

ICESat-2 RH98 and ALS RH99 had the best agreement among the height pairs compared- R^2 0.54 and ME -1.43 m. Popescu et al., (2018) in their study to validate simulated ICESat-2 canopy height based on photon level comparisons, reported RMSD of 3.2 m which is lower than the results in this study (RMSD 4.76 m for ICESat-2 RH98). This may be because this study used discrete return lidar data, which may have higher variations than using photon counting lidar.

Canopy heights from ICESat-2 ATL08 data product underestimated the canopy heights when compared with ALS for ICESat-2 RH98 and ALS RH99 pair (MD = -1.43 m). Several factors can contribute to the underestimation of the canopy height by spaceborne lidar. For ICESat-2, the small probability of detecting the treetop may lead to an underestimation of canopy height when the number of photons within the segment is low. This finding concurs with the recent study of Neuenschwander et al., (2020) who reported a MD of -3.05 m for canopy heights derived from ICESat-2 and ALS. Mulverhill et al., (2022) in comparing canopy height over different forested ecosystems of Canada found MD of -0.55 m and RMSD of 4.87 m. This poorer performance of ICESat-2 canopy heights could be due to various factors such as sub-optimal sampling by the ICESat-2 sensor, and reduced performance of ICESat-2 ATL08 filtering algorithms in classifying off-terrain point (Malambo & Popescu, 2021). ICESat-2 produces a

high-frequency micro-pulse laser producing height values every 0.7 m on the surface, however it records only 0 - 4 photons from an emitted laser pulse over vegetation surfaces (Neuenschwander & Pitts, 2019) whereas the ALS data used in this study has average point density of 2 pts/m^2. Therefore, there is a chance of characterizing forest canopies inadequately in some areas. Moreover, the lower sampling rate increases the chance of missing the canopy tops that leads to underestimation of relatively higher-resolution ALS estimates. With lower sampling rates, noise filtering algorithms and classification of photon used in ICESat-2 product generation performs poorly and thus, may lead to underestimation of canopy heights (Malambo & Popescu, 2021). There is an increasing agreement for the ICESat-2 canopy metrics with increasing height percentiles (Table 1.2). Higher agreement is observed for higher height percentiles (RH98) than RH90 and RH95 due to better characterization of the canopy top (Figure 1.19 - 1.21).

This study also evaluated the agreement of canopy heights derived from ICESat-2 and ALS using the beam combinations (weak and strong) in relation to data acquisition time (day and night). There was a higher agreement in canopy heights measured with strong beam at night than any other combination of beam type and time of acquisition. Weak beam data acquired at night had lower RMSD (RMSD = 4.33 m) than strong beam data acquired during the day (RMSD = 4.75 m) for the RH98 pair which aligns with study by Liu et al., (2021) who found RMSD of 5.07 m and 7.99 m for weak and night, and weak and day respectively. One of the reasons for higher accuracy of night data could be the absence of solar background noise at night and higher number of points from strong beams facilitating better estimation of canopy height (Malambo & Popescu, 2021).

Another important factor impacting the canopy height was the canopy structure within the study area. Increasing canopy cover has a positive impact on ICESat-2 agreement which

explains better performance in evergreen forest (average canopy cover of 55%) whereas woody wetlands (average canopy cover of 47%) and deciduous forests (average canopy cover of 44%) had lowest agreement, which is in line with other studies like Malambo & Popescu, (2021). We found best agreement for the stands with >65% canopy cover. This is consistent with the findings from Neuenschwander et al., (2020) who observed the best agreement between ICESat-2 and ALS ranging between 40% and 85% which also implies that very high or very low canopy cover may not produce sufficient ground or canopy photons respectively. When canopy cover exceeds 90%, the mean difference also increases which is also observed by Mulverhill et al., (2022). Except for woody wetlands, our result showed high agreement of canopy heights derived from ICESat-2, where about 90% of ALT08 heights were within 95% confidence interval of ALS height estimates.

Among different forest types and their height classes, except for the woody wetlands in <10 m height class, ICESat-2 overestimated the canopy heights in median values. Other studies have also reported that ICESat-2 tend to overestimate canopy heights in dwarf shrubland whereas with taller canopy heights, the ICESat-2 tends to underestimate the canopy height (Liu et al., 2021). Evergreen forests in Mississippi are comprised of coniferous species like loblolly pine, slash pine, and longleaf pine with dense canopies, which show better performance for height estimation using lidar. Malambo & Popescu, (2021) also found better agreement between ICESat-2 and ALS in conifer forest than other environments. On the other hand, there was poor agreement in woody wetlands (average canopy cover of 47%) and deciduous forests (average canopy cover of 44%). Woody wetlands (vegetation cover >20%, soil periodically saturated or covered with water) signifies a sparse forest with low canopy cover, which may be the cause for poor performance of ICESat-2. Similarly, in our study the deciduous forests had among the

lowest mean canopy cover (44%), which could be the reason for its poor performance among other forest types. Neuenschwander et al., (2016) also discussed limitations in the ICESat-2 retrieval of terrain height in the ecosystem of deciduous forests, which ultimately had an impact on estimations of canopy height.

For all physiographic regions, except for the alluvial plain, 90% of ICESat-2 canopy heights were within 95% confidence interval of ALS (max and RH98) height estimates (Table 1.7). The black prairie also showed the lowest MD and RMSD values as compared to other physiographic regions. The equivalence test also suggested that ICESat-2 performs best for the black prairie physiographic region with the lowest threshold value of similarity whereas the alluvial plain had the greatest threshold value. Also, the boxplot of canopy heights by physiographic regions showed good agreement between ICESat-2 and ALS and greater MD for the higher height classes. As the height class increased, the agreement between the height products decreased. Similar results were also observed by Mulverhill et al. (2022). Overall, there was good correspondence between ICESat-2 and ALS for lower height classes i.e., 0-10 m and 11-20 m, across various physiographic regions which shows potential of integrating two data sources for forest monitoring studies. All the physiographic regions in the <10 m height class showed ICESat-2 overestimating the canopy heights and gradually shifts to an underestimation as canopy height increased. The reason for this shift with canopy height for ICESat-2 is unclear, more related research could help improve the canopy height retrieval algorithm for ICESat-2. Another reason could be due to the impact of using discrete categories of height classes based on ALS which generated somewhat artificial over and underestimates at the low and high extremes of the canopy heights respectively. Also using new versions of data products would provide

better estimates of canopy height therefore we encourage other users to use the latest versions of these data products for research and applications.

ICESat-2 seems to overestimate canopy heights for height class <10 m irrespective of the frequency of disturbances but in height classes >10 m, the ICESat-2 underestimated the canopy height. Differences between ICESat-2 and ALS increased with increasing canopy height. For height classes 11-20 m (Figure 1.22 and 1.23), the ICESat-2 and ALS have similar values compared to height classes such as 21-30 m and over 30 m. This suggests that tall trees are difficult to estimate than shorter ones.

Since we do not know if the disturbance is a stand-replacing disturbance or not, the differences would be greater in burned areas than in harvested areas, since burned areas are characterized by more heterogeneous forest structures following disturbance. If standing dead trees remained after disturbance, ICESat-2, ALS or both may have difficulty capturing the regeneration in such heterogeneous conditions. Even though the ICESat-2 underestimates canopy height, both height products captured patterns of height increment with a corresponding increase in the time since disturbance.

Overall, the ICESat-2 seems to underestimate the canopy height for height class >10 m in all cases. This could be associated with the differences in the pulse density from the two different lidar sensors. The ICESat-2 illuminates the nominal 17 m diameter footprint on the surface every 70 cm in the along-track direction and detects 0-4 photons over vegetations (Neuenschwander & Magruder, 2019). This lower number of returns may not be sufficient to estimate accurate canopy height at the footprint level. Another reason for the underestimation could be due to the high variance in estimated canopy height within the ICESat-2 segment, especially when the landcover within the segment is heterogeneous. Studies measuring the precision of individual

tree heights undertaken independently by different mensurationists demonstrate that difference in measurements for the same trees ranged between 0.1 and 4.2 m (Luoma et al., 2017). Moreover, the FIA guide indicates that the tolerance of the tree height measurement can be up to ± 10 % of true tree height (US Forest Service, 2007). The MD observed between the canopy height products from ICESat-2 and ALS along with the equivalence test in this study demonstrate that the differences are within the tolerance and hence the ICESat-2 canopy height data can be used for reliable estimates.

The results from this study showed a good level of agreement between canopy height products from ICESat-2 and ALS. However, there were some unexpected observations that may be associated with the ICESat-2 data processing algorithms. The differences in the estimates were particularly due to the extreme estimates caused by noise and point cloud classification algorithms. Therefore, it is necessary to adequately clean the data by removing the outliers before using the ICESat-2 data. Another important thing to consider is that the discrete return systems can also be biased upwards as a function of leading-edge ranging (Queinnec et al., 2021). Besides, it is also important to co-register all the dataset before carrying out further analysis. Results in this study are based on version 4 of the ICESat-2 ATL08 products. The ATL08 products are continuously updated with some improvements in the product. However, validating each version is also equally important to understand the performance of the product. This shows potential for integrating spaceborne lidar data into large scale forest monitoring activities with other optical datasets like Landsat and Sentinel-2. Since ICESat-2 has global coverage, unlike GEDI which does not have spatial coverage outside 51.6°N - 51.6°S latitude, it has greater potential in integrating with other data products (Dubayah et al., 2020).

This study provides insight in comparison between ICESat-2 and ALS data that will be useful to guide integration with other data sources in the future. ICESat-2 synergy with finer resolution dataset like Sentinel-2 data could be used to generate wall-to-wall estimate of forest structure. ICESat-2 data provides global spatial coverage as compared to ALS and could be used to augment the representation of ALS to inform generation of a wall-to-wall canopy height product. This could be further used to assess forest monitoring activities like ours over larger area to study impacts over disturbed areas. Another application would be to provide consistent measures of global tree heights which is critical for biomass estimation.

1.6 Conclusions

In this study, we evaluated the performance of ICESat-2 ATL08 canopy height products. The accuracy of the canopy height products from ICESat-2 was evaluated with reference to high resolution ALS data products of the same year. Overall, results indicate agreement between ICESat-2 and ALS derived canopy heights. Canopy height estimates from ICESat-2 varied with forest types, canopy structure and physiographic regions. Estimation of canopy height using high beam at night produced the most accurate estimation of canopy height. For forests with a moderate canopy cover, ICESat-2 provides accurate estimates. It shows potential to estimate canopy heights with a high degree of accuracy, especially for evergreen forests and other ecosystems similar to those found in the Black Prairie region. Another important application of ICESat-2 could be to detect forest disturbances and its recovery trajectory.

From this study, we conclude that ICESat-2 can provide reliable canopy height estimates with high accuracy. It has potential to provide information on canopy height throughout the globe. Incorporating this data with other data sources such as optical images, and RADAR will further expand its application at multiple spatial and temporal scales. The findings presented in

this research provide information on the accuracy of the ICESat-2 canopy height product and its accuracy over different scenarios. It demonstrates the value and potential of integrating the use of diverse data sources for forest structure monitoring.

CHAPTER II

MODELS TO PREDICT AIRBORNE LASER SCANNING CANOPY HEIGHT METRICS FROM ICESAT-2 SPACEBORNE LIDAR

2.1 Introduction

Canopy height has been used in deriving individual tree and stand-level variables such as standing volume, biomass, carbon stock, stand growth, productivity, and site index (Jurjević et al., 2020). Researchers have emphasized the importance of tree height in estimating above ground biomass (Wang et al., 2016), its relation to tree diversity (Zhang et al., 2022) and habitat for wildlife (Vaglio Laurin et al., 2019). Recent development in remote sensing technology like Terrestrial Laser Scanning (TLS), Airborne Lidar Scanning (ALS), and Unmanned Aerial Vehicles (UAV) have the prospect of precisely measuring tree height (Zhang et al., 2022) saving time and money. Among them, ALS has become popular for estimating canopy height and forest biomass across landscapes (Boudreau et al., 2008; Wang et al., 2016). Traditional forest inventories measure forest attributes such as canopy height, canopy cover, distribution of vertical layers, and biomass at local level and then extrapolated over a landscape either to estimate or derive those attributes using principles of statistical sampling. However, air and spaceborne lidar systems have the capability to measure these attributes at a wider scale and a much faster rate, saving time and money (Wulder et al., 2012).

Lidar remote sensing assists in the direct measurement and estimation of several crucial forest characteristics such as canopy height, sub-canopy topography, and the vertical distribution

of intercepted surfaces between the canopy top and the ground. Other forest structural characteristics, such as above-ground biomass, are modeled or inferred from these direct measurements (Dubayah & Drake, 2000). The laser beams from the lidar sensor penetrate forest canopy and provide details of ground vegetation. Because of this ability and independence from solar illumination, lidar-derived Canopy Height Models (CHM) are used to estimate tree height, and canopy cover (Ma et al., 2017). High-resolution canopy height models derived from ALS can provide detailed information on the vertical structure of forests. However, when compared to satellite data of similar resolution and extent, the ALS data are very expensive. Therefore, it is important to use a cost-effective approach that best meets monitoring goals and quantify forest resources from local to global scales. Spaceborne lidar missions, like ICESat-2, are capable of directly measuring canopy heights globally and provide a critical observation needed to improve our understanding of global carbon stocks (Neuenschwander & Magruder, 2019). ICESat-2 data provides a new opportunity to directly measure the height and distribution of boreal forest and other forests, which would otherwise be omitted from the next generation accounting of forest biomass using only ALS.

ICESat-2 ATL08 data products have been used to determine terrain and canopy height over different forest types and ecozones (Malambo & Popescu, 2021). Many studies have used ALS data as a reference to compare ICESat-2 canopy heights and have shown good results (Liu et al., 2021; Queinnec et al., 2021). Wang et al., (2019) compared field measured height with ALS and Terrestrial Laser Scanner (TSL) and found that ALS based tree height estimates and field measurements have high correlation (R^2 = 0.94) and low error (RMSE = 1.69m). Liu et al., (2021) compared canopy heights derived from ICESat-2 with airborne lidar and reported

moderate correlation (R^2 = 0. 61) showing potential of ICESat-2 to estimate canopy height with good accuracy.

Many airborne lidar datasets have been acquired over time under the USGS 3D Elevation Program (3DEP). However, ALS data are still not always open access, they are limited in terms of spatial and temporal coverage and are expensive and therefore, are unsuited for routine applications. Freely available ALS standard canopy height data with global coverage could aid in efficient canopy height estimation. Next generation lidar instruments like ICESat-2 are capable of global-scale mapping of forest canopy characteristics (Finley et al., 2017). It provides an opportunity to create wall-to-wall predictive maps of forest variables using statistical models to obtain ALS standard data products. Statistical models could be developed using a small subset of available ALS data to provide insights beyond the location of ALS measurements. Therefore, this study aims to develop models to predict ALS canopy height using freely available ICESat-2 ATL08 canopy height data and generate wall to wall forest canopy height maps over the study area.

2.2 Methods

2.2.1 Study area

The study area is the same as Chapter I (Figure 2.1). A detailed description of the study area is presented in Section 1.3.1 of Chapter I.

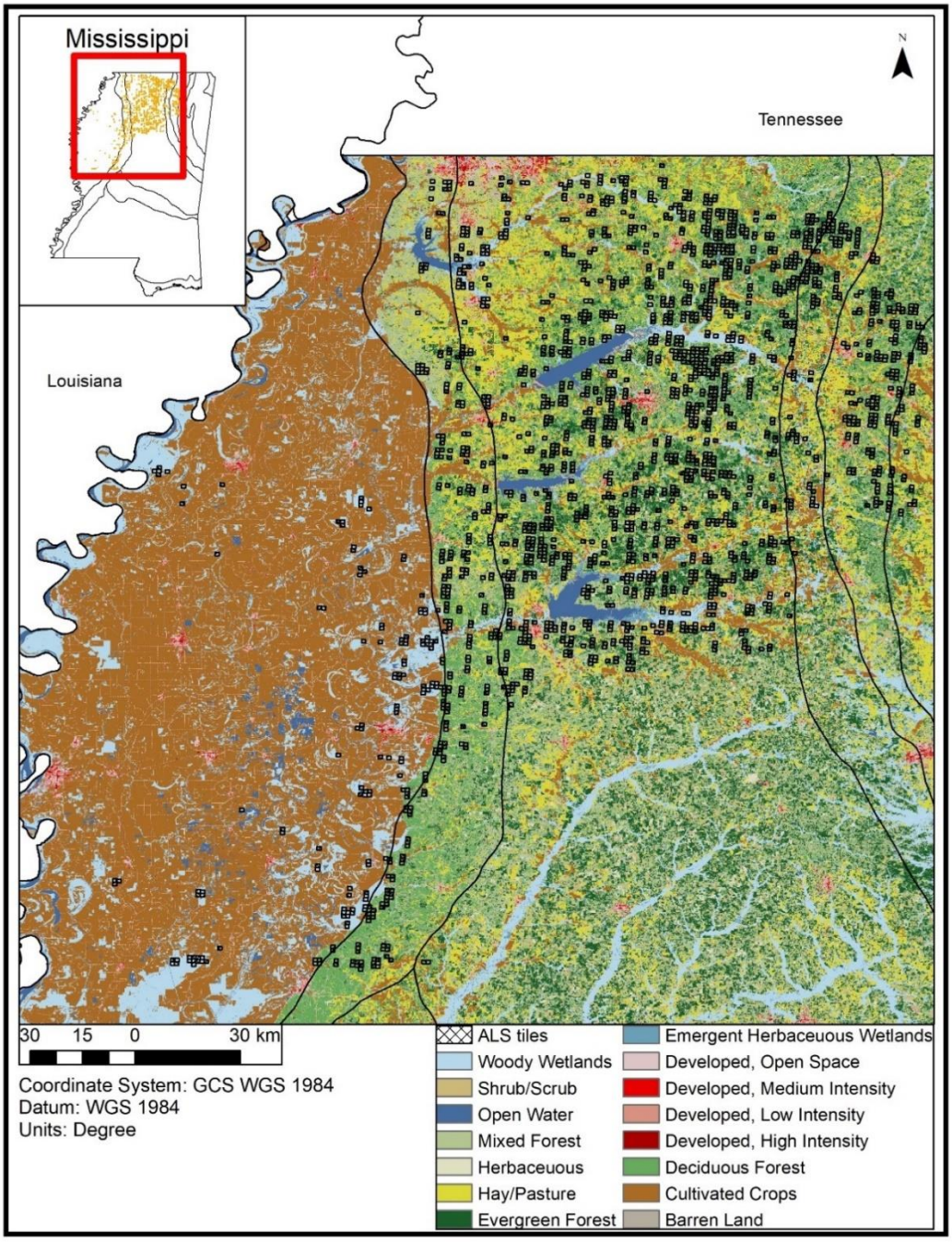

Figure 2.1 Map showing the study area within Mississippi state. The land use and land cover type are extracted from the National Land Cover Database (NLCD) 2019 (MRLC, 2022).

2.2.2 Datasets

The data used in this study are ALS and ICESat-2 ATL08 data from 2018 to 2020, the same data used in Chapter I. However, only the strong beams data acquired at night were used for the model development as our findings from Chapter I and other earlier studies have suggested that these datasets have lower statistical error (Liu et al., 2021; Neuenschwander et al., 2020). A detailed description of the data is presented in Section 1.3.2 of Chapter I.

2.2.3 Data management

Further data cleaning was carried out to obtain clean data for modeling purpose. Firstly, we filtered ICESat-2 footprints using the following criteria:

1. A relative uncertainty value of less than 20 m for canopy height (h_canopy_uncertainty <20 m) (Liu et al., 2022);
2. Estimated forest canopy height should be greater than 2 m and less than 60 m.

Secondly, we tested the datasets for possible outlying observations for all data using the Median Absolute Deviation (MEAD) using Equation (2.1) (Leys et al., 2013). Any observation outside the median ± 3 × MEAD was considered an outlier and removed from the dataset. This approach is not sensitive to outliers and is a more robust measure of dispersion that is easy to implement (Leys et al., 2013).

$$MEAD = bM_i\left(\left|x_i - M_j(x_j)\right|\right) \tag{2.1}$$

where x_i is the set of n original observations, M_j is the median of original observations, M_i is the median of the series, and b = 1.4826 is a constant associated with the normality assumption of the data without regarding the abnormality due to outliers (Leys et al., 2013).

2.2.4 Variable description and regression models

The exploratory data analysis suggested a linear relationship between ICESat-2 and ALS height metrics. Therefore, linear regression was used to model ALS canopy height metrics from a set of selected ICESat-2 derived predictors. The description of the variables used in the model is shown in Table 2.1.

Table 2.1 Description of variables used in model development.

Variable	Variable type		Description
CHM max	Response	(Continuous)	Canopy Height Model derived maximum canopy height
ALS max	Response	(Continuous)	ALS maximum canopy height
ALS RH99	Response	(Continuous)	ALS 99th percentile canopy height
ICESat-2 max*	Predictor	(Continuous)	ICESat-2 maximum canopy height
ICESat-2 RH98*	Predictor	(Continuous)	ICESat-2 98th percentile canopy height
Forest type	Predictor	(Categorical)	Deciduous, Evergreen, Mixed, Woody wetlands
Physiographic regions	Predictor	(Categorical)	Black Prairie, Pontotoc Ridge, Flatwoods, North central hills, Loess hill, Alluvial plain
Disturbance presence	Predictor	(Binary)	Yes or no
Percent canopy cover	Predictor	(Binary)	0 to 1
Signal to Noise Ratio (SNR)*	Predictor	(Continuous)	Ratio of the number of ATL08 signal photons to the number of noise photons per segment
Terrain height*	Predictor	(Continuous)	Height of terrain

* indicates ICESat-2 parameters.

Mississippi consists of 11 different physiographic regions, however the ALS data we used to develop the model were available only for six physiographic regions. Therefore, to predict the ALS height over the 6 physiographic regions the study used a linear mixed effects

model with physiographic region as a random variable, whereas for predicting the canopy height over the entire state of Mississippi, the study used a fixed effects model.

First, the data was grouped by beam type and time of acquisition and divided into four subsets: strong beam data acquired at day, strong beam data acquired at night, weak beam data acquired at day, and weak beam data acquired at night. Then, the group that had the best evaluation statistics was used for model development. Both a linear fixed effects model (LM) and linear mixed effects model (LME) were created to predict ALS canopy height. Mixed effect models are primarily used to describe relationships between response variables and covariates in data that has been classified into one or more categories (Pinheiro et al., 2006). The fixed effects explain the variations whereas the random effects organize the unexplained variation (Robinson and Hamann, 2010). For LM, the study used forest types, canopy cover, disturbance presence, Signal to Noise Ratio (SNR), and year since disturbance as fixed effects. Whereas the random effect of physiographic regions was incorporated in the mixed effects model.

The mixed-effect model was fitted using the lme function in 'nlme' package (Pinheiro et al., 2022) in R version 4.1.1. The general expression for a fixed and mixed model is defined in Equation 2.2 and 2.3 respectively. Residual plots of the models were visually assessed to evaluate the model assumptions.

$$Y_i = f(\boldsymbol{X}_i, \beta_i) + \varepsilon_i \tag{2.2}$$

$$Y_i = f(\boldsymbol{X}_i, \alpha, \beta_i) + \varepsilon_i \tag{2.3}$$

where, Y_i is a vector of ALS canopy height (dependent variables); f is the model equation form; $\boldsymbol{X_i}'$s is a matrix of the selected predictor variables; α is a vector of random-effect parameters; β_i is a vector of fixed-effects parameters; and ε_i is the error term.

To remedy the potential effect of collinearity, variance inflation factors (VIFs) were also used to investigate the relationships among variables.

2.2.5 Model evaluation and validation

The entire dataset was randomly split into two parts, with 75% for model development and 25% for validation. Validation data was then used to calculate model fit statistics including Mean Deviation (MD), Mean Absolute Deviation (MAD), Fit Index (FI), and Root Mean Squared Error (RMSE) to determine the accuracy of model estimations (Equation 2.4 – Equation 2.7). The cross-validation process was repeated 20 times and the evaluation statistics were obtained by averaging over 20 iterations. Models that had smaller values of MD, MAD, and RMSE and higher values of FI were preferred as the best fit model.

$$Mean\ Deviation\ (MD) = \sum_{i=1}^{n}\left(\frac{y_i - \hat{y}_i}{n}\right) \tag{2.4}$$

$$Mean\ Absolute\ Deviation\ (MAD) = \sum_{i=1}^{n}\left(\frac{|y_i - \hat{y}_i|}{n}\right) \tag{2.5}$$

$$Fit\ Index\ (FI) = 1 - \left(\frac{\sum_{i=1}^{n}(y_i - \hat{y}_i)^2}{\sum_{i=1}^{n}(y_i - \bar{y}_i)^2}\right) \tag{2.6}$$

$$Root\ Mean\ Square\ Error\ (RMSE) = \sqrt{\frac{1}{n} \times \sum\nolimits_{i=1}^{n}(y_i - \hat{y}_i)^2} \tag{2.7}$$

y_i and $\hat{y}_i$ are observed and predicted values of the dependent variable; $\bar{y}_i$ is the mean of the dependent variable; and n is the number of observations.

2.2.6 Interpolation

Spatial interpolation is a method based on the Tobler's first law of geography that states that “everything is related to everything else, but near things are more related than distant things” (Tobler, 1970). Additionally, the Third Law of Geography hypothesizes that “near” things in similar geographic conditions should be more similar instead of things that are near only in spatial distance (Zhu et al., 2018). Regarding forest canopy height, it can be influenced by local environmental factors such as slope, aspect, and solar radiation (Simard et al., 2011; Tao et al., 2016). Based on these ideas we can infer that the canopy height of trees close to each other have similar geographic conditions and are more related than distant trees. Consequently, interpolation can be used to obtain a uniform canopy height map over the study area.

To obtain a uniform canopy height map over the study area, we used Ordinary Kriging (OK) interpolation method to interpolate canopy height from ICESat-2, ALS, and predicted canopy heights. OK of the canopy height data points was performed using the geostatistical analyst tool in ArcGIS software with the inclusion of a maximum of 5 data points at each interpolation node.

2.3 Results

Graphical analysis showed a linear relationship of ICESat-2 and ALS derived canopy heights for all pairs. For each linear fixed effect and linear mixed effect model of CHM max, ALS max and ALS RH99, the models were run twice to obtain only the significant variables (p-value <0.05) (Table 2.2 - 2.4). The variance inflation factor (VIF) among the variables were also computed to investigate the relationships among variables. The VIF values for all the variables: ICESat-2 canopy height (1.10), forest type (1.93), physiographic regions (1.62), disturbance

history (1.15), canopy cover (1.28), and SNR (1.01) were found to be <2 which indicate that the variables were not correlated.

In the case of the CHM max fixed-effect model, ICESat-2 max, forest type, SNR, canopy cover, SNR, and disturbance presence were statistically significant whereas terrain height was not (p-value < 0.05) (Table 2.2). Among the forest types, CHM max was predicted highest for deciduous forest whereas the other forest types had smaller predicted CHM max. Similarly, the higher CHM max was predicted when disturbance was not present. Similar results were also seen in the mixed-effect model.

Table 2.2 Parameters, estimates, standard errors (SE), and t-values for the CHM max model

Variable	Parameter	Estimate	SE	|t-value|	p-value
LM					
Intercept	b_1	6.1636	0.1528	40.331	< 0.001
ICESat-2 max*	b_2	0.8071	0.0046	174.993	< 0.001
Forest type (FT)	b_3 = deciduous	0			
	b_3 = evergreen	-1.3668	0.0651	20.984	< 0.001
	b_3 = mixed	-0.4372	0.0678	6.444	< 0.001
	b_3 = woody wetlands	-0.7597	0.0656	11.575	< 0.001
Disturbance	b_4= yes	-0.4365	0.0522	8.358	< 0.001
SNR*	b_5	0.0011	0.0006	2.085	< 0.001
Canopy cover	b_6	1.5250	0.2028	7.519	0.037
LME					
Intercept	b_1	5.8576	0.2022	28.972	< 0.001
ICESat-2 max*	b_2	0.8087	0.0046	174.838	< 0.001
Forest type (FT)	b_3 = deciduous	0			
	b_3 = evergreen	-1.3976	0.0663	21.069	< 0.001
	b_3 = mixed	-0.4629	0.0683	6.774	< 0.001
	b_3 = woody wetlands	-0.5644	0.0751	7.51	< 0.001
Disturbance	b_4 = yes	-0.4363	0.0523	8.344	< 0.001
SNR*	b_5	0.0013	0.0006	2.449	0.014
Canopy cover	b_6	1.8185	0.2087	8.71	< 0.001

LM = Linear fixed effect model; LME = Linear mixed effect model; SE = Standard Error; SNR = Signal to Noise Ratio; * indicates ICESat-2 parameters

For the ALS max fixed-effect model, all the predictor variables (ICESat-2 max, forest type, SNR, canopy cover, and disturbance presence) were statistically significant (Table 2.3). Among the forest types, ALS max was predicted highest for deciduous forest whereas the other forest types had smaller predicted ALS max. Similarly, the higher ALS max was predicted when disturbance was not present. Similar result was observed in the mixed-effects model except that lower ALS max was predicted with increasing terrain height.

Table 2.3 Parameters, estimates, standard errors (SE), and t-values for the ALS max model

Variable	Parameter	Estimate	SE	|t-value|	p-value
LM					
Intercept	b_1	6.5015	0.1828	35.572	< 0.001
ICESat-2 max*	b_2	0.8053	0.0047	172.623	< 0.001
Forest type (FT)	b_3 = deciduous	0			
	b_3 = evergreen	-1.3973	0.0657	21.257	< 0.001
	b_3 = mixed	-0.4801	0.0682	7.038	< 0.001
	b_3 = woody wetlands	-0.8377	0.0780	10.735	< 0.001
Disturbance	b_4= 1	-0.4964	0.0526	-9.43	< 0.001
SNR*	b_5	0.0013	0.0006	2.274	0.023
Canopy cover	b_6	1.4086	0.2080	6.771	1.33
LME					
Intercept	b_1	6.3516	0.2374	26.754	< 0.001
ICESat-2 max*	b_2	0.8037	0.0047	1.72	< 0.001
Forest type (FT)	b_3 = deciduous	0			
	b_3 = evergreen	-1.4357	0.0667	21.512	< 0.001
	b_3 = mixed	-0.5130	0.0688	7.460	< 0.001
	b_3 = woody wetlands	-0.7096	0.0847		
Disturbance	b_4= yes	-0.5017	0.0526	9.534	0.007
SNR*	b_5	0.0015	0.0006	2.666	< 0.001
Canopy cover	b_6	1.6923	0.2134	7.929	< 0.001
Terrain height*	b_7	-0.0033	0.0011	26.754	0.004

LM = Linear fixed effect model; LME = Linear mixed effect model; SE = Standard Error; SNR = Signal to Noise Ratio; * indicates ICESat-2 parameters.

Also, for the ALS RH99 fixed-effect model, ICESat-2 RH98, forest type, SNR, canopy cover, and disturbance presence were statistically significant whereas terrain height was not

(Table 2.4). Among the forest types, ALS RH99 was predicted highest for deciduous forest whereas the other forest types had smaller predicted ALS RH99. Similarly, the ALS RH99 was predicted higher when disturbance was not present. Similar results were also seen in the mixed-effects model.

Table 2.4 Parameters, estimates, standard errors (SE), and t-values for the ALS RH99 model

Variable	Parameter	Estimate	SE	|t-value|	p-value
LM					
Intercept	b_1	6.1485	0.1454	42.276	< 0.001
ICESat-2 RH98*	b_2	0.8064	0.0045	179.738	< 0.001
Forest type (FT)	b_3 = deciduous	0			
	b_3 = evergreen	-1.2851	0.0636	20.206	< 0.001
	b_3 = mixed	-0.4212	0.0663	6.352	< 0.001
	b_3 = woody wetlands	-0.8155	0.0640	12.736	< 0.001
Disturbance	b_4= 1	-0.5010	0.0511	9.812	< 0.001
SNR*	b_5	0.0024	0.0005	4.488	< 0.001
Canopy cover	b_6	0.5162	0.1980	2.61	0.009
LME					
Intercept	b_1	5.9372	0.1751	33.913	< 0.001
ICESat-2 RH98*	b_2	0.8054	0.0045	179.409	< 0.001
Forest type (FT)	b_3 = deciduous	0			
	b_3 = evergreen	-1.3197	0.0648	20.350	< 0.001
	b_3 = mixed	-0.4468	0.0669	6.683	< 0.001
	b_3 = woody wetlands	-0.6951	0.0723	9.61	< 0.001
Disturbance	b_4= 1	-0.5058	0.0512	9.882	< 0.001
SNR*	b_5	0.0025	0.0005	4.7166	< 0.001
Canopy cover	b_6	0.7418	0.2042	3.63	< 0.001

LM = Linear fixed effect model; LME = Linear mixed effect model; SE = Standard Error; SNR = Signal to Noise Ratio; * indicates ICESat-2 parameters.

The standardized residual vs. fitted plots were also evaluated for both the LM and LME for CHM max, ALS max, and ALS RH99 (Figure 2.2 – 2.4). Both the LM and LME showed a similar residual value in all cases.

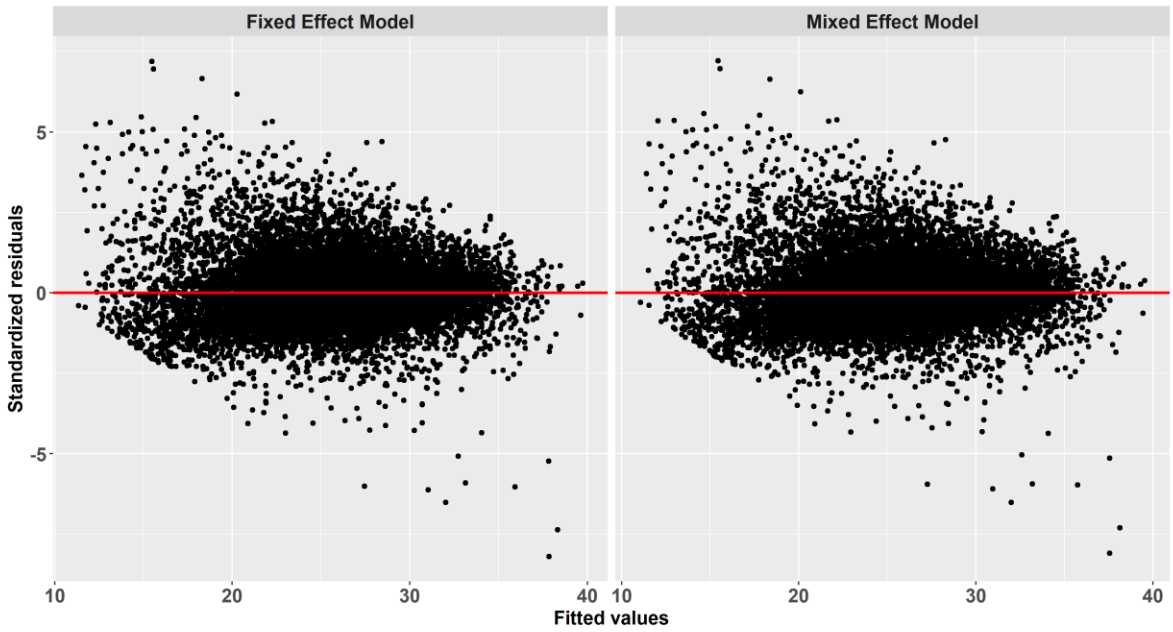

Figure 2.2 Standardized residuals plotted against fitted values of CHM max for LM and LME models.

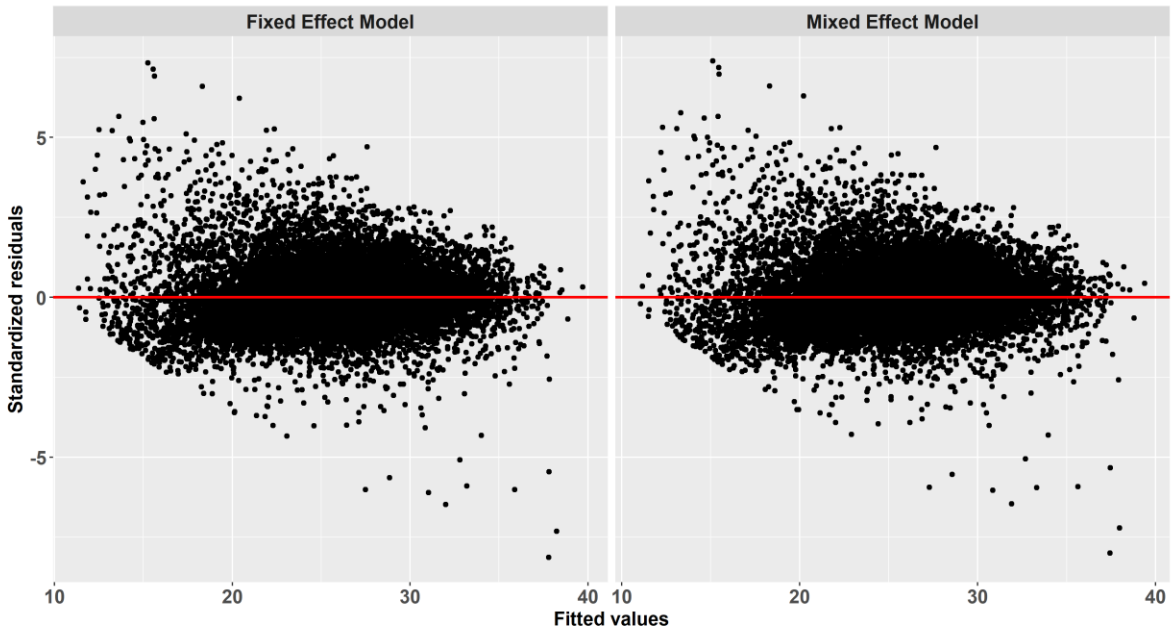

Figure 2.3 Standardized residuals plotted against fitted values of ALS max for LM and LME models.

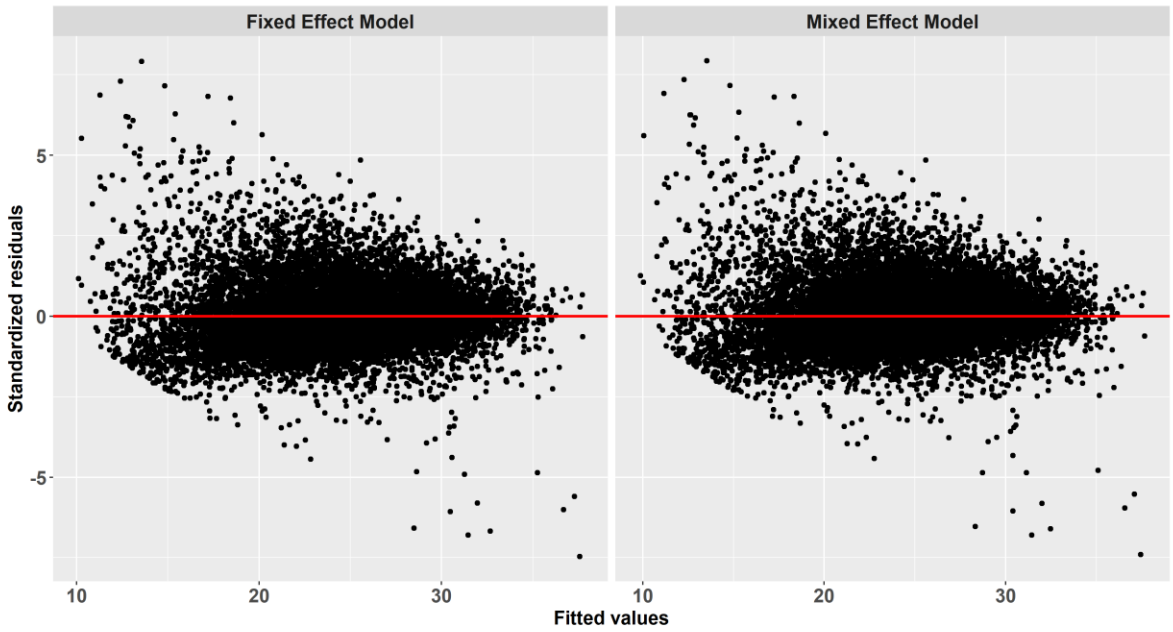

Figure 2.4 Standardized residuals plotted against fitted values of ALS RH99 for LM and LME models.

Inclusion of the physiographic regions as a random effect produced slightly better evaluation statistics for ALS canopy height models (Table 2.5). A small reduction in MAD and RMSE was observed in the LME. Among CHM max, ALS max and ALS RH99 canopy height predictions, the LME model for ALS RH99 had the highest FI (0.73) and lowest RMSE (2.63).

Table 2.5 Cross validation results for comparison of LM and LME models.

Response variable	Model	MD	MAD	FI	RMSE
CHM max	LM	0.0011	1.9711	0.7213	2.7286
	LME	0.0007	1.9687	0.7219	2.7255
ALS max	LM	0.0087	1.9656	0.7228	2.7101
	LME	0.0089	1.9638	0.7235	2.7070
ALS RH99	LM	0.0150	1.8886	0.7358	2.6383
	LME	0.0150	1.8879	0.7362	2.6363

LM = Linear fixed effect model; LME = Linear mixed effect model; MD = Mean deviation; MAD = Mean absolute deviation; FI = Fit index; RMSE = Root mean square error.

We discovered that the LME was superior to the LM for predicting ALS metrics using ANOVA model comparison (Table 2.6), as evidenced by the AIC, BIC, and log likelihood of the two models.

Table 2.6 Comparison of fixed- and mixed-effects models for predicting ALS metrics using ICESat-2 derived metrics. AIC = Akaike Information Criterion, BIC = Bayesian Information Criterion. Smaller values of AIC, BIC, and larger values of Log-Likelihood are preferred.

Response variable	Model	AIC	BIC	Log-Likelihood	p-value
CHM max	LM	67541.61	67632.11	-33758.81	<.0001
	LME	67505.43	67603.47	-33739.71	
ALS max	LM	67663.25	67746.21	-33820.62	<.0001
	LME	67635.44	67725.95	-33805.72	
ALS RH99	LM	66942.97	67025.94	-33460.48	<.0001
	LME	66929.52	67020.03	-33452.76	

LM = Linear fixed effect model; LME = Linear mixed effect model

The cross-validation result, standardized residual plots, and ANOVA comparison show that the LME performs slightly better than the LM, therefore this study used the LME to predict ALS canopy height within the study area and the LM to predict ALS height over the entire state of Mississippi for which physiographic information was incomplete.

Since, ICESat-2 canopy height data collected throughout the Mississippi covered the majority of the areas (Figure 1.3), we interpolated canopy height for ICESat-2 as well as predicted ALS over the whole state of Mississippi. Predicted CHM max, ALS max and ALS RH99 canopy heights over all of Mississippi can be found in Appendix B (Figure B.1 – B.3).

2.4 Discussion

In this study, we used linear regression models to estimate ALS canopy height from ICESat-2 canopy height metrics. Studies on lidar have shown potential of relative height (RH) percentiles in regression models for predictions (Ku et al., 2012). For example, Sheridan et al.,

(2014) used the 90th height percentile calculated from ALS as one of the best predictors of gross volume of Pacific Northwest FIA plots. There are several factors that influence ICESat-2 canopy height estimates such as site, biome, data acquisition time and beam strength (Liu et al., 2021; Malambo & Popescu, 2021; Varvia et al., 2022). Yu et al., (2022) suggested that strong beams at night are most suitable for retrieving canopy height estimates, which was the case in this study.

An important predictor with positive influence on canopy height observed in this study was canopy cover, which is in line with the finding of Mulverhill et al., (2022) who found significant positive influence of forest canopy cover on ICESat-2 canopy height. In our study, canopy height models for CHM max, ALS max, and ALS RH99 predicted canopy heights with higher estimates as canopy cover increased. Narine et al., (2019) also found canopy cover to be an important predictor to estimate aboveground biomass using simulated ICESat-2 data. Similarly, another important predictor with positive influence on ALS canopy height is the SNR. Researchers have shown that SNR is an influential variable and higher SNR is important to generate more accurate terrain and canopy heights (Liu et al., 2021; Popescu et al., 2018). Studies have shown that in case of higher SNR, most signal photons can be separated from noise photons and therefore lower RMSE can be seen in determining the canopy heights (Wang et al., 2019). A study by Popescu et al., (2018) used night data with higher SNR values and generated more accurate estimated canopy height as compared to their corresponding reference data with a RMSE of 3.77 m. The models in our study also showed that SNR had significant positive impact on ALS canopy height prediction with low standard error.

The negative effect of disturbance presence on canopy height implies that ALS predicts smaller canopy height when measuring canopy heights in presence of disturbance. This finding is consistent with Mulverhill et al., (2022) who found lower canopy heights in forests following

disturbances. However, the limitation of this study is that we do not know if the disturbance is a stand-replacing disturbance or not. If standing dead trees persisted after disturbance, it may be difficult to capture the regenerating vegetation height under such heterogeneous conditions.

Physiographic regions have a considerable impact on dominant height, stand basal area, and site index (Amateis et al., 2006). While fitting equations for canopy height estimates, using the LME method with physiographic regions as a random variable produced smaller MD and RMSE, and more reliable results than the standard LM model. Therefore, it is important to consider the uncertainty in the physiographical aspect on canopy height estimation using ICESat-2. However, the gain in precision was minimal in this study.

The model's ability to predict ALS standard canopy height has practical relevance. Studies have used ALS height metrics to estimate volume, basal area, and above ground biomass with good accuracy ($R^2 > 0.8$) (Lim et al., 2003; Lim et al., 2006). This predictive ability offers new opportunities for enhanced forest monitoring, management, and planning. Moreover, the results presented in this study was used to model ALS canopy height only over a small part of Mississippi. However, it can be used to facilitate extrapolating the data to provide wall-to-wall coverage over larger areas such as the whole state. Moreover, the predictions could also be improved by combining lidar data with other optical dataset like Landsat and Sentinel-2 (Jiang et al., 2022).

2.5 Conclusions

The use of the LME technique while fitting equations for ALS canopy height prediction produced smaller MAD and RMSE than using LM model. This study showed that the linear mixed effect modeling approach can produce more reliable results than a standard fixed effect model. The FI values obtained from the regression models, ranging from 0.72 to 0.73, highlight

the predictive ability of ICESat-2 metrics to characterize canopy height. While using ICESat-2 to predict ALS height, it is important to filter the observations by strong beam data acquired at night and integrate variables like forest types, physiographic regions, terrain height, SNR, canopy cover and disturbance history. Hence, from this study we conclude that ICESat-2 data can be used to predict ALS standard canopy height using statistical models with good accuracy. However, the limitation of this study is that the model did not include additional variables like slope, aspect, forest stand structure, density or seasonally affected variables (i.e., leaf on and leaf off), which could influence canopy height or sensor returns. Therefore, the inclusion of such variables in the canopy height models could further improve the model's predictive power. Moreover, this study focused only on a part of Mississippi, so scaling-up to regional and continental scales should be done cautiously and variations in forest types and topography must be taken into account as these factors influence the accuracy of estimates.

REFERENCES

Akay, A. E., Oğuz, H., Karas, I. R., & Aruga, K. (2009). Using LiDAR technology in forestry activities. *Environmental Monitoring and Assessment*, *151*(1–4), 117–125. https://doi.org/10.1007/S10661-008-0254-1

Alves, L. F., Vieira, S. A., Scaranello, M. A., Camargo, P. B., Santos, F. A. M., Joly, C. A., & Martinelli, L. A. (2010). Forest structure and live aboveground biomass variation along an elevational gradient of tropical Atlantic moist forest (Brazil). *Forest Ecology and Management*, *260*(5), 679–691. https://doi.org/10.1016/J.FORECO.2010.05.023

Amateis, R. L., Prisley, S. P., Burkhart, H. E., & Liu, J. (2006). The effect of physiographic region and geographic locale on predicting the dominant height and basal area of loblolly pine plantations. *Southern Journal of Applied Forestry*, *30*(3), 147–153. https://doi.org/10.1093/SJAF/30.3.147

Beland, M., Parker, G., Sparrow, B., Harding, D., Chasmer, L., Phinn, S., Antonarakis, A., & Strahler, A. (2019). On promoting the use of lidar systems in forest ecosystem research. *Forest Ecology and Management*, *450*, 117484. https://doi.org/10.1016/J.FORECO.2019.117484

Boudreau, J., Nelson, R. F., Margolis, H. A., Beaudoin, A., Guindon, L., & Kimes, D. S. (2008). Regional aboveground forest biomass using airborne and spaceborne LiDAR in Québec. *Remote Sensing of Environment*, *112*(10), 3876–3890. https://doi.org/10.1016/J.RSE.2008.06.003

Chen, Q., Gong, P., Baldocchi, D., & Tian, Y. Q. (2007). Estimating basal area and stem volume for individual trees from lidar data. *Photogrammetric Engineering and Remote Sensing*, *73*(12), 1355–1365. https://doi.org/10.14358/PERS.73.12.1355

Conrad, O., Bechtel, B., Bock, M., Dietrich, H., Fischer, E., Gerlitz, L., Wehberg, J., Wichmann, V., & Böhner, J. (2015). System for Automated Geoscientific Analyses (SAGA) v. 2.1.4. *Geoscientific Model Development*, *8*(7), 1991–2007. https://doi.org/10.5194/GMD-8-1991-2015

Danson, F. M., Gaulton, R., Armitage, R. P., Disney, M., Gunawan, O., Lewis, P., Pearson, G., & Ramirez, A. F. (2014). Developing a dual-wavelength full-waveform terrestrial laser scanner to characterize forest canopy structure. *Agricultural and Forest Meteorology*, *198–199*, 7–14. https://doi.org/10.1016/J.AGRFORMET.2014.07.007

Day, J. W., Boesch, D. F., Clairain, E. J., Kemp, G. P., Laska, S. D., Mitsch, W. J., Orth, K., Mashriqui, H., Reed, D. J., Shabman, L., Simenstad, C. A., Streever, B. J., Twilley, R. R., Watson, C. C., Wells, J. T., & Whigham, D. F. (2007). Restoration of the Mississippi Delta: Lessons from hurricanes Katrina and Rita. *Science*, *315*(5819), 1679–1684. https://doi.org/10.1126/SCIENCE.1137030/ASSET/76E26C9E-2363-43D4-AD56-9BFCD078C930/ASSETS/GRAPHIC/315_1679_F3.JPEG

di Sacco, A., Hardwick, K. A., Blakesley, D., Brancalion, P. H. S., Breman, E., Cecilio Rebola, L., Chomba, S., Dixon, K., Elliott, S., Ruyonga, G., Shaw, K., Smith, P., Smith, R. J., & Antonelli, A. (2021). Ten golden rules for reforestation to optimize carbon sequestration, biodiversity recovery and livelihood benefits. *Global Change Biology*, *27*(7), 1328–1348. https://doi.org/10.1111/GCB.15498

Dubayah, R., Blair, J. B., Goetz, S., Fatoyinbo, L., Hansen, M., Healey, S., Hofton, M., Hurtt, G., Kellner, J., Luthcke, S., Armston, J., Tang, H., Duncanson, L., Hancock, S., Jantz, P., Marselis, S., Patterson, P. L., Qi, W., & Silva, C. (2020). The Global Ecosystem Dynamics Investigation: High-resolution laser ranging of the Earth's forests and topography. *Science of Remote Sensing*, *1*, 100002. https://doi.org/10.1016/J.SRS.2020.100002

Dubayah, R. O., & Drake, J. B. (2000). Lidar Remote Sensing for Forestry. *Journal of Forestry*, *98*(6), 44–46. https://doi.org/10.1093/JOF/98.6.44

Finley, A. O., Datta, A., Cook, B. D., Morton, D. C., Andersen, H. E., & Banerjee, S. (2017). Applying nearest neighbor gaussian processes to massive spatial data sets: Forest canopy height prediction across Tanana valley Alaska. *Journal of Computational and Graphical Statistics*, *28*(2), 401–414. https://doi.org/10.48550/arxiv.1702.00434

Grala, K., Grala, R. K., Hussain, A., Cooke, W. H., & Varner, J. M. (2017). Impact of human factors on wildfire occurrence in Mississippi, United States. *Forest Policy and Economics*, *81*, 38–47. https://doi.org/10.1016/J.FORPOL.2017.04.011

GreenValley International (2022). Retrieved October 5, 2022, from https://greenvalleyintl.com/

Guan, H., Su, Y., Sun, X., Xu, G., Li, W., Ma, Q., Wu, X., Wu, J., Liu, L., & Guo, Q. (2020). A marker-free method for registering multi-scan terrestrial laser scanning data in forest environments. *ISPRS Journal of Photogrammetry and Remote Sensing*, *166*, 82–94. https://doi.org/10.1016/J.ISPRSJPRS.2020.06.002

Guo, Q., Li, W., Yu, H., & Alvarez, O. (2010). Effects of topographic variability and lidar sampling density on several DEM interpolation methods. *Photogrammetric Engineering and Remote Sensing*, *76*(6), 701–712. https://doi.org/10.14358/PERS.76.6.701

Harrod, R. J., Peterson, D. W., Povak, N. A., & Dodson, E. K. (2009). Thinning and prescribed fire effects on overstory tree and snag structure in dry coniferous forests of the interior Pacific Northwest. *Forest Ecology and Management, 258*(5), 712–721. https://doi.org/10.1016/J.FORECO.2009.05.011

Hodgson, M. E., & Bresnahan, P. (2004). Accuracy of airborne lidar-derived elevation: Empirical assessment and error budget. *Photogrammetric Engineering and Remote Sensing, 70*(3), 331–339. https://doi.org/10.14358/PERS.70.3.331

Holmgren, P., Thuresson, T., Holmgren, P., & Thuresson, T. (1996). Satellite remote sensing for forestry planning-A review. *Scandinavian Journal of Forest Research, 13*, 90–110. https://doi.org/10.1080/02827589809382966

Huang, C., Goward, S. N., Masek, J. G., Thomas, N., Zhu, Z., & Vogelmann, J. E. (2010). An automated approach for reconstructing recent forest disturbance history using dense Landsat time series stacks. *Remote Sensing of Environment*, *114*(1), 183–198. https://doi.org/10.1016/J.RSE.2009.08.017

Hyyppä, J., Hyyppä, H., Inkinen, M., Engdahl, M., Linko, S., & Zhu, Y. H. (2000). Accuracy comparison of various remote sensing data sources in the retrieval of forest stand attributes. *Forest Ecology and Management*, *128*(1–2), 109–120. https://doi.org/10.1016/S0378-1127(99)00278-9

Jiang, F., Sun, H., Ma, K., Fu, L., & Tang, J. (2022). Improving aboveground biomass estimation of natural forests on the Tibetan Plateau using spaceborne LiDAR and machine learning algorithms. *Ecological Indicators*, *143*, 109365. https://doi.org/10.1016/J.ECOLIND.2022.109365

Jurjević, L., Liang, X., Gašparović, M., & Balenović, I. (2020). Is field-measured tree height as reliable as believed – Part II, A comparison study of tree height estimates from conventional field measurement and low-cost close-range remote sensing in a deciduous forest. *ISPRS Journal of Photogrammetry and Remote Sensing*, *169*, 227–241. https://doi.org/10.1016/J.ISPRSJPRS.2020.09.014

Kayitakire, F., Hamel, C., & Defourny, P. (2006). Retrieving forest structure variables based on image texture analysis and IKONOS-2 imagery. *Remote Sensing of Environment, 102*(3–4), 390–401. https://doi.org/10.1016/J.RSE.2006.02.022

Ku, N. W., Popescu, S. C., Ansley, R. J., Perotto-Baldivieso, H. L., & Filippi, A. M. (2012). Assessment of available rangeland woody plant biomass with a terrestrial LIDAR system. *Photogrammetric Engineering & Remote Sensing*, 78(4), 349-361. https://doi.org/10.14358/PERS.78.4.349

Landfire (2011). Retrieved October 5, 2022, from https://landfire.gov/documents/SW_GA.pdf

Leys, C., Ley, C., Klein, O., Bernard, P., & Licata, L. (2013). Detecting outliers: Do not use standard deviation around the mean, use absolute deviation around the median. *Journal of Experimental Social Psychology*, *49*(4), 764–766. https://doi.org/10.1016/J.JESP.2013.03.013

Li, W., Guo, Q., Jakubowski, M. K., & Kelly, M. (2012). A new method for segmenting individual trees from the lidar point cloud. *Photogrammetric Engineering and Remote Sensing*, *78*(1), 75–84. https://doi.org/10.14358/PERS.78.1.75

Lim, K. S., Treitz, P. M., Lim, K. S., & And Treitz, P. M. (2006). Estimation of above ground forest biomass from airborne discrete return laser scanner data using canopy-based quantile estimators. *Http://Dx.Doi.Org/10.1080/02827580410019490*, *19*(6), 558–570. https://doi.org/10.1080/02827580410019490

Lim, K., Treitz, P., Wulder, M., St-Onge, B., & Flood, M. (2003). *LiDAR remote sensing of forest structure*. https://doi.org/10.1191/0309133303pp360ra

Liu, A., Cheng, X., & Chen, Z. (2021). Performance evaluation of GEDI and ICESat-2 laser altimeter data for terrain and canopy height retrievals. *Remote Sensing of Environment*, *264*, 112571. https://doi.org/10.1016/J.RSE.2021.112571

Liu, X., Su, Y., Hu, T., Yang, Q., Liu, B., Deng, Y., Tang, H., Tang, Z., Fang, J., & Guo, Q. (2022). Neural network guided interpolation for mapping canopy height of China's forests by integrating GEDI and ICESat-2 data. *Remote Sensing of Environment*, *269*, 112844. https://doi.org/10.1016/J.RSE.2021.112844

Luoma, V., Saarinen, N., Wulder, M. A., White, J. C., Vastaranta, M., Holopainen, M., & Hyyppä, J. (2017). Assessing precision in conventional field measurements of individual tree attributes. *Forests 2017, Vol. 8, Page 38*, *8*(2), 38. https://doi.org/10.3390/F8020038

Ma, Q., Su, Y., & Guo, Q. (2017). Comparison of canopy cover estimations from airborne LiDAR, aerial imagery, and satellite imagery. *IEEE Journal of Selected Topics in Applied Earth Observations and Remote Sensing*, *10*(9), 4225–4236. https://doi.org/10.1109/JSTARS.2017.2711482

Malambo, L., & Popescu, S. C. (2021). Assessing the agreement of ICESat-2 terrain and canopy height with airborne lidar over US ecozones. *Remote Sensing of Environment*, *266*, 112711. https://doi.org/10.1016/J.RSE.2021.112711

Manzanera, J. A., García-Abril, A., Pascual, C., Tejera, R., Martín-Fernández, S., Tokola, T., & Valbuena, R. (2016). Fusion of airborne LiDAR and multispectral sensors reveals synergic capabilities in forest structure characterization. *Http://Dx.Doi.Org/10.1080/15481603.2016.1231605*, *53*(6), 723–738. https://doi.org/10.1080/15481603.2016.1231605

Mississippi Automated Resource Information System (2022). Retrieved October 9, 2022, from https://www.maris.state.ms.us/#gsc.tab=0

Mississippi State University (2022). *Mississippi Climate | Department of Geosciences at Mississippi State University*. Retrieved August 30, 2022, from https://www.geosciences.msstate.edu/state-climatologist/climate/

Morgan, C., DeMatteis, J., & Barber, E. (2012). *Forest legacy program: Prepared by the Mississippi Forestry Commission - 2007 - 2012* (Issue March 2007).

Mulverhill, C., Coops, N. C., Hermosilla, T., White, J. C., & Wulder, M. A. (2022). Evaluating ICESat-2 for monitoring, modeling, and update of large area forest canopy height products. *Remote Sensing of Environment*, *271*, 112919. https://doi.org/10.1016/J.RSE.2022.112919

Multi-Resolution Land Characteristics Consortium (U.S.). National Land Cover Dataset (NLCD) (2022). [Research Triangle Park, NC]: [Multi-Resolution Land Characteristics Consortium]. Retrieved August 25, 2022, from https://www.mrlc.gov/data

Narine, L. L., Popescu, S., Neuenschwander, A., Zhou, T., Srinivasan, S., & Harbeck, K. (2019). Estimating aboveground biomass and forest canopy cover with simulated ICESat-2 data. *Remote Sensing of Environment*, *224*, 1–11. https://doi.org/10.1016/J.RSE.2019.01.037

Neuenschwander, A., Guenther, E., White, J. C., Duncanson, L., & Montesano, P. (2020). Validation of ICESat-2 terrain and canopy heights in boreal forests. *Remote Sensing of Environment*, *251*, 112110. https://doi.org/10.1016/J.RSE.2020.112110

Neuenschwander, A. L., & Magruder, L. A. (2019). Canopy and terrain height retrievals with ICESat-2: A first look. *Remote Sensing 2019, Vol. 11, Page 1721*, *11*(14), 1721. https://doi.org/10.3390/RS11141721

Neuenschwander, A. L., Magruder, L. A., Baghdadi, N., Swatantran, A., & Thenkabail, P. S. (2016). The potential impact of vertical sampling uncertainty on ICESat-2/ATLAS terrain and canopy height retrievals for multiple ecosystems. *Remote Sensing 2016, Vol. 8, Page 1039*, *8*(12), 1039. https://doi.org/10.3390/RS8121039

Neuenschwander, A., & Pitts, K. (2019). The ATL08 land and vegetation product for the ICESat-2 Mission. *Remote Sensing of Environment*, *221*, 247–259. https://doi.org/10.1016/J.RSE.2018.11.005

Oswalt, S. N. (2019). Mississippi's forests, 2017. *Resource Bulletin SRS-226. Asheville, NC: U.S. Department of Agriculture Forest Service, Southern Station.*, *226*, 1–68. https://doi.org/10.2737/SRS-RB-226

Pinheiro, J., & Bates, D. (2006). *Mixed-effects models in S and S-PLUS.* Springer science & business media.

Pinheiro, J., Bates, D., DebRoy, S., Sarkar, D., and R core Team. (2022). nlme: linear and nonlinear mixed effects models. *R package version* 3.1-155. https://cran.r-project.org/package=nlme

Popescu, S. C., Zhou, T., Nelson, R., Neuenschwander, A., Sheridan, R., Narine, L., & Walsh, K. M. (2018). Photon counting LiDAR: An adaptive ground and canopy height retrieval algorithm for ICESat-2 data. *Remote Sensing of Environment*, *208*, 154–170. https://doi.org/10.1016/J.RSE.2018.02.019

Queinnec, M., White, J. C., & Coops, N. C. (2021). Comparing airborne and spaceborne photon-counting LiDAR canopy structural estimates across different boreal forest types. *Remote Sensing of Environment*, *262*, 112510. https://doi.org/10.1016/J.RSE.2021.112510

R Core Team (2021). R: A language and environment for statistical computing. R Foundation for Statistical Computing. Vienna, Austria. Retrieved from https://www.R-project.org/

Rahimizadeh, N., Babaie Kafaky, S., Sahebi, M. R., & Mataji, A. (2020). Forest structure parameter extraction using SPOT-7 satellite data by object- and pixel-based classification methods. *Environmental Monitoring and Assessment*, *192*(1), 1–17. https://doi.org/10.1007/S10661-019-8015-X/FIGURES/9

Robinson, A. P., & Froese, R. E. (2004). Model validation using equivalence tests. *Ecological Modelling*, *176*(3–4), 349–358. https://doi.org/10.1016/J.ECOLMODEL.2004.01.013

Robinson, A. P., & Hamann, J. D. (2010). *Forest analytics with R: an introduction*. Springer Science & Business Media.

Rödig, E., Cuntz, M., Rammig, A., Fischer, R., Taubert, F., & Huth, A. (2018). The importance of forest structure for carbon fluxes of the Amazon rainforest. *Environmental Research Letters*, *13*(5), 054013. https://doi.org/10.1088/1748-9326/AABC61

Seidl, R., Fernandes, P. M., Fonseca, T. F., Gillet, F., Jönsson, A. M., Merganičová, K., Netherer, S., Arpaci, A., Bontemps, J. D., Bugmann, H., González-Olabarria, J. R., Lasch, P., Meredieu, C., Moreira, F., Schelhaas, M. J., & Mohren, F. (2011). Modelling natural disturbances in forest ecosystems: a review. *Ecological Modelling*, *222*(4), 903–924. https://doi.org/10.1016/J.ECOLMODEL.2010.09.040

Sheridan, R. D., Popescu, S. C., Gatziolis, D., Morgan, C. L. S., & Ku, N. W. (2014). Modeling forest aboveground biomass and volume using airborne LiDAR metrics and Forest Inventory and Analysis data in the Pacific Northwest. *Remote Sensing 2015, Vol. 7, Pages 229-255*, *7*(1), 229–255. https://doi.org/10.3390/RS70100229

Simard, M., Pinto, N., Fisher, J. B., & Baccini, A. (2011). Mapping forest canopy height globally with spaceborne lidar. *Journal of Geophysical Research: Biogeosciences*, *116*(G4), 4021. https://doi.org/10.1029/2011JG001708

Tao, S., Guo, Q., Li, C., Wang, Z., & Fang, J. (2016). Global patterns and determinants of forest canopy height. *Ecology*, *97*(12), 3265–3270. https://doi.org/10.1002/ECY.1580

Tello, M., Cazcarra-Bes, V., Pardini, M., & Papathanassiou, K. (2018). Forest structure characterization from SAR tomography at L-band. *IEEE Journal of Selected Topics in Applied Earth Observations and Remote Sensing*, *11*(10), 3402–3414. https://doi.org/10.1109/JSTARS.2018.2859050

Thatcher, C. A., Lukas, V., & Stoker, J. M. (2020). The 3D Elevation Program and energy for the Nation. *Fact Sheet*. https://doi.org/10.3133/FS20193051

Tian, X., & Shan, J. (2021). Comprehensive Evaluation of the ICESat-2 ATL08 Terrain Product. *IEEE Transactions on Geoscience and Remote Sensing*, *59*(10), 8195–8209. https://doi.org/10.1109/TGRS.2021.3051086

Tinkham, W. T., Mahoney, P. R., Hudak, A. T., Domke, G. M., Falkowski, M. J., Woodall, C. W., & Smith, A. M. S. (2018). Applications of the United States Forest Inventory and Analysis dataset: A review and future directions. *Canadian Journal of Forest Research. 48: 1251-1268.*, *48*(11), 1251–1268. https://doi.org/10.1139/CJFR-2018-0196

Tobler, W. R. (1970). A computer movie simulating urban growth in the Detroit region. *Economic Geography*, *46*, 234. https://doi.org/10.2307/143141

US Forest Service (2007). Retrieved September 30, 2022, from https://www.fs.usda.gov/srsfia/data_acquisition/SRS%20401_MARCH_2012%20ALL%20Complete_FINAL_.pdf

US Geological Survey, USGS 3D Elevation Program Digital Elevation Model (2019). Retrieved June 7, 2022, from http://prd-tnm.s3.amazonaws.com/index.html?prefix=StagedProducts/Elevation/metadata/MS_Central_Delta_2018_D18/MS_MississippiDelta_3_2018

Vaglio Laurin, G., Ding, J., Disney, M., Bartholomeus, H., Herold, M., Papale, D., & Valentini, R. (2019). Tree height in tropical forest as measured by different ground, proximal, and remote sensing instruments, and impacts on above ground biomass estimates. *International Journal of Applied Earth Observation and Geoinformation*, *82*, 101899. https://doi.org/10.1016/J.JAG.2019.101899

van Leeuwen, M., & Nieuwenhuis, M. (2010). Retrieval of forest structural parameters using LiDAR remote sensing. *European Journal of Forest Research*, *129*(4), 749–770. https://doi.org/10.1007/S10342-010-0381-4/TABLES/3

Van Rossum, G., & Drake, F. L. (2009). *Python 3 Reference Manual.* Scotts Valley, CA: CreateSpace.

Varvia, P., Korhonen, L., Bruguière, A., Toivonen, J., Packalen, P., Maltamo, M., Saarela, S., & Popescu, S. C. (2022). How to consider the effects of time of day, beam strength, and snow cover in ICESat-2 based estimation of boreal forest biomass? *Remote Sensing of Environment*, *280*, 113174. https://doi.org/10.1016/J.RSE.2022.113174

Wang, Y., Lehtomäki, M., Liang, X., Pyörälä, J., Kukko, A., Jaakkola, A., Liu, J., Feng, Z., Chen, R., & Hyyppä, J. (2019). Is field-measured tree height as reliable as believed – A comparison study of tree height estimates from field measurement, airborne laser scanning and terrestrial laser scanning in a boreal forest. *ISPRS Journal of Photogrammetry and Remote Sensing*, *147*, 132–145. https://doi.org/10.1016/J.ISPRSJPRS.2018.11.008

Wang, Y., Li, G., Ding, J., Guo, Z., Tang, S., Liu, R., & Chen, J. (2016). A combined GLAS and MODIS estimation of the global distribution of mean forest canopy height. *Remote Sensing of Environment*, *174*, 24–43. https://doi.org/10.1016/J.RSE.2015.12.005

Wickham, J., Stehman, S. v., Sorenson, D. G., Gass, L., & Dewitz, J. A. (2021). Thematic accuracy assessment of the NLCD 2016 land cover for the conterminous United States. *Remote Sensing of Environment*, *257*, 112357. https://doi.org/10.1016/J.RSE.2021.112357

Wulder, M. A., Bater, C. W., Coops, N. C., Hilker, T., & White, J. C. (2008). The role of LiDAR in sustainable forest management. *Forestry Chronicle*, *84*(6), 807–826. https://doi.org/10.5558/TFC84807-6

Wulder, M. A., White, J. C., Nelson, R. F., Næsset, E., Ørka, H. O., Coops, N. C., Hilker, T., Bater, C. W., & Gobakken, T. (2012). Lidar sampling for large-area forest characterization: A review. *Remote Sensing of Environment*, *121*, 196–209. https://doi.org/10.1016/J.RSE.2012.02.001

Yu, J., Nie, S., Liu, W., Zhu, X., Lu, D., Wu, W., & Sun, Y. (2022). Accuracy assessment of ICESat-2 ground elevation and canopy height estimates in mangroves. *IEEE Geoscience and Remote Sensing Letters*, *19*. https://doi.org/10.1109/LGRS.2021.3107440

Zahawi, R. A., Dandois, J. P., Holl, K. D., Nadwodny, D., Reid, J. L., & Ellis, E. C. (2015). Using lightweight unmanned aerial vehicles to monitor tropical forest recovery. *Biological Conservation*, *186*, 287–295. https://doi.org/10.1016/J.BIOCON.2015.03.031

Zhang, J., Zhang, Z., Lutz, J. A., Chu, C., Hu, J., Shen, G., Li, B., Yang, Q., Lian, J., Zhang, M., Wang, X., Ye, W., & He, F. (2022). Drone-acquired data reveal the importance of forest canopy structure in predicting tree diversity. *Forest Ecology and Management*, *505*, 119945. https://doi.org/10.1016/J.FORECO.2021.119945

Zhu, A., Lu, G., Liu, J., Qin, C., & Zhou, C. (2018). Spatial prediction based on Third Law of Geography. *Https://Doi.Org/10.1080/19475683.2018.1534890*, *24*(4), 225–240. https://doi.org/10.1080/19475683.2018.1534890

APPENDIX A

EQUIVALENCE TEST FIGURES

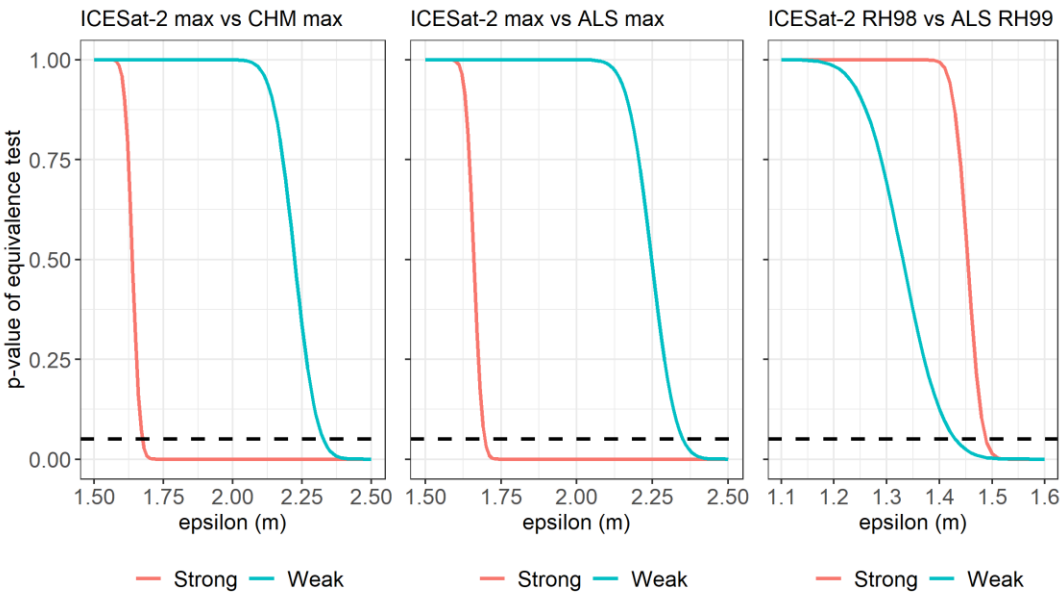

Figure A.1 Equivalence test for strong and weak beams from ICESat-2 and ALS

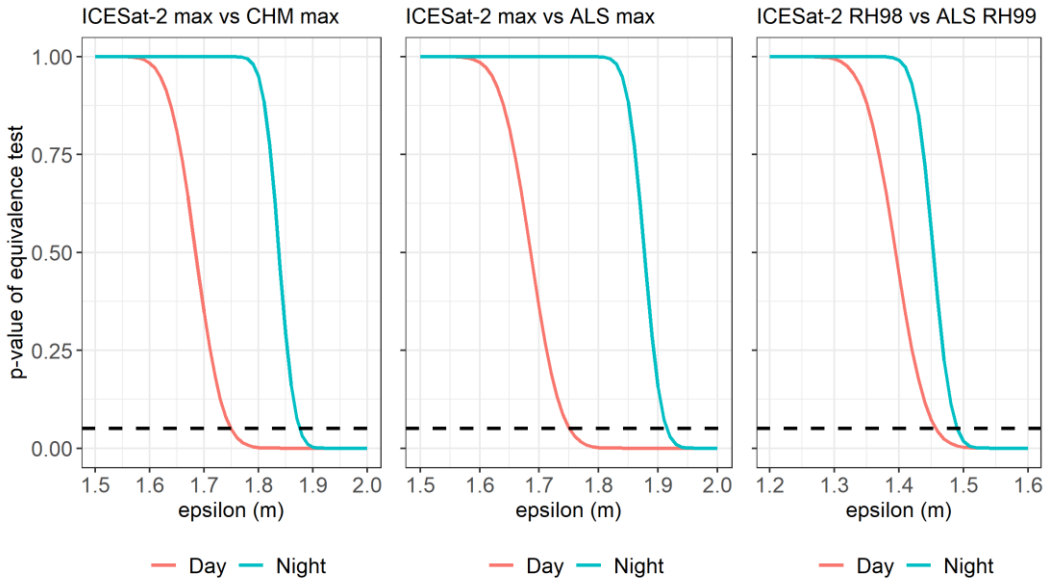

Figure A.2 Equivalence test for day and night beams from ICESat-2 and ALS

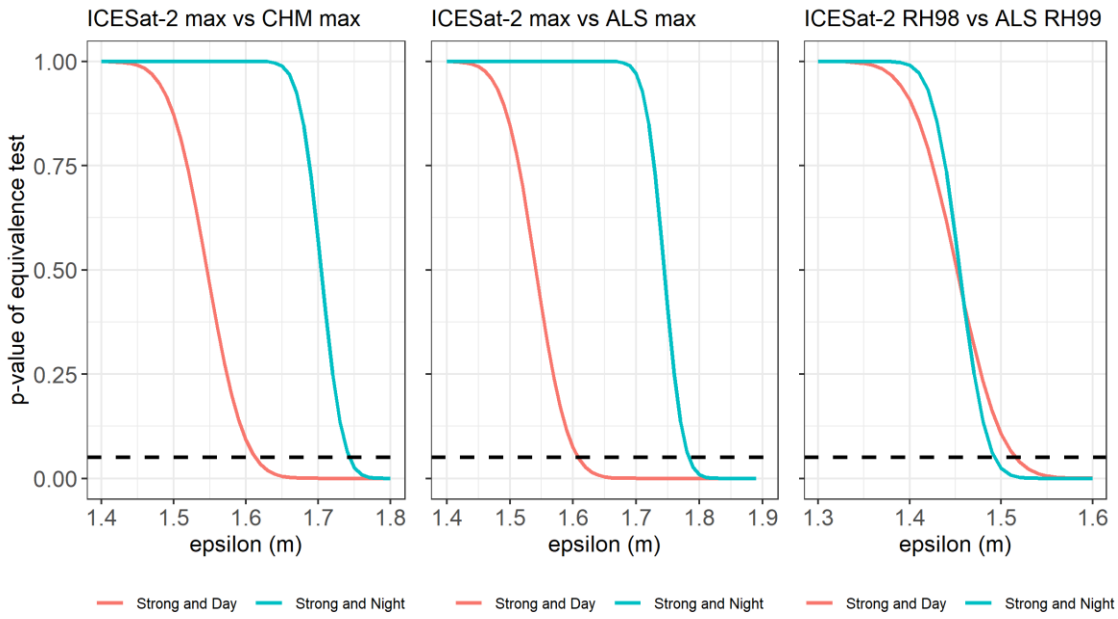

Figure A.3 Equivalence test for strong and day/night data from ICESat-2 and CHM max

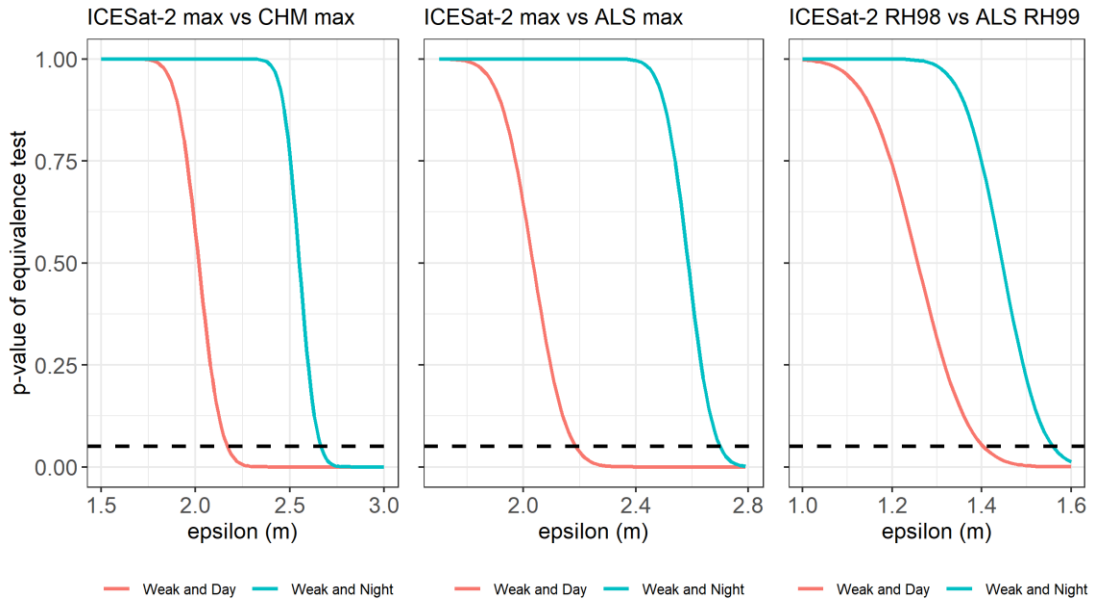

Figure A.4 Equivalence test for weak and day/night data from ICESat-2 and CHM max

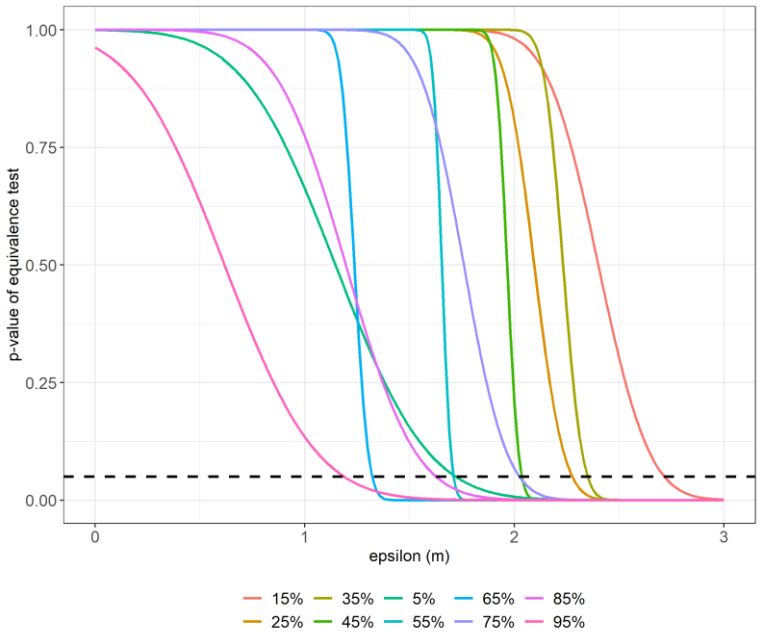

Figure A.5 Equivalence test for canopy cover for ICESat-2 max vs. CHM max

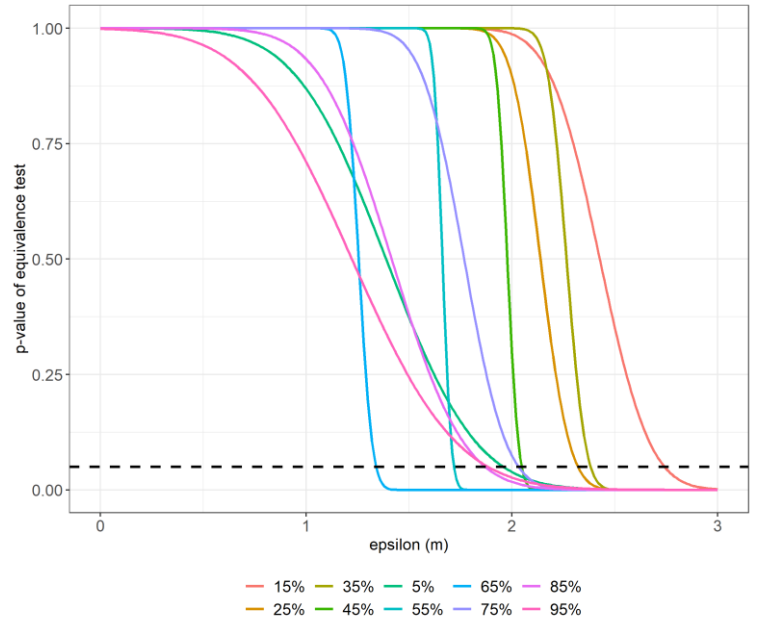

Figure A.6 Equivalence test for canopy cover for ICESat-2 vs. ALS max

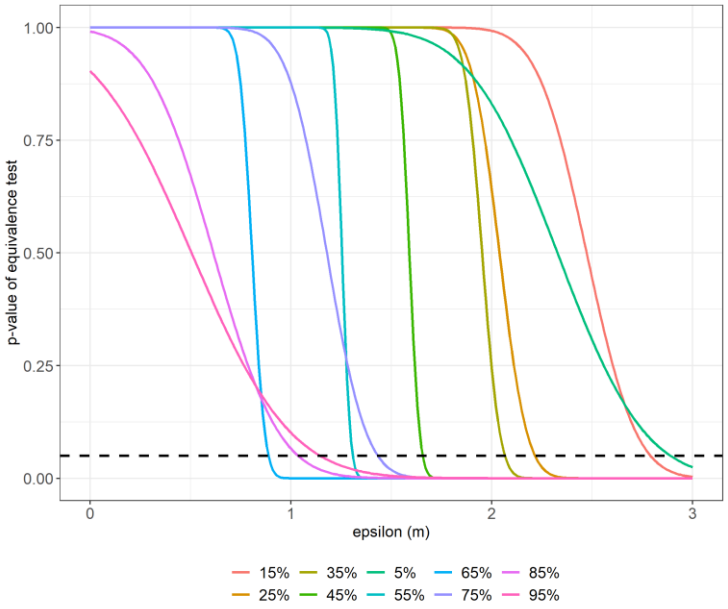

Figure A.7 Equivalence test for canopy cover for ICESat-2 RH98 vs. ALS RH99

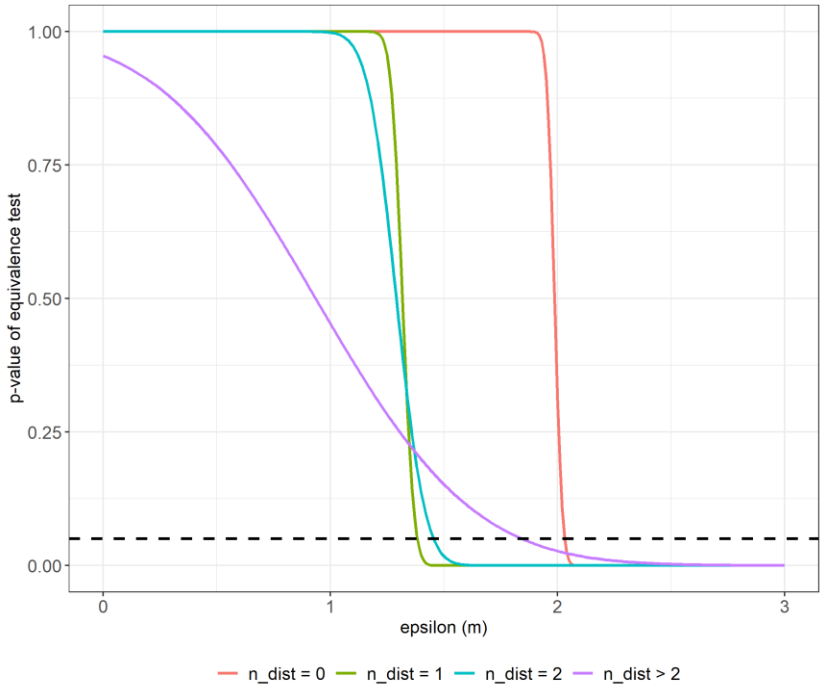

Figure A.8 Equivalence test for disturbance frequency for ICESat-2 max vs. CHM max

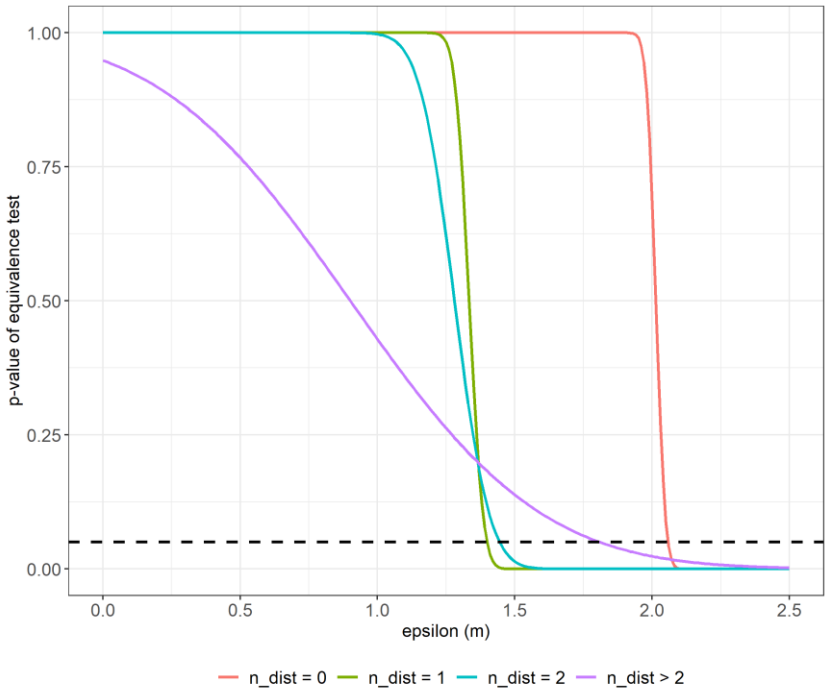

Figure A.9 Equivalence test for disturbance frequency ICESat-2 max vs. ALS max

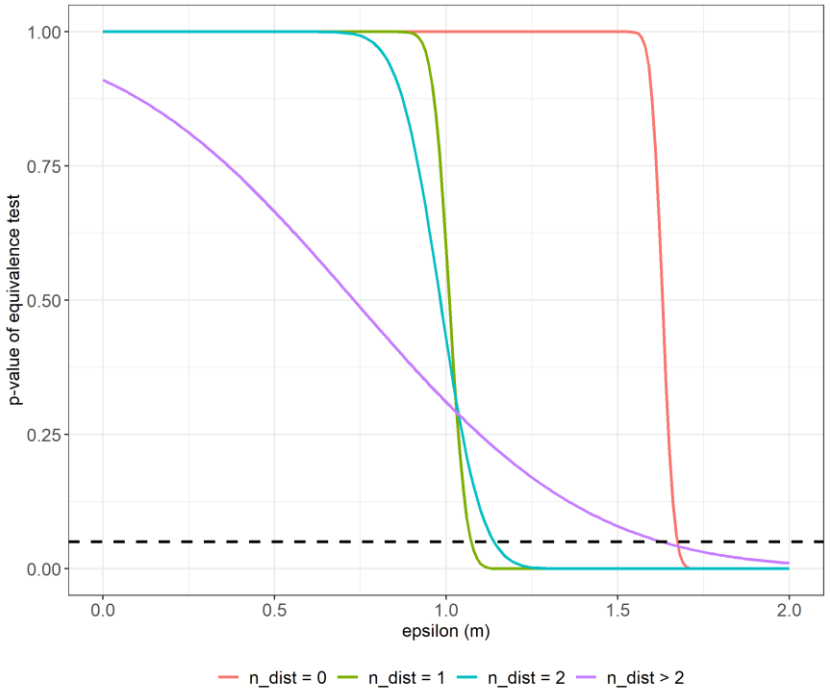

Figure A.10 Equivalence test for disturbance frequency of ICESat-2 RH98 vs. ALS RH99

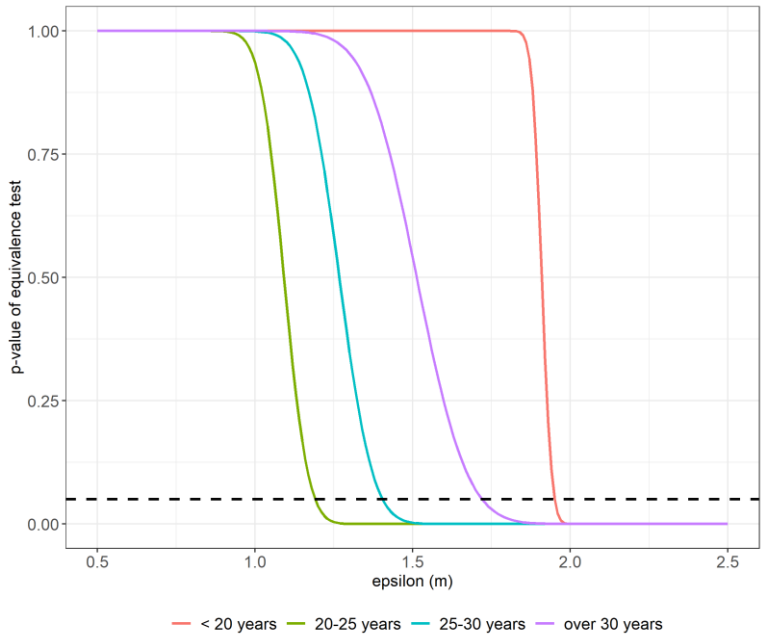

Figure A.11 Equivalence test for time since disturbance of ICESat-2 max vs. CHM max

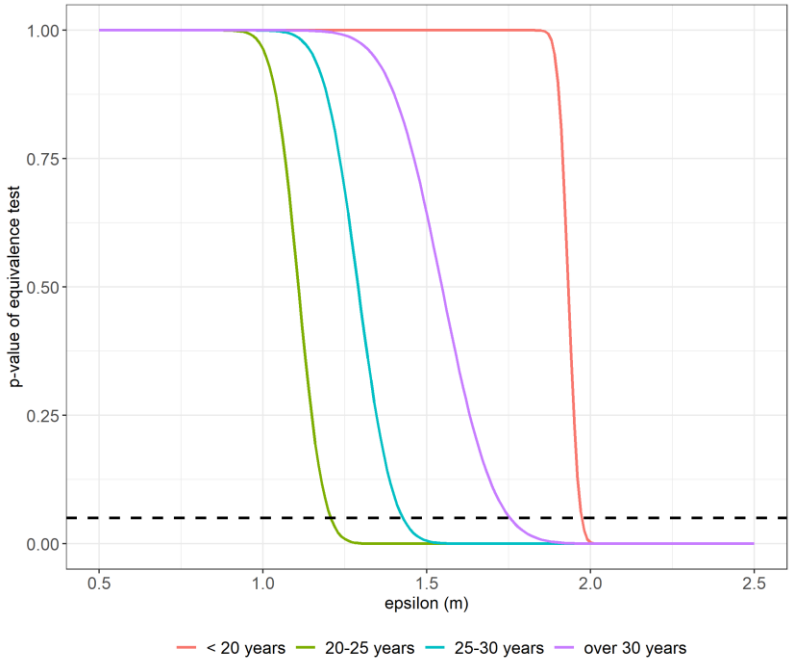

Figure A.12 Equivalence test for time since disturbance of ICESat-2 max vs. ALS max

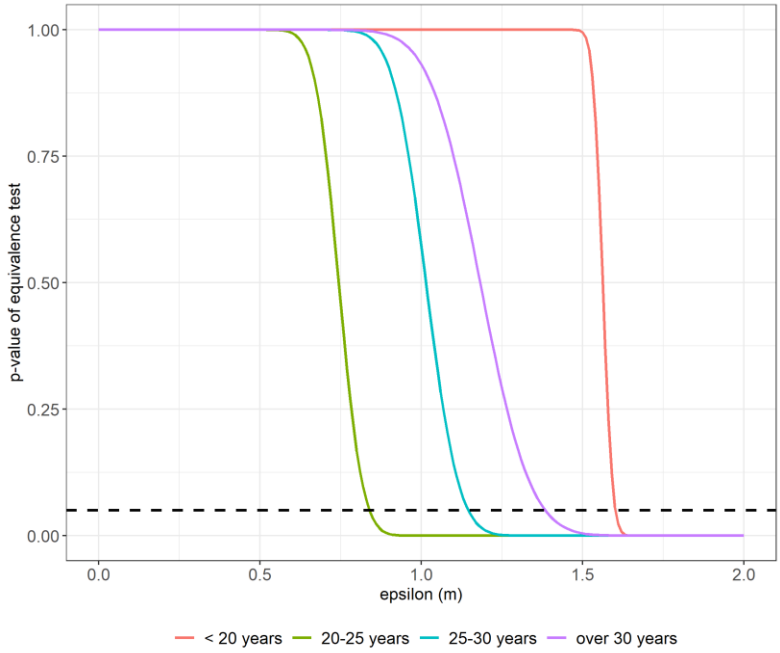

Figure A.13 Equivalence test for time since disturbance of ICESat-2 RH98 vs. ALS RH99

APPENDIX B

INTERPOLATED CANOPY HEIGHT MAPS OF MISSISSIPPI

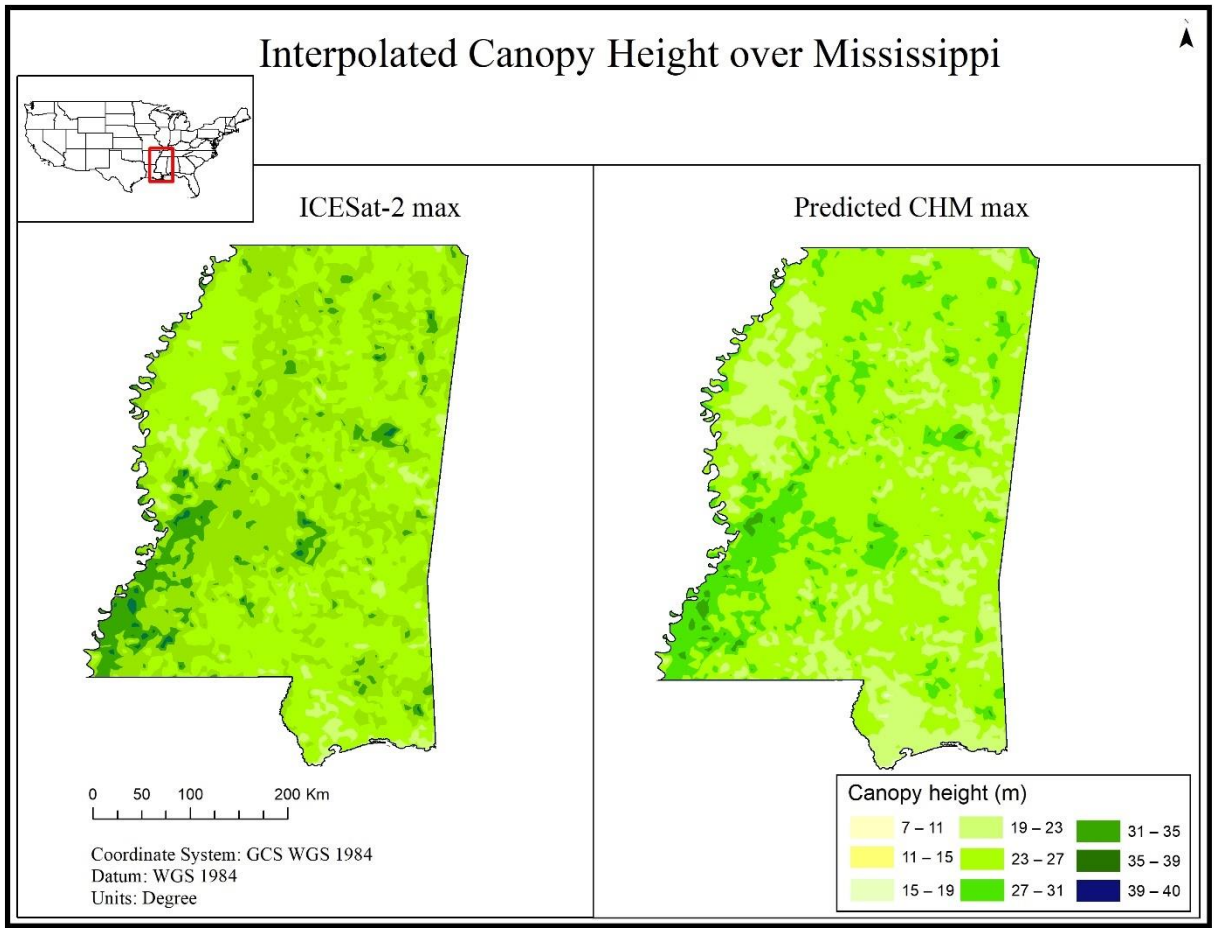

Figure B.1 Observed ICESat-2 max vs. predicted CHM max canopy heights over Mississippi

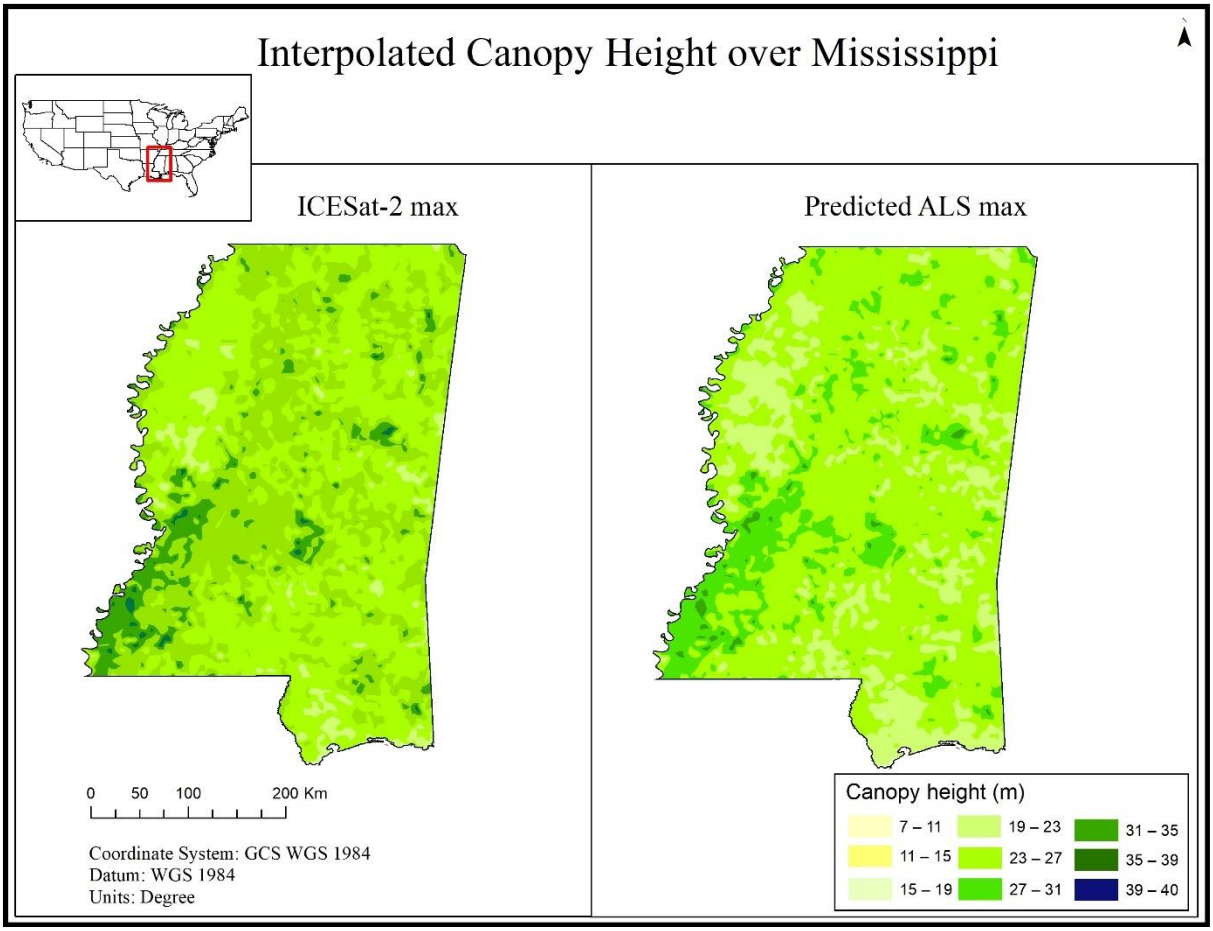

Figure B.2 Observed ICESat-2 max vs. predicted ALS max canopy heights over Mississippi

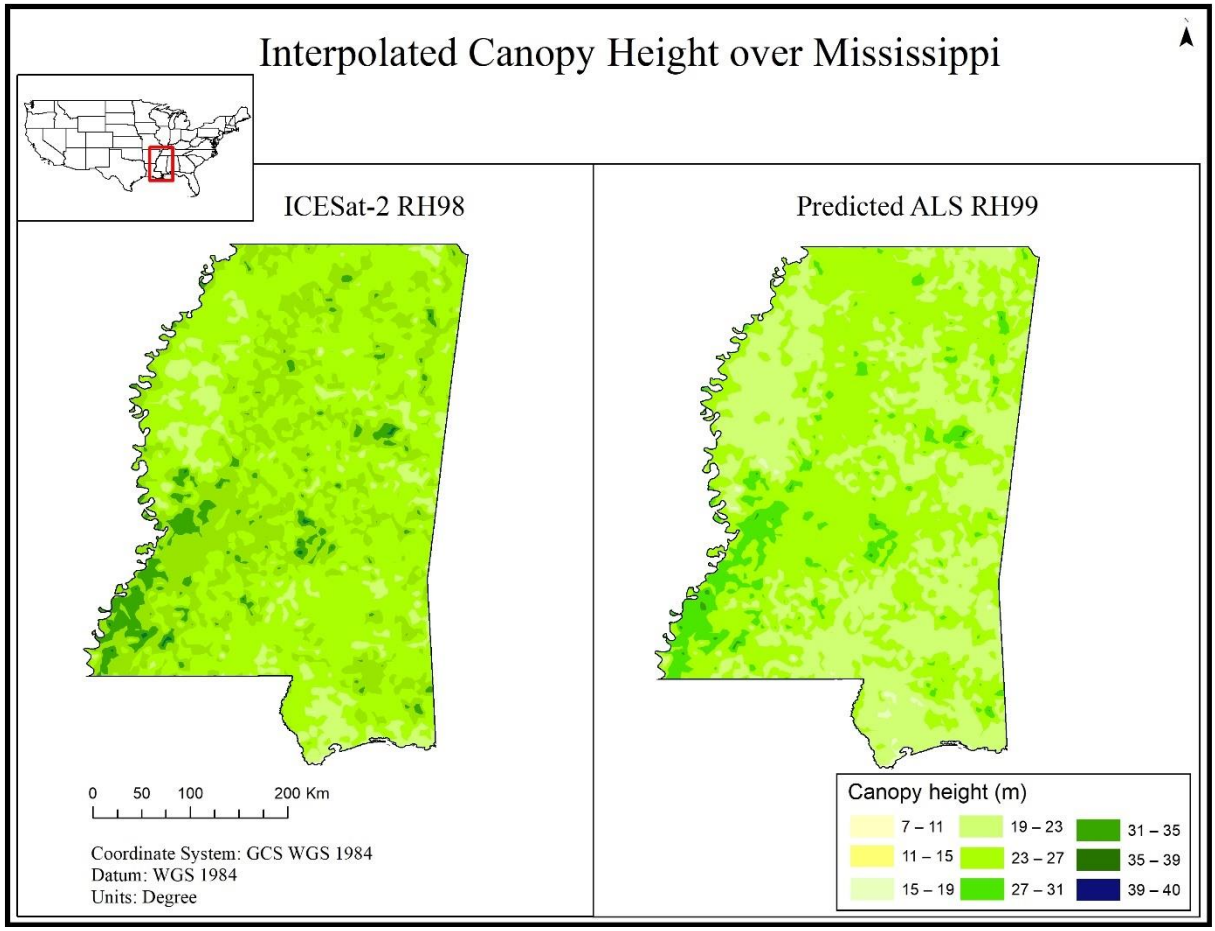

Figure B.3 Observed ICESat-2 RH98 vs. predicted ALS RH99 canopy heights over Mississippi